Strongly Coupled Bayesian Models for Interacting Object and Scene Classification Processes

Tina Ehtiati

Department of Electrical and Computer Engineering
McGill University, Montreal

February 2007

A Thesis submitted to the Faculty of Graduate Studies and Research
in partial fulfillment of the requirement for the degree of
Doctor of Philosophy

Your file Votre référence
ISBN: 978-0-494-32177-5
Our file Notre référence
ISBN: 978-0-494-32177-5

Abstract

In this thesis, we present a strongly coupled data fusion architecture within a Bayesian framework for modeling the bi-directional influences between the scene and object classification mechanisms. A number of psychophysical studies provide experimental evidence that the object and the scene perception mechanisms are not functionally separate in the human visual system. Object recognition facilitates the recognition of the scene background and also knowledge of the scene context facilitates the recognition of the individual objects in the scene. The evidence indicating a bi-directional exchange between the two processes has motivated us to build a computational model where object and scene classification proceed in an interdependent manner, while no hierarchical relationship is imposed between the two processes. We propose a strongly coupled data fusion model for implementing the feedback relationship between the scene and object classification processes. We present novel schemes for modifying the Bayesian solutions for the scene and object classification tasks which allow data fusion between the two modules based on the constraining of the priors or the likelihoods. We have implemented and tested the two proposed models using a database of natural images created for this purpose. The Receiver Operator Curves (ROC) depicting the scene classification performance of the likelihood coupling and the prior coupling models show that scene classification performance improves significantly in both models as a result of the strong coupling of the scene and object modules.

ROC curves depicting the scene classification performance of the two models also show that the likelihood coupling model achieves a higher detection rate compared to the prior coupling model. We have also computed the average rise times of the models' outputs as

a measure of comparing the speed of the two models. The results show that the likelihood coupling model outputs have a shorter rise time. Based on these experimental findings one can conclude that imposing constraints on the likelihood models provides better solutions to the scene classification problems compared to imposing constraints on the prior models.

We have also proposed an attentional feature modulation scheme, which consists of tuning the input image responses to the bank of Gabor filters based on the scene class probabilities estimated by the model and the energy profiles of the Gabor filters for different scene categories. Experimental results based on combining the attentional feature tuning scheme with the likelihood coupling and the prior coupling methods show a significant improvement in the scene classification performances of both models.

Résumé

Dans cette thèse, nous présentons une architecture de fusion de données fortement couplée à l'intérieur d'un cadre bayésien pour la modélisation des influences bidirectionelles entre les mécanismes de classification de scène et d'objet. Un certain nombre d'études psychophysiques apportent des preuves expérimentales que les mécanismes de perception d'objet et de scène ne sont pas séparés fonctionnellement dans le système visuel humain. La reconnaissance d'objet facilite la reconnaissance de l'arrière-plan d'une scène et la connaissance du contexte d'une scène facilite aussi la reconnaissance des objets individuels de la scène. Les preuves indiquant un échange bidirectionnel entre les deux processus nous ont motivés à construire un modèle computationnel dans lequel la classification d'objet et de scène procèdent de façon interdépendante, alors qu'aucune relation hiérarchique n'est imposée entre les deux processus. Nous proposons un modèle de fusion de données fortement couplé pour implémenter la relation de feedback entre les processus de classification de scène et d'objet. Nous présentons de nouvelles techniques pour modifier les solutions bayésiennes pour les tâches de classification de scène et d'objet qui permettent la fusion de données entre les deux modules en se basant sur la contrainte des probabilités a priori ou des vraisemblances. Nous avons implémenté et testé les deux modèles proposés en utilisant une base de donnée d'images naturelles créés à cet escient. Les courbes de caractéristique d'opération du récepteur (Receiver Operator Curve - ROC) décrivant la performance en classification de scène des modèles par couplage de vraisemblance et par couplage de probabilité a priori montrent que le fort couplage des modules de scène

et d'objet resulte en une amélioration significative de la performance en classification de scène des deux modèles.

Les courbes ROC décrivant la performance en classification de scène des deux modèles montrent aussi que le modèle par couplage de vraisemblance atteint un taux de détection plus élevé que le modèle par couplage de probabilité a priori. Nous avons aussi calculé les temps de montée moyens des sorties des modèles comme mesure de comparaison de la vitesse des deux modèles. Les résultats montrent que les sorties du modèle par couplage de vraisemblance ont un temps de montée plus court. En se basant sur ces résultats expérimentaux, on peut conclure qu'imposer des contraintes sur les modèles par vraisemblance fournir de meilleures solutions aux problèmes de classification de scène qu'imposer des contraintes sur les modèles par probabilité a priori.

Nous avons aussi proposé une technique de modulation par trait attentionel qui consiste au réglage des réponses des images en entrée à la banque de filtres de Gabor en se basant sur les probabilitées de classes de scènes estimées par le modèle et les profils energétiques des filtres de Gabor pour différentes catégories de scènes. Des résultats expérimentaux basés sur la combinaison de la technique de réglage par trait attentionel avec les méthodes par couplage de vraisemblance et par couplage de probabilité a priori montrent une amélioration significative de la performance en classification de scène pour les deux modèles.

Acknowledgements

I would like to express my great gratitude to my supervisor, Dr. James J. Clark, for his encouragement and guidance throughout my Ph.D. program, and for his time and patience in the course of writing this thesis. I have been most fortunate to be able to use his wealth of knowledge and experience as his Ph.D. student during the past four years. I would also like to thank my thesis committee members, Dr. Tal Arbel and Dr. Michael Langer for their supervision on my thesis progress.

I would like to thank my friends in the Centre for Intelligent Machines, Wei Sun, Sandra Skaff, Li Jie, Muhua Li, and Fatima Drissi-Smaili for their companionship which made my years of Ph.D. studies more fruitful and enjoyable. I thank Vincent Levesque for the French translation of the abstract of this thesis.

My special gratitude goes to my family members, my parents Mohammad Ali Ehtiati and Servat Rostamkhani, and my husband Zahir Albadawi, for all the support they gave me throughout my research work.

The research described in this thesis was funded by Precarn Incorporated, as well as through research grants to the supervisor from the Institute for Robotics and Intelligent Systems (IRIS).

Table of Contents

List of Figures

List of Tables

Chapter 1

Introduction

1.1 Motivation

Natural scene categorization is one of the most relevant evolutionary tasks of the human visual system. The great efficiency of this task as performed by humans has stimulated much research in the fields of neural physiology, psychophysics, and computational neuroscience. Contrary to our daily experience of the effortlessness with which natural scene recognition is performed in humans, this is one of the hardest tasks for machine vision, and one that the modern state of the art computer vision algorithms have yet to accomplish. This difficulty is to a great extent due to the vast variability among the scenes belonging to similar categories of natural scenes. The question of choosing appropriate scene representations that are capable of capturing the main characteristics of scene categories without being too sensitive to intra-class variabilities, and are therefore useful for the scene recognition task, has been the subject of extended research in the domain of computer vision.

In this work we have looked into the literature in neurophysiology and psychophysics in order to gain an understanding of how the human visual system performs scene recognition and categorization and to apply similar models and mechanisms to the computer vision systems for achieving more efficient scene recognition capabilities. In this endeavor we have found that the hierarchical view of the

human visual system, which has been supported by neuro-physiological findings, has led to the general conclusion that understanding the meaning of scenes is a high level visual task which takes place as the end result of a progressive reconstruction of the retinal image. The hierarchical architecture of the visual system implies that understanding the content of local regions of scenes, and recognition of objects in the scene, are the pre-requisite of understanding the meaning of the whole scene. On the other hand we have found that experimental results in the domain of psychophysics have provided evidence that scene understanding can take place independently from object recognition. These results have been interpreted as evidence that some sort of high-level abstract representations of scenes, or "gists" of scenes, are rapidly extracted by the visual system, bypassing the object recognition stage [76][77]. The low-pass spatial frequency content of the scenes have been suggested as a candidate for the computational definition of "gists" since they provide an encoding of the scene that is useful for categorizing scene information across scene classes. Psychophysical experimental results have furthermore shown that scene context can be processed and accessed early enough to influence the recognition of objects. These experiments imply that the abstract conceptual representations of scenes may be formed before the identification of the objects which are semantically associated with them.

In general, it is far from being settled what is actually the relationship between the scene recognition process and object recognition process in the human visual process, and what actually happens in a brief viewing of a scene. It is still an open debate in psychophysics whether the objects in the scene are perceived before the scene identity is produced based on the list of objects and their relations, or the scene context is

grasped independently and perhaps prior to recognizing objects. But by looking into the psychophysical and the neuro-physiological findings one can conclude that there is adequate evidence to suggest that scene and object perception are not unrelated and disparate mechanisms, but they are correlated and facilitate each other, implying that they may share computational resources. Scene-contextual constraint is available early enough and is robust enough to influence the recognition of objects, and also identification of the object in a scene promotes the understanding of the meaning of the scene, implying a bidirectional exchange between the two processes. Our goal in this thesis is to provide an account of how such a bidirectional influence is computationally possible. What would be a computational model for implementing the mutual influence between the two processes?

1.2 Objectives

We would like to build a computational model where the scene recognition and object recognition mechanisms do not relate to each other in a hierarchical relationship, but rather run in parallel. Our objective is to build a computational model where the two recognition stages occur in parallel, but constantly feedback information to each other in order to enhance the performance of the two processes. The idea is that as soon as there is any information for any possible levels of recognition, our model takes advantage of it. In this model an early sensory information extraction stage precedes the semantic recognition stages. The scene recognition process is performed based on sensory information from all locations in the scene, or "global" scene information. The object recognition stage is performed based on local sensory information extracted from local

regions in the image. The computational scheme chosen for scene recognition stage must be capable of eliciting an estimation of the scene identity rapidly and independently of the object recognition stage, based on the gist type global scene features given to it. The object module must in parallel produce the most likely candidate interpretations of individual objects based on local image features. The information inferred by each of the two recognition processes is projected to the other process, where the set of associations that corresponds to the relevant content is activated. In implementing such a model the main questions to address are the following: How are the associations between scenes and objects represented? How can the results of the scene recognition process become available to the object recognition process and vise versa?

In this work we propose using strongly coupled data fusion architecture within a Bayesian framework to model the associations between the scene and the object recognition mechanisms. The function of each recognition process is modeled using Bayesian inference methods. The strongly coupled data fusion architecture ensures that when the *a priori* constraints built into the scene recognition process and the object recognition process fail to provide a unique solution for one of the processes, the knowledge inferred from the other module can be combined as part of the module estimation process in order to further constrain the solution. Motivated by the strongly coupled data fusion architecture we present a scheme for modifying the Bayesian solutions for the scene and the object recognition processes in order to incorporate the possibility of information sharing between the two processes. The strongly coupled data fusion architecture allows two approaches to implementing the interactions between the two modules. In the first approach, the two modules interact through the prior terms of

the Bayesian formulation. In this approach the *a priori* models of the scene and object modules are modified in order to allow constraints built into the solution process based on information coming from the other module. This variation of the model is strongly coupled in terms of priors. In the second approach, the likelihood models of each module are reformulated in order to allow data fusion with the other module. This variation of the model is strongly coupled in terms of likelihoods. Both variations of the model we present are examples of recurrent strongly coupled architecture.

A computational scheme for producing features that capture the context of the scenes was first proposed by Oliva and Torralba [70]. In their work a holistic representation of the scene based on oriented bandpass filters is used as the context features. This image representation encodes spatially localized structural information. The potential of this representation for serving as features for the computational scene categorization task has been investigated and demonstrated. Furthermore Torralba and Oliva [94] have proposed a novel Bayesian approach to contextual object detection. Their approach is based on conditioning the statistics of the low level contextual features of the scene according to the presence or absence of objects. They show that the scene contexts can provide an estimate of the likelihood for finding certain classes of objects in the scene. Murphy et al [65] have further extended this idea and combined the scene classification and object detection task by maximizing a conditional joint probability density model that represents the likelihood of different scene classes and the presence of different object classes in certain locations, as constrained by the global contextual features.

Our approach has the architectural advantage that the scene identification and object identification are capable of functioning independently. When one of the processes does not have enough information in order to create a plausible hypothesis, the strong coupling data fusion scheme between the two processes can be used in order to obtain further evidence for creating a hypothesis. Furthermore, our approach is different from [65] in the sense that we do not just use conditional likelihoods, but rather we use a full Bayesian formulation in which the *a priori* scene and object models play a crucial role.

Visual attention is considered to be one of the first and foremost means of controlling the flow of information between the different levels of visual processing. It has been shown that the function of attention is tightly associated with object recognition process in human vision. Numerous studies have probed the function of attention, demonstrating attentional control over stimuli with complex and conjugate features. In this work we have investigated the usefulness and efficacy of an attentional process in the scene recognition process. We have implemented the attentional process for scene recognition by adding a feature tuning stage in which the high-level information inferred from the scene recognition process is used to bias image responses to selected spatial frequency and orientation features that provide higher discrimination for scene classification task.

1.3 Contributions

The following is a list of the main contributions made in this thesis, most of which have been published in Ehtiati and Clark [18][19]:

1. We propose a model in which the process of scene categorization and the process of categorization of individual objects in the scene feedback information to each other in order to enhance the performance of both processes. The main characteristic of this model is that the feedback between the two processes is implemented in a way which allows the two processes to function in parallel, with no hierarchical relationship being imposed between the two processes. The proposed architecture allows the two processes to function independently, within their individual required timeframes and without receiving any feedback from the other process, but as soon as any information is available by one of the processes it becomes available to the other process through the feedback connections between the two processes.

2. We propose a strongly coupled data fusion model for implementing the feedback relationship between the scene categorization and the object categorization processes. We present a Bayesian interpretation of the strongly coupled data fusion architecture which allows imposing constraints on either the likelihood models or the prior models of the scene and object categorization processes based on feedback from the other process.

3. We present experimental results which show that the feedback implemented between the scene categorization and the object categorization processes increases the performance of scene categorization task. We also investigate the robustness of the model function to noise and variability in data such as scale and orientation variations.

4. We present a variation of the model in which a top-down attentional modulation effect from the high-level scene inference process to the lower level scene feature extraction process is incorporated with the objective of making the scene

categorization process more efficient. In this variation of the model we use the hypothesis formed by the scene categorization process to bias global image responses to selected spatial frequencies and orientations. We show that the effect of combining feature tuning with the strongly coupled models is to increase the performance of scene categorization.

1.4 Overview of the Thesis

This thesis is organized as the following. In chapter 2 we examine the current theories and findings in the domain of cognitive sciences about scene perception and the relationship between scene perception and object perception, with the goal of motivating the model presented in this thesis. In chapter 3 we first give a short background on different computational schemes for scene representation and classification and motivate and present our choice for the model's formulation of scene classification process. In the second part of this chapter we discuss briefly different computational schemes for object representation and classification and motivate and present our choice for the model's formulation of object categorization module. In chapter 4 we discuss the implementation of the feedback between the scene and the object categorization processes. In this chapter we present the mathematical methodology we have developed through which the information produced by the two sensory information processing modules, the scene classification module and the object classification module can become available to each other and be considered as part of the information processing problem solved in each module. The methodology we present here is motivated by the field of data fusion. In this chapter we propose two approaches for implementing the interactions between the

scene classification and the object classification modules based on a Bayesian strongly coupled data fusion architecture, the strongly coupled priors model and the strongly coupled likelihoods model. In chapter 5 we present the experimental results from the implementation of the strongly coupled scene and object classification models presented in chapter 4. We first demonstrate selective examples where the scene module or the object module cannot perform the scene or the object classification task reliably when they function independently, but the strong coupling of the two modules improves the initial classification results. In this chapter we also present the statistical evaluation of the models performances and address the issue of statistical meaningfulness of the presented results using receiver operating characteristic (ROC) curves. The statistical evaluation of the adaptive priors and the adaptive likelihood models provide a basis for comparing these two models. In this chapter we also give a description of the database we have created for the purpose of these experiments. In chapter 6 we attempt to establish the main characteristics of the models such as predictability, speed, and robustness to input image variations. In chapter 7 we present a variation of the model which incorporates a top-down attentional feedback from the high-level scene inference process to the lower level scene feature extraction process. In this chapter we show that the attentional modulation effect enhances the scene categorization performance. Chapter 8 provides conclusion for the current work and suggestions for future work.

Chapter 2

Cognitive Models of Scene and Contextual Object Perception

We often take our ability to quickly and accurately understand real-world scenes for granted. It is normal for us to be able to rapidly grasp the meaning of different scenes while scanning through different channels on the TV, the downtown of Montreal with high buildings and people and cars moving around, a courtroom full of people and furniture, a boat sailing in the sea, etc. We are able to efficiently and accurately recognize and categorize the new scene types without our visual system requiring significant amounts of time to adjust and tune itself.

The rapid apprehension of the world by the human visual system has been the subject of many psychophysical studies. Potter *et al.* utilized rapid serial visual presentations (RSVP) of images to find out that subjects could understand a visual scene with exposures of as brief as 100 ms, and might be able to extract semantic information about scene context from presentations as brief as 80 ms [76][77]. Furthermore, they demonstrated that while the semantic information of a scene is quickly extracted, it requires a few hundred milliseconds (about 300 ms) to be consolidated into memory. These results have been interpreted as evidence that a high-level abstract representation of the visual scene, which can be accessed very rapidly, is continually generated by the visual system. This representation, which is called the "gist" of a scene, is defined as a conceptual summary of the principal semantic features of the scene as perceived in a brief viewing. In other words, the gist of the scene is the conceptual content of the scene

understood in a glance. In experiments performed by Standing *et al* [86] and Standing [87] it is shown that our visual memory performs very well in identifying scenes viewed previously among very large sets of old and new scenes. One possible explanation of this performance can be that in this task only the gist of the scenes are required for recognition of old scenes.

Some evidence for abstract representations of scenes also comes from the phenomenon of *boundary extension* [46][35]. Boundary extension is a type of memory distortion in which observers report having seen not only information that was physically present in the scene, but also information that they have extrapolated outside the scene's boundaries. Similarly, in visual false memory experiments, participants report that they remember having seen, in a previously presented picture, objects that are contextually related to that scene but that were not in the picture. Such memory distortions might be the byproduct of an efficient mechanism for extracting and encoding the gist of a scene.
It is interesting to compare the capacity of our brain for holding gist of scenes with its capacity to hold details of objects in scenes. The limits of our perception of objects during RSVP experiments has been studied by Rensink *et al.*[80] and O'Regan *et al* [73]. They used the "mud splash" technique of masking a change in the scene by making several simultaneous conspicuous changes at different locations in the scene (similar to the effect of a mud splash on a car windscreen). They show that when the attentional effect introduced by visual transients accompanying a change in the scene is masked, changes to retinotopically large portions of the scene sometimes can fail to be detected by viewers. This is more likely to occur when the regions are not linked to the scene's overall meaning. This striking phenomenon has been termed "change blindness". The

phenomenon of change blindness is especially interesting since it challenges the view of the "picture in the head", or an exact and detailed internal representation of the visual world in our brain, which is usually assumed in the passive vision theories. Change blindness is better explained when the active vision perspective is adopted. O'Regan *et al* [72] show that for objects directly fixated change detection ability is high.

2.1 The Content of the Gist of a Scene

Other investigators have attempted to elucidate the nature of information captured by the gist of a scene. What is the nature of information that we perceive and understand when we rapidly glance at the world?

Mandler and Parker have suggested that three types of information are remembered from a picture: i) an inventory of objects, ii) descriptive information of the physical appearance and other details of the objects, iii) spatial relationships between the objects [58]. Freidman and colleagues proposed that early scene recognition involves the identification of at least one obligatory object [30]. In their model, the obligatory object serves as a contextual pivotal point for the recognition of other parts of the scene. They have also provided evidence that objects can be recognized independently, without facilitation by the global scene context. Bar and Ullman [3] show that an ambiguous object becomes recognizable when another object that is contextually associated with it, is placed in an appropriate spatial relation to it.

On the other hand, other researchers have supported the idea that early scene processing is based on global scene information rather than local object information. Wolfe speculates that the spatial layout of the scene and a general impression of the low-

level features that fill the scene (e.g., texture, etc.) contribute to the understanding of the conceptual content of a scene [108]. Metzger and Antes [62] show that contextual information is extracted before observers can saccade towards the portions of the picture that were rated as contributing most to the context of the scene, and possibly even before the recognition of individual objects. Loftus *et al* [56] furthermore show that observers process the most informative portions of an image earliest.

Biederman *et al.* [5] found that recognition of objects is impaired when the objects are embedded in a randomly jumbled scene rather than a coherent scene. Biederman's finding implies that some kind of global context of the scene is registered in the early stages of scene perception, which can modulate the object recognition mechanism. His conclusions regarding scene perception parallel concepts in the auditory studies of sentence and word comprehension. He suggests using an analogy with analysis of language material, that scenes could be regarded as *schemas*, providing a frame in which objects are viewed. He identifies several physical (support, interposition) and semantic (probability, position, size) constraints, which objects must satisfy within a scene, similar to the syntactic and grammatical rules of language [6]. He shows that scenes with typical physical and structural regularities which follow contextual semantic rules facilitate object recognition as compared to scenes where these rules and regularities are violated.

Boyce et al. [9] have demonstrated that objects are more difficult to identify when located against a contextually inconsistent background, given a briefly flashed scene (150 ms) as compared with the effect of a meaningless background that was equated for visual appearance.

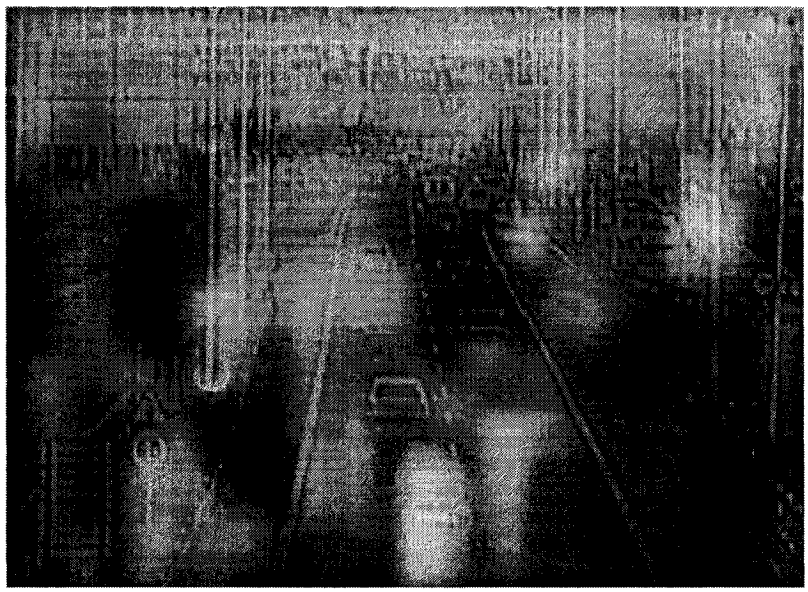

Figure 2.1 Example of a hybrid image used by Oliva and Shyns is shown. The hybrid images are produced by combining the low frequency components of the amplitude and phase spectra of one scene with the high frequency components of another scene. This example mixes the low frequency component of a city scene with a high frequency component of a highway.(Taken from the paper by Oliva and Schyns [66])

Recent computational work has suggested that global features such as spatial frequencies of the images are often sufficient for categorizing different environments without explicit recognition of objects [94]. Oliva and Schyns [66][67] show that a scene can be identified by global scene information independent of the identities of individual objects in the scene. They have demonstrated that scenes can be identified from low-pass spatial frequency filtered images that preserve the relationship between large scale structures in the scene but lacks the visual detail for identifying individual objects in the scene. They also show that when participants in the experiment have to identify scenes created by the superimposition of a low-pass filtered image and a high-pass filtered image from a very brief view (50 ms), they tend to base their interpretations on the low

frequency information rather than the high frequency information. This interpretation for gist of scenes is specifically interesting in the light of the experimental results of Hubel and Weisel [45] which provide evidence for the presence of oriented band-pass filters at the early stages of the visual pathway. An example of the superimposed images used by Oliva and Schyns is shown in figure (2.1).

2.2 Scene Context and Object Perception

Some discrepancies appear to exist between the different theories and experimental results described in section 2.1. Although intuitively much of the meaning of a scene is defined by the objects that comprise the scene (it is hard to imagine a scene that does not contain any objects), there is evidence that it is possible to produce a "gist" of a scene independent of constituent objects, and furthermore this "gist" modulates object recognition. On the other hand there is evidence from the experiments that at least some sort of object recognition is present even in the early stages of scene perception. At least some objects are recognized in the brief viewings of cluttered scenes. So the question which arises is that are the objects in the scene perceived first, and then the scene identity is produced based on the list of these objects and their relations? Or is the scene context grasped independently, and perhaps prior to recognizing objects? How are the two perceptions related? Is object recognition part of early scene perception? These questions have been the topic of an open debate by the psychophysical community for more than two decades [33][16][41].

The *perceptual schema model* proposes that expectations derived from knowledge about the composition of a scene type interact with the perceptual analysis of

objects in the scene [62][5][6][74]. This model is supported by studies of scene consistency and object detection. This view suggests that scene context information can be processed and accessed early enough to influence recognition of objects contained in the scene, even inhibiting recognition of inconsistent ones [7]. The *priming model*, on the other hand, proposes that the locus of the contextual effect is at the stage where a structural description of an object is matched against long-term memory representations [30][3]. This model suggests that the activation of a certain scene context primes the stored representations of context-consistent object types, and facilitates convergence to the most likely interpretations during the object recognition process. This model implies a definition of scene context independent of the identity of the objects semantically associated with the scene.

Regardless of the mechanism, both the priming model and the perceptual schema model claim that scene context facilitates consistent objects more than inconsistent ones. These theories predict that we should observe a correlation of object identification performance with scene context categorization performance [22]. In contrast, a third theory called the *functional isolation model,* proposes that object identification is isolated from expectations derived from scene knowledge [40]. Henderson and colleagues, who propose this view, predict that experiments examining the perceptual analysis of objects should find no systematic relation between object and scene recognition performance. Hollingworth and Henderson [40] mention that whereas objects tend to have a highly constrained set of component parts and relations between parts, a scene places far less constraint on objects and spatial relationship among objects.

2.3 Hints from Neurophysiology

The ventral visual pathway, linking the primary visual cortex through inferior temporal cortex to the prefrontal cortex, is generally known as the "what" visual pathway, as it is responsible for object recognition through integrating features [101][50][64][98]. Given the hierarchical structure of the visual system many have proposed models in which the elementary features of the objects are first processed and then bound together for object recognition [96][107]. Although many studies have revealed the cortical mechanisms involved in the recognition of individual objects, in comparison little work has been done to reveal the neural underpinnings of scene perception and contextual object recognition. Neuro-imaging studies have shown that a region in the parahippocampal cortex (PHC) responds preferentially to topographical information and spatial landmarks, the Parahippocampal place area (PPA) [1][21][57]. This region has an important role in large scale integration [54] and is increasingly being speculated to be a module for scene analysis [20][88]. Experimental results have also shown that objects may be grouped by physical appearance in the occipital visual cortex [36][91], by basic level categories in the anterior temporal cortex [78][39][17], by contextual relations in the parahippocampal cortex (PHC) [4], and by semantic relations in the prefrontal cortex (PFC) [31]. Bar has performed experiments in order to investigate the cortical areas involved during a contextual processing [4]. He designed experiments in which he compares the fMRI signal elicited during the recognition of visual objects that are highly associated with a certain context with that elicited by objects that are not associated with any unique context. He reports that the largest focus of differential activity is in the posterior PHC, which is the site that encompasses PPA. The other foci of activation are

found in the superior orbital sulcus (SOS) and the retro-splenial cortex (RSC), which have also been implicated in the analysis of spatial information. Despite much speculation in the neuro-physiological literature there is still no consensus and no clear answer as to how the scene contextual information useful for analysis of objects is represented, retained and stored in the brain, and how exactly the cortical processing takes advantage of the associations between scenes and objects.

One interesting observation is related to the PFC. It has been shown explicitly that PFC receives direct magnocellular connections from early visual cortex. Also PFC activity increases as a function of the number of alternative interpretations that can be produced about an object image based on its low spatial frequency [83]. It is proposed that low spatial frequencies in the image are extracted quickly and projected into PFC using fast anatomical connections, possibly the magnocellular pathway. This projection is faster than the thorough bottom-up pathway, and therefore can trigger a top-down processing which facilitates object recognition [46][11].

2.4 Summary

The question of the relationship between the scene recognition process and object recognition process in human visual system, especially in brief viewings of scenes, is still unanswered. But there is adequate evidence to suggest that scene and object perception are not unrelated and disparate mechanisms, but are correlated and influence and facilitate each other. Psychophysical evidence shows that scene-contextual constraint is available early enough and is robust enough to influence the recognition of objects. Other experimental results show that the identification of the objects in a scene

promotes the understanding of the meaning of the scene. One can hypothesize that there is a bidirectional exchange of information between the two processes, without one process being necessarily pre-requisite of the other. Our goal in this thesis is to provide an account of how such a bidirectional influence is computationally possible while retaining biological plausibility. What would be a computational model for implementing the mutual influence between the two processes?

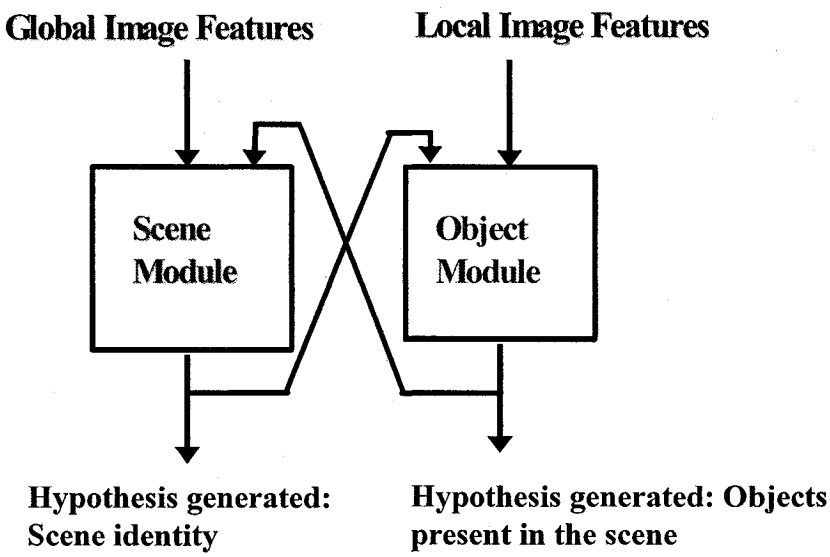

Figure 2.2 A model is presented where the two mechanisms of scene and object recognition occur in parallel, but constantly feedback information to each other so that as soon as there is any information for any possible stages of recognition (scene or object), the model takes advantage of it.

In figure (2.2) we present the general architecture of the model we propose for implementing the bi-directional relationship between the scene recognition and the object recognition process. The model consists of two modules, the scene module and the object modules, which encapsulate the process of scene recognition and object recognition. The main characteristic of this model is that the scene recognition and

object recognition mechanisms do not relate to each other in a hierarchical relationship, but rather run in parallel. The model has to be implemented in a fashion that although the two processes occur in parallel, they constantly feedback information to each other in order to enhance the performance of the two processes. In the next chapter we discuss the computational formulation for each of the two modules.

Chapter 3

Computational Models for Natural Scene and Object Classification

In the previous chapter we examined the current theories and findings in the domain of cognitive sciences about scene perception and the relationship between scene perception and object perception. We explained that, contrary to seminal approaches to vision which viewed scene perception as a result of a hierarchical visual organization, there is strong evidence that scenes can be understood very rapidly and independently of the recognition of the constituent objects. We found that there is strong psychophysical evidence that the two processes of scene perception and object perception are correlated, with the results of each process affecting and constraining the outcome of the other process. This motivates us to investigate the possibility of computational implementation of a model which incorporates this bi-directional relationship.

Our goal is not to build a high performance scene classification or object classification model per se; but to build a model which allows the two processes to interact with each other, and see if such an interaction entails any significant increase in the scene and object classification performance compared to an implementation with no feedback. As mentioned previously our proposed model has two modules for scene classification and object identification, which are able to function either independently or with feedback, based on availability of information from the other module. In this chapter we discuss the formulation of each of the modules as they function separately. In section 3.1 we first give a short background on different computational schemes for

scene representation and classification and motivate our choice for the model's formulation for scene classification. In section 3.2 we discuss briefly different computational schemes for object representation and classification and motivate our choice of formulation of the model's object module. In the following chapter we will continue the discussion with the implementation of the feedback between the two modules.

3.1 Computational Model for Scene Classification

The scene classification problem is one of the most challenging problems in computer vision. Given an arbitrary scene, we would like to describe it as belonging to a semantically meaningful category. A complete approach to scene classification should address the issues of feature selection (scene representation), feature organization, and classification. One computational approach to scene representation and classification is to view it as a process that combines low level image features (color, orientation, texture, etc.) to form progressively higher level constructs such as regions, *geons*, objects, and finally complex scenes. This approach is motivated by the hierarchical view of the visual system where at the earliest stage from retina to V1 simple features such as lines and edges are processed, in visual cortex V4 more complex features such as curve contours or 3D orientations are being processed. Cells responding to complex object patches are found in the anterior regions of IT, and finally in PPA layout of scenes are processed. This approach to human vision has been challenged by recent findings in psychophysics which suggest that scene understanding can happen independently from object recognition (see the discussion found in chapter 2). In parallel, a new computational

approach to scene representation and classification has been developed which processes low level features directly without the creation of intermediate progressive levels of abstraction. In the following section we briefly review some of the more recent work in this area in order to motivate our choice of scene representation and scene classification method.

3.1.1 Review of Computational Models for Scene Representation and Classification

A number of recent studies have presented approaches to classify scene images using global cues (e.g. power spectrum, color histogram information). Gorkani and Picard [34] discriminate between photos of city scenes and photos of landscape scenes using a multiscale steerable pyramid to find dominant orientations in 4x4 sub-blocks of the image. The image is classified as a city scene if enough sub-blocks have strong dominant vertical orientations, or alternatively medium-strong vertical orientation and also horizontal orientation. Yiu [110] uses the same dominant orientation features and also color information, to classify indoor and outdoor scenes using nearest neighbor and support vector machine classifiers. Szummer and Picard [90] combine color histogram features and DCT-based features capturing shift invariant intensity variations over a range of scales to discriminate between indoor and outdoor images. They report that k-nearest neighborhood classifiers performed as well as more sophisticated classification methods such as neural networks. They deal with the problem of combining local and global properties through a multi-stage classification method. They divide the images into sub-block and classify the sub-blocks independently and then perform another stage of classification on these results for the image as a whole. The disadvantage of this

method is that spatial location information is not used for classification of sub-blocks; therefore the individual sub-block classifiers are less accurate than the whole image classifier.

Carson *et al* [13] propose a representation of images based on blobs. Each blob is a coherent color-texture region. All the blobs in all image categories are clustered into a set of canonical blobs using Gaussian models. Each image is then assigned a score vector which measures the nearest distance of each canonical blob to the image. These score vectors are used to train a classifier.

The configurational recognition scheme proposed by Lipson [55] is a knowledge-based scene classification method. Images from 4 classes of scenery (snowy mountains, snowy mountains with lakes, fields, and waterfalls) are described by model templates which encode the common global scene configuration structure (relations between the color, spatial location, and highpass frequency content of different regions of the image). The disadvantage of this model is that the templates have to be handcrafted for each scene category layout. These templates are fine for scene categories that are geometrically well defined such as "sky over mountain over lake or snowy mountain with blue sky", but the method cannot be generalized to broader categories or scenes where parts and objects are randomly localized (such as rooms and indoors). An image is classified to the category whose model template best matches the image by deformable template matching (which requires heavy computation, despite the fact that the images are sub-sampled to low resolutions) using a nearest neighbor classification method. To avoid the drawbacks of manual templates, a learning scheme that automatically constructs scene templates from a few examples is proposed by [79].

Yu [111] uses statistical learning methods to learn templates of the image from a training set. Vector quantized color histograms are computed for sub-blocks of images. Then a one-dimensional hidden Markov model is trained along vertical or horizontal segments of specific scene layouts, such as sky-mountain-river scenes. Her results show that the one-dimensional model cannot describe the spatial relationships well, and a two-dimensional generalization such as Markov random fields would be more desirable.

One of the important applications of scene classification is in image retrieval systems. State of the art image retrieval systems such as QBIC [27], Virage [38], and VisualSEEK [85] represent images via a set of low level feature attributes such as color histograms and primitive texture measures. Retrieval is performed by matching the feature attributes of the query image with those of the database images. The user builds a query by selecting colors from a palette, a texture from a chart, and then weighting the color features versus the texture features. The image retrieval system FourEyes [63] learns the relevant feature weight combinations based on user's feedbacks on several example images. A successful categorization of images in the database greatly enhances the performance of the content-based image retrieval system by filtering out images from irrelevant classes during matching, but presently these systems are not very efficient in learning scene categories of higher levels of abstraction (for example a classification such as outdoor versus indoors) based on the low-level representations of the image content. One attempt at remedying this problem is the hierarchical clustering scheme proposed by Zhang and Zhong [112,113], which uses self-organizing maps to cluster images into groups of visually similar images based on color and texture features.

Vailaya et al [99, 100] also address the problem of high level scene classification in image retrieval systems. They use a procedure which qualitatively measures the saliency of features (color histogram, DCT coefficients, and edge direction histograms) for a hierarchical classification of database images first into city images vs. landscapes. Then the subset of landscape images is classified into sunset, forest, and mountain classes. Plots of intra-class and inter-class distance distributions are used to qualitatively determine the discrimination ability of a feature towards a specific classification problem. A Bayesian approach is used for classification, where the probabilistic models (class-conditional distributions of the various low-level features) are estimated using the Vector Quantization method during a training phase. A minimum description length type principle is used to determine the optimal codebook size representing a particular class of images from the training samples.

Huang et al [42] also propose a scheme for automatic hierarchical image classification. They use banded color correlograms as image features. They reduce the dimensionality of the feature vectors by singular value decomposition. An iterative method is then used for constructing a hierarchical classification tree, based on normalized cuts. The singular value decomposition method not only reduces the dimensionality of the data but also re-arranges the feature space to reflect the major correlation patterns in the data and ignore the less important variations.

Oliva and Torralba [68][69][95][94] have proposed a method for scene categorization based on the statistics of the natural images. Badley [2], Oliva et al [70], and Oliva and Torralba [68] have shown that the statistics of the natural images follow particular regularities and that the averaged power spectra of different categories of

scenes exhibit different orientation and spatial frequency distributions. They have used spatial frequency and orientation tuned filters to create a representation of scenes based on their characteristic power spectra.

Our design goal to avoid a hierarchical relationship between the object and the scene modules constrains us to choose a model which adopts a direct scene representation approach as opposed to a hierarchical scene representation. The model proposed by Oliva and Torralba captures the main insights which the other models in line with the direct scene representation, such as Gorkani and Picard [34], Szummer and Picard [90], and Vailaya et al [99][100] offer. In terms of scene feature selection, sampling of the low frequency content of the scene power spectra using a bank of Gabor filters is founded on the psychophysical findings which provide evidence for scene recognition based on low frequency content of images. These features capture multi-scale information from images, similar to multi-scale steerable pyramids and DCT based features, and can be computed in parallel over the whole image. In fact, Oliva has proposed that these features can serve as a computational account for "gist" features, since based on them the scenes can be rapidly and directly be identified [71]. In terms of feature organization, Oliva and Torralba use principal components analysis (PCA) for maximizing variability among features of different classes. The method proposed by Oliva and Torralba is successful in categorizing scenes at basic level classes, such as street, buildings, highways, and beach scenes, which is not achieved by the other methods. Motivated by this discussion we have based our formulation of the scene module based on the work of Oliva and Torralba; therefore, we present a detailed discussion of their model in the following section.

3.1.2 Oliva and Torralba Model for Natural Scene Representation and Classification

Oliva et al [70], and Oliva and Torralba [68] have shown that the averaged power spectra of different categories of scenes exhibit different orientation and spatial frequency distributions.

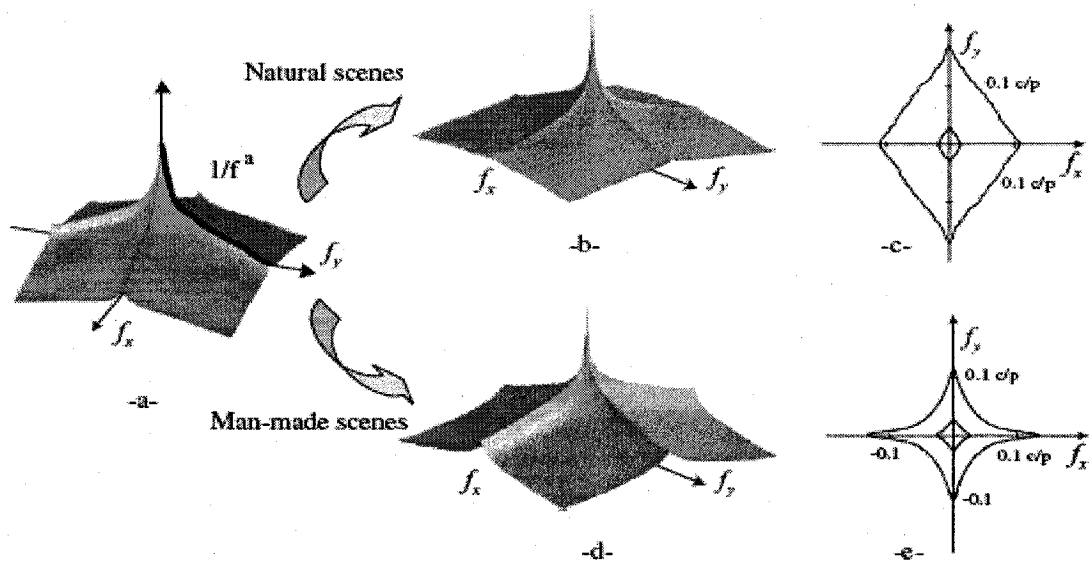

Figure 3.1. (a) Mean power spectrum averaged from 12000 images. (b) Mean power spectra computed for 6000 images of man-made scenes. (d) Mean power spectra of images from natural scenes. (c) and (e) are contour plots of respective power spectra, the contour is chosen so that the sum of the components inside the section represents 50% (and 80%) of the total energy of the spectra. Units are in cycles per pixel. (Image taken from reference [94]).

Figure 3.1, which illustrates results from Torralba and Oliva [94], emphasizes the differences in the mean power spectra computed for images of man-made and natural environments. In both sets of images the energy of the power spectra is concentrated mainly on the low spatial frequencies. What distinguishes the two sets of images is their distribution of energy in the lower frequencies. For the man-made scenes there is a very pronounced bias towards horizontal and vertical orientations in the power spectra, which

can be explained by the fact that in man-made environments the structural elements of the scene are organized mainly in horizontal or vertical layers. The power spectra of the natural scenes have a tendency to be more isotropic as compared to the man-man made scenes, but still there is a more energy concentrated on the vertical spatial frequencies, as a lot of natural scenes are organized along layers parallel to the horizon.

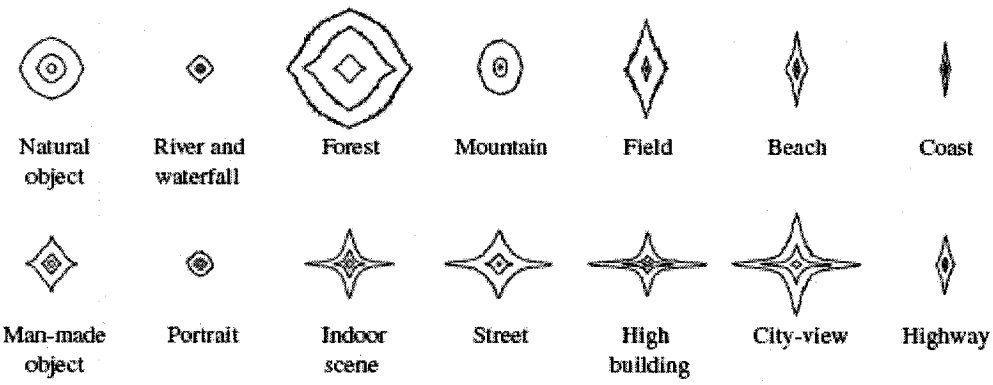

Figure 3.2. Spectral signatures of 14 different image categories is presented. Each spectral signature is obtained by averaging the power spectra of a few hundred images per category. The contour plots represent 60%, 80%, and 90% of the energy of the spectra. (Taken from reference [95])

Figure 3.2, which illustrates results from Torralba and Oliva [95], shows the spectral signatures of 14 different categories of scenes. One striking result is that basic level classes of scenes such as streets, highways, buildings, and indoor scenes have typical spectral signatures. The difference among the spectra of various man-made categories lies in the relationship between the horizontal and vertical contours at different spatial scales. On the other hand, the spectra of the natural scenes exhibit a broader range of variations. Large scale scene categories dominated by the horizon, have a high percentage of the energy concentrated on the vertical orientation, but in scenes

that the background is closer the spectral signature becomes more isotropic, and denser in the high spatial frequencies.

In general the shape of the spectral signatures is correlated with the scales (sizes) of the main components of the image. How the image is broken down into smaller surfaces, for example a lot of clutter in the image versus large areas of smooth surfaces, or finer texture versus coarser texture, influences the shape of the spectra. Each scene category follows certain coarse spatial arrangements of its constituent structural elements. These different organizational laws can provide signatures for certain scene categories. Attributes such as smoothness, roughness, texture, and orientation in certain directions of constituting elements of scenes (e.g. trees in forest scenes, buildings in street scenes) provide information which differs from one scene category to another. These attributes can be captured in second order statistics of images, as encoded in the Fourier spectra of the images. In [70] Oliva and Torralba show that it is possible to construct representations of scene context based on sampling the power spectra of images using oriented bandpass (Gabor) filters. The power spectrum of an image is computed by taking the squared magnitude of its discrete Fourier transform (DFT):

$$\Gamma(k_x, k_y) = \frac{1}{N^2}\left|I(k_x, k_y)\right|^2 \tag{3.1}$$

where

$$I(k_x, k_y) = \frac{1}{N^2}\sum_{x=0}^{N-1}\sum_{y=0}^{N-1} i(x, y)\exp(-\frac{j2\pi}{N}(x k_x + y k_y)) \tag{3.2}$$

where $f_x = k_x/N$ and $f_y = k_y/N$ are the discrete spatial frequencies. The power spectrum $\Gamma(k_x, k_y)$ encodes the energy density of different spatial frequencies over the

whole image. The power spectrum is normalized with respect to its variance for each spatial frequency as:

$$\Gamma'(k_x, k_y) = \frac{\Gamma(k_x, k_y)}{std(\Gamma(k_x, k_y))} \tag{3.3}$$

where

$$std(\Gamma(k_x, k_y)) = \sqrt{E\left[\left(\Gamma(k_x, k_y) - E[\Gamma(k_x, k_y)]\right)^2\right]} \tag{3.4}$$

This normalization compensates for the $1/f^{\alpha}$ shape of the power spectrum. PCA applied directly to the power spectra thus computed gives the main components that take into account the structural variability between different images. But these spectral representations of images are feature vectors of very high dimensions. To reduce dimensionality Oliva and Torralba propose sampling the power spectrum by a set of narrow-band Gabor filters tuned to different spatial frequencies, from low spatial frequencies to high spatial frequencies (figure 3.3).

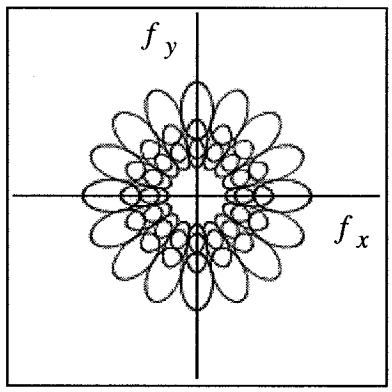

Figure 3.3. Coverage of the spatial frequency domain by a bank of 24 Gabor filters.

In spatial domain, the Gabor function is a complex exponential modulated by a Gaussian function:

$$G(x,y)=\frac{1}{2\pi\sigma_x\sigma_y}\exp\left[-\frac{1}{2}\left(\frac{x'^2}{{\sigma_x}^2}+\frac{y'^2}{{\sigma_y}^2}\right)\right]\exp[2\pi j\frac{x'}{\lambda}] \tag{3.5}$$

where $x'=x\cos(\theta)+y\sin(\theta)$ and $y'=-x\sin(\theta)+y\cos(\theta)$. The filter is tuned to the wavelength λ (or radial frequency $f_r=1/\lambda$). Filters of arbitrary orientations are obtained by rotations of the x, y coordinates, and the angle parameter θ defines the orientation of the 2-dimensional sinusoid. The parameters $\sigma_x\}$ and σ_y define the Gaussian envelope along the x and y axes. The transfer function of a Gabor filter tuned to a radial frequency f_r and with the orientation determined by the angle θ is given as:

$$G(f_x,f_y)=K\exp\left[-\frac{1}{2}\left(\frac{(f'_x-f_r)^2}{\sigma_{f_x}^2}+\frac{f'^2_y}{\sigma_{f_y}^2}\right)\right] \tag{3.6}$$

where $f'_x=f_x\cos(\theta)+f_y\sin(\theta)$ and $f'_y=-f_x\sin(\theta)+f_y\cos(\theta)$, $K=2\pi\sigma_x\sigma_y$ is a constant, and $\sigma_{f_x}=\frac{1}{2\pi\sigma_x}$ and $\sigma_{f_y}=\frac{1}{2\pi\sigma_y}$ define the shape and the frequency resolution of the Gabor filter. A self-similar set of the Gabor filters bank is obtained by the rotation and the scaling of the expression (3.6). Sampling the power spectrum with the bank of Gabor filters produces a higher resolution of frequency sampling in the low spatial frequencies and a lower resolution of frequency sampling in the higher frequencies. We choose the frequency bandwidth and orientation bandwidth of the Gabor filters in order to have a uniform covering of the spatial-frequency domain, with minimum amount of overlap between filters. The representation of scene context using Gabor filters are specifically interesting in the light of the experimental results of Hubel

and Weisel [44] which provide evidence for the presence of oriented band-pass filters at the early stages of the visual pathway.

Given an image, the feature vector obtained through sampling of its power spectrum with a bank of Gabor filters is given as:

$$\Gamma_{f_r,\theta} = \iint \Gamma(f_x, f_y) G^2_{f_r,\theta}(f_x, f_y) d f_x d f_y \tag{3.7}$$

Each $\Gamma_{f_r,\theta}$ is the output energy for a Gabor filter with the spatial frequency given by radial frequency f_r and the direction θ. This computation in the Fourier domain is equivalent to the convolution of the image with the corresponding bank of Gabor filters in the spatial domain:

$$V(x, y, f_r, \theta) = \iint I(\xi, \eta) G_{f_r,\theta}(x-\xi, y-\eta) d\xi \quad d\eta \tag{3.8}$$

or for the discrete case:

$$V(x, y, f_r, \theta) = \left| \sum_{\xi,\eta=1}^{N} I(\xi, \eta) G_{f_r,\theta}(x-\xi, y-\eta) \right| \tag{3.9}$$

where $I(\xi,\eta)$ is the input image and $V(x, y, f_r, \theta)$ is the output amplitude at the location x, y of a Gabor filter tuned to radial frequency f_r and orientation θ.

In order to reduce the dimensionality of the representation and also to capture the variability of the features Oliva and Torralba decompose the image features $V(x, y, f_r, \theta)$ into their principal components (PC). Principal Components Analysis (PCA) gives orthogonal axes (principal components) that best represent the variance of the data distribution. This method reduces dimensionality by taking into account the components that are responsible for most variability among the images in a feature

space. To this purpose covariance matrices are formed for each f_r and θ using feature vectors $V(x, y, f_r, \theta)$ obtained from all training images in the database. The decomposition of the covariance matrices produces the eigenvectors $\psi_n(x, y, f_r, \theta)$. The coefficients $a_{f_r,\theta,d}$ are produced by the projection of the image features $V(x, y, f_r, \theta)$ onto the principal components $\psi_d(x, y, f_r, \theta)$.

$$V(x, y, f_r, \theta) \cong \sum_{d=1}^{D} a_{f_r,\theta,d} \psi_d(x, y, f_r, \theta) \tag{3.10}$$

The coefficients $\{a_{f_r,\theta,n}\}$ for the radial frequencies f_r and orientations θ and the principal components $d = 1...D$ are used as an estimation of the context features of the images. The dimensionality of the context features depend on the choice of the number of filters in the Gabor set and the choice of D. We will discuss the effect of choice of D in our model further in chapter 5. The coefficients $\{a_{f_r,\theta,d}\}$ incorporate information about the spectral characteristics of the images and their spatial arrangements. The ability of this representation for scene categorization task and its ability to account for attributes meaningful to observers has been investigated and demonstrated in Oliva and Torralba [37].

3.1.3 Proposed Scene Module Formulation

We choose the feature vector $V_G = \{a_{f_r,\theta,d}\}$ as the scene representation for our model, and we call V_G the global image feature. Assuming m scene classes $S_1, S_2, \ldots, S_m$, and global context features V_G of an input image given to the scene module, the probability

of the input image belonging to each scene class s_j is computed by the following Bayesian formulation:

$$P(S_j|V_G) = \frac{P(V_G|S_j)P(S_j)}{P(V_G)} \tag{3.11}$$

$P(S_j)$ is the a priori probability of each scene category which can be determined by the statistics of the image database or be initially assumed equal for all scene categories. $P(V_G)$ is a normalization factor, computed as $P(V_G) = \sum_j P(V_G|S_j)P(S_j)$. The hypothesis formed by the scene module is based on the maximum *a posteriori* estimation of the $P(S_j|V_G)$ over different scene classes.

The likelihood probability density $P(V_G|S_j)$ can be estimated by a semi-parametric method such as finite mixtures or by non-parametric methods such as histogram estimation or kernel density estimation. We choose the semi-parametric method of finite mixtures since the histogram estimation method and kernel density estimation method both run into problems with high dimensional data sets. The problem imposed by the kernel density estimators is that we have to retain all the data set values in order to estimate the probability density function for a given data point. The problem with the histogram estimation method is that the amount of information needed for density estimation depends on the number of bins, and this number increases considerably in high-dimensional data. But in finite mixture models much of the computational burden is shifted to the training stage, and relatively less computation is required for estimating the density at a given point after training. The only values we need to retain after training are the estimated parameter values. The semi-parametric

model allows us to retain some flexibility in choosing the shape of the distribution during the estimation process compared to the parametric methods. But the choice of the number of the mixtures replaces the problems of choice of bin width or window width (smoothing parameters).

The probability density function representing the likelihood $P(V_G|S_j)$ is modeled as a mixture of Gaussians as follows:

$$P(V_G|S_j) = \sum_{k=1}^{K} b_{k,j} G\left(V_G; \mu_{k,j}, \Sigma_{k,j}\right) \tag{3.12}$$

where G is a multivariable Gaussian function of V_G, with a mean $\mu_{k,j}$, and covariance matrix $\Sigma_{k,j}$. The subscript j shows that the probability density function $P(V_G|S_j)$ is estimated over images from scene class S_j. The mixing coefficients $b_{k,j}$ are the weights of each Gaussian. The choice of the number of the Gaussians used for modeling the likelihood model probability density function is discussed further in chapter 5. The number of Gaussians K in the mixture model is a parameter of the model which can be adjusted based on the performance results. The model parameters $\mu_{k,j}, \Sigma_{k,j}$, and $b_{k,j}$ are estimated using the expectation-maximization (EM) algorithm and the hand-labeled training images belonging to each scene category S_j. The EM algorithm [60] is an iterative optimization method which maximizes the posterior probability of the model parameters given the data set and consists of a procedure in two consecutive steps, the expectation step and the maximization step. If the training set contains images I_h, for $h = 1...H$, where the feature vector V_h is the global image feature corresponding to I_h,

the E-step computes the probability of every data point V_h in the training set belonging to each cluster $\tau^t_{k,j,h}$ at the iteration t as the following:

$$\tau^t_{k,j,h} = \frac{b^t_{k,j} G\left(V_h; \mu^t_{k,j}, \Sigma^t_{k,j}\right)}{\sum_{k=1}^{K} b^t_{k,j} G(V_h; \mu^t_{k,j}, \Sigma^t_{k,j})} \tag{3.13}$$

The M-step uses the estimated $\tau^t_{k,j,h}$ from the E-step to update the model parameters $\mu^{t+1}_{k,j}$, $\Sigma^{t+!}_{k,j}$, and $b^{t+1}_{k,j}$ as follows:

$$b^{t+1}_{k,j} = \sum_{h=1}^{H} \tau^t_{k,j,h} \tag{3.14}$$

$$\mu^{t+1}_{k,j} = \frac{\sum_{h=1}^{H} V_h \tau^t_{k,j,h}}{\sum_{h=1}^{H} \tau^t_{k,j,h}} \tag{3.15}$$

$$\Sigma^{t+1}_{k,j} = \frac{\sum_{h=1}^{H} \tau^t_{k,j,h} (V_h - \mu^{t+1}_{k,j})(V_h - \mu^{t+1}_{k,j})^T}{\sum_{h=1}^{H} \tau^t_{k,j,h}} \tag{3.16}$$

The M-step maximizes the joint likelihood of the training data in order to estimate the updated model parameters.

Since the whole data set is used at each iteration, a massive database imposes a high computational load on the training stage. Also the EM algorithm requires estimation of initial values for the parameter models, which does not impose a problem for the mixing parameters, but computation of initial values for the mean and the covariance matrix impose problems for sparse data sets. The algorithm iterates until the changes in estimates in each iteration are less than a chosen tolerance level, which can be adjusted based on model performance.

3.2 Computational Model for Object Classification

Replicating the human ability to recognize different object categories is one of the most difficult challenges which face computational vision scientists in this decade. Humans are able to recognize more than 10^4 categories of objects by the time they are six years old, and keep learning more through life [8]. The literature on the topic of object presentation and object recognition is very rich, but one can generalize the various approaches to three general dichotomies. The early approach to object presentation was to consider an object as made up of a distinctive collection of features, and to attempt to achieve recognition through detection of features and their combinations. Marr [59] and Biederman [8] proposed a different view of the vision process, in which a 2-dimensional retinal image is first transformed to a 3-dimensional representation, which forms a basis for recognition. Based on this view, Biederman proposed an elaborate theory for object recognition, where objects are represented as collection of geometric icons (geons), which are 3-dimensional shapes that produce viewpoint invariant 2-dimensional projections. An alternative "appearance-based" view of object representation was proposed by Poggio and Edelman [75] and Tarr and Bulthoff [92] that suggests objects are recognized on the basis of a small number of stored 2-dimensional views. The main challenge of all three approaches is that in order to capture the great diversity of forms and appearances of objects, the models must contain hundreds, and sometimes thousands of parameters. Estimation of these parameters involves batch training with large sets of examples. Compounding this difficulty are other factors such as occlusion, clutter, lighting and shading, view points, scales, all of which make recognition harder. Recent work has highlighted the ability of humans to learn object categories from small number

of examples and in an incremental manner (as opposed to the large training sets and batch learning common in computational vision methods) and have attempted to replicate these abilities into computational vision algorithms [24][22][25].

In view of the complications of an elaborate model for object category representation, we searched for a relatively simple method which would be adequate for our experimental setup of discrimination among a few chosen set of object classes. Some recent work on object classification focuses on special interest categories: human faces [53] [82][89][84][103], pedestrians [104], hand written digits [52], and automobiles [84] [26]. Instead we need a method that would apply well to a variety of different object categories. Researchers who have addressed the problem of multi-category recognition [26][106][12] choose rich representation models with many parameters for object categories in order to be able to capture the diversity of different category appearances. They do not deal with variability in view-point and lighting and occlusion explicitly, but as additional factors for intra-class variability, therefore there is no requirement for alignment of objects, lighting normalization, or segmentation of the images as a preprocessing stage.

We define our problem as recognizing one object category out of a number of possible object categories, from image patches which have been extracted from a natural scene image. Our goal is to extract some local information about the probabilities of having different object categories in that location of image. Image patches are extracted from a tessellation of the scene image in different scales, so a patch may be dominated by one object or part of an object, or be a cluttered part of the scene with no dominant object, or belong to the background. There is generally a lot of clutter and occlusion

present in the images and few patches in a scene may contain a dominant un-occluded object. The objects appear in a variety of scales and from different view points which are only constrained by the scene context (certain view points of objects, or certain scales of objects, are very improbable in certain scene contexts).

In choosing a model for representing different object categories we rely on experimental results presented by Oliva and Torralba [95]. In order to study the effect of scale in their proposed method for scene representation, they have also experimented with close-up images (or cropped sections of images) which contain mainly one object category. Their results show that the some object categories can be characterized by their mean power spectra. For example fig 3.2 shows characteristic spectra for man made objects versus natural objects. Motivated by this result we have investigated the possibility of categorizing image patches containing our chosen set of object classes (vehicles, buildings, furniture, people, and plants) using spectrum-based features. We created a set of image patches in different scales, by cropping the scene images in our data base by hand and selecting patches which bound one whole object. We did not impose a limitation on objects view points or orientations, but these factors are highly constrained by the scene context. Our experiments indicate that we can use the features extracted by sampling the mean power spectra, as explained in detail in section 3.1.2, for a reliable classification of object-patches, within this chosen set of object categories. We would like to emphasize that we do not claim that this method can serve as a successful object category model in general. The object categories we have chosen differ in texture, dominant orientation of structural components, and smoothness of surfaces, which may count for the success of this modeling for our purposes. The utility of this model may

break however, with a different choice of object categories. The PCA stage in feature extraction maximizes the variability of the selected features among the chosen classes. We choose a probabilistic framework for classification in these experiments, and the statistical modeling of the object category features allows us to deal with the problems of variations in view point, occlusion, background clutter, and lighting implicitly as intra-category variability. We deal with the problem of scale more explicitly in the model which is discussed in detail in the following section.

3.2.1 Proposed Object Module Formulation

Given an input image to the model, the object module estimates the probability of presence of objects from different object categories in local regions of the image (image patches). The object module processes local information while the scene module processes global scene information. Local regions of an image may be extracted using different methods. We choose a sliding rectangular window for extracting patches from the image, where the center of the sliding window moves on an evenly sampled grid in order to provide a uniform covering of the image. Patches of different sizes are used for extracting regions of different scales in the image. Each scale is denoted by T_l, with $l = 30,50,70,90,110$ pixels, corresponding to patches with height of 30, 50, etc. pixels. For each extracted patch the feature vector $V_L = \{a_{f_r,\theta},_d\}$ is computed using the Oliva and Torralba method described in section 3.1.2.

The probability of a patch of scale T_l representing an object belonging to one of the n different object classes $O_1, O_2, \ldots, O_n$ is given by:

$$P_{T_l}(O_i|V_L) = \frac{P_{T_l}(V_L|O_i)\,P_{T_l}(O_i)}{P_{T_l}(V_L)} \tag{3.17}$$

At the learning stage, for each scale T_l, the probability density function representing the likelihood $P_{T_l}(V_L|O_i)$ is estimated using EM algorithm and a mixture of Gaussians model, using the feature vector V_L of all training image patches of scale T_l that represent an object of class O_i. $P_{T_l}(O_i)$ is the *a priori* probability of the object class which can be determined by enumerating the object patches of particular scale in the image database or initially be assumed equal for all object classes. The data prior model is computed as $P_{T_l}(V_L) = \sum_i P_{T_l}(V_L|O_i)P_{T_l}(O_i)$.

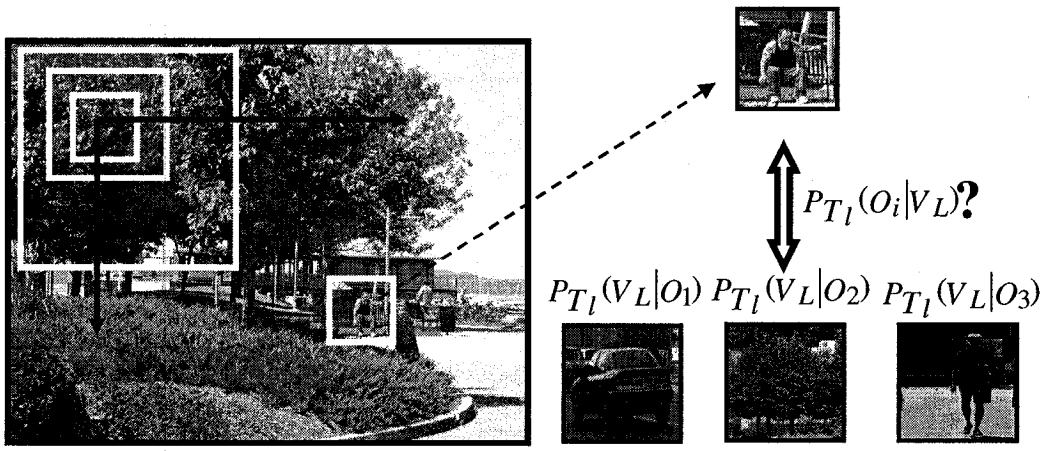

Figure 3.4. Local patches are extracted from each image using sliding window of different scales. For each local patch of scale T_l, the probability of the presence of different classes of objects are estimated using likelihood models which are built by patches of the same scale.

Our goal in building this model is to make it possible for the scene module and the object module to interact with each other. The scene module creates a hypothesis about the whole scene, while the object module creates a hypothesis linked to local regions of the scene. Therefore we have two ways of having the scene module and the

object module interact. We can either let each local region propagate the results of its local processing to the scene module independently, and then average or aggregate the results of the independent interactions of each local region with the whole scene, at the scene level. Or we can combine the results of local processing of the regions produced by the object module before any interaction with the scene module and then adjust the scene module according to the combination of the object module results. This issue is actually the crux of the model and one of the most important problems to resolve. In order to address this issue we have to decide what kind of information we want to transfer between the two modules. There are three types of information produced by the object module, the identity of the objects, the scales, and the locations of the objects. The scene module can make use of all these three types of information to adjust its estimate of the scene type, although they may not be necessary. In the present implementation of the model, we focus on the identity of the objects. We would want to pass the information extracted by the object module about the possible object categories present in the image to the scene module but not specific information about their locations or scales. In this case there is no need for local region processes interacting individually with the scene module. Therefore we integrate the local hypotheses represented by the posterior $P_{T_l}(O_i|V_L)$ from different patch locations and different scales into one hypothesis which we represent by $P(O_i|\{V_L\})$. One can think of averaging all the probability distributions $P_{T_l}(O|V_L)$ over all the patches of different scales and different locations. But a simple averaging of the probability distributions would run into

several issues. We propose a weighted average of the distributions using the following technique:

1. A weighted average is computed where the posterior probability distributions which present low certainty decisions (based on the preset decision thresholds) are assigned a lower weight compared to posterior probability distributions which present high certainty decisions. (We do not want a lot of regions with posteriors representing uncertain decisions cancel out the effect of regions with certain decisions).
2. The distributions are weighted according to their scale, with a higher weight for distributions belonging to larger scale regions and a smaller weight for distributions belonging to smaller scale regions. Certainty or uncertainty of decision for larger scale regions has more effect on the weighted average compared to certainty or uncertainty of decision for smaller scale regions. The adverse effect of this weighting is that the effects of many small instances of an object have to aggregate to have the effect of one instance of object in a larger scale, which may not be always meaningful.

In order to resolve the issue of over-counting evidence we take the following measures:

1. We start computing the local estimation with the patches of highest scale, and at each scale level we discard all the smaller scale patches falling inside a higher scale patch with a high certainty decision. We also avoid over-counting evidence for objects which are self-similar in different scales (e.g. plants).

2. We discard regions with small likelihood values, regions which the measurements do not give evidence that one of the known object categories is present, regions with unknown objects, or background clutter. In such a case the Bayesian formulation copies the prior model to the posterior. In the future design of the model this issue will cause a problem because we count evidence for wrong regions.
3. In order to avoid over-counting evidence from overlapping regions we compare the change in the posterior estimation for regions in a neighborhood and if the changes in probability values are smaller than a threshold, we discard the overlapping patch.

The global probability distribution $P(O \mid \{V_L\})$ is thus created as a weighted average over the local posterior probability distributions, with the probability $P(O_i \mid \{V_L\})$ containing information about the frequency of presence of object category O_i across all scales and across all locations in the scene.

3.3. Summary

We use the scene representation introduced by Oliva and Torralba, based on the sampling of the mean power spectrum of images with Gabor filters of different scales and orientations, for scene categorization. We also use a similar representation for extracting features from local image regions for object categorization. Figure (3.5) presents a general schema of the model discussed in this chapter. The function of the scene and the object modules are formulated using Bayesian inference processes. In the

next chapter we will propose a method for incorporating feedback between the two modules' processes.

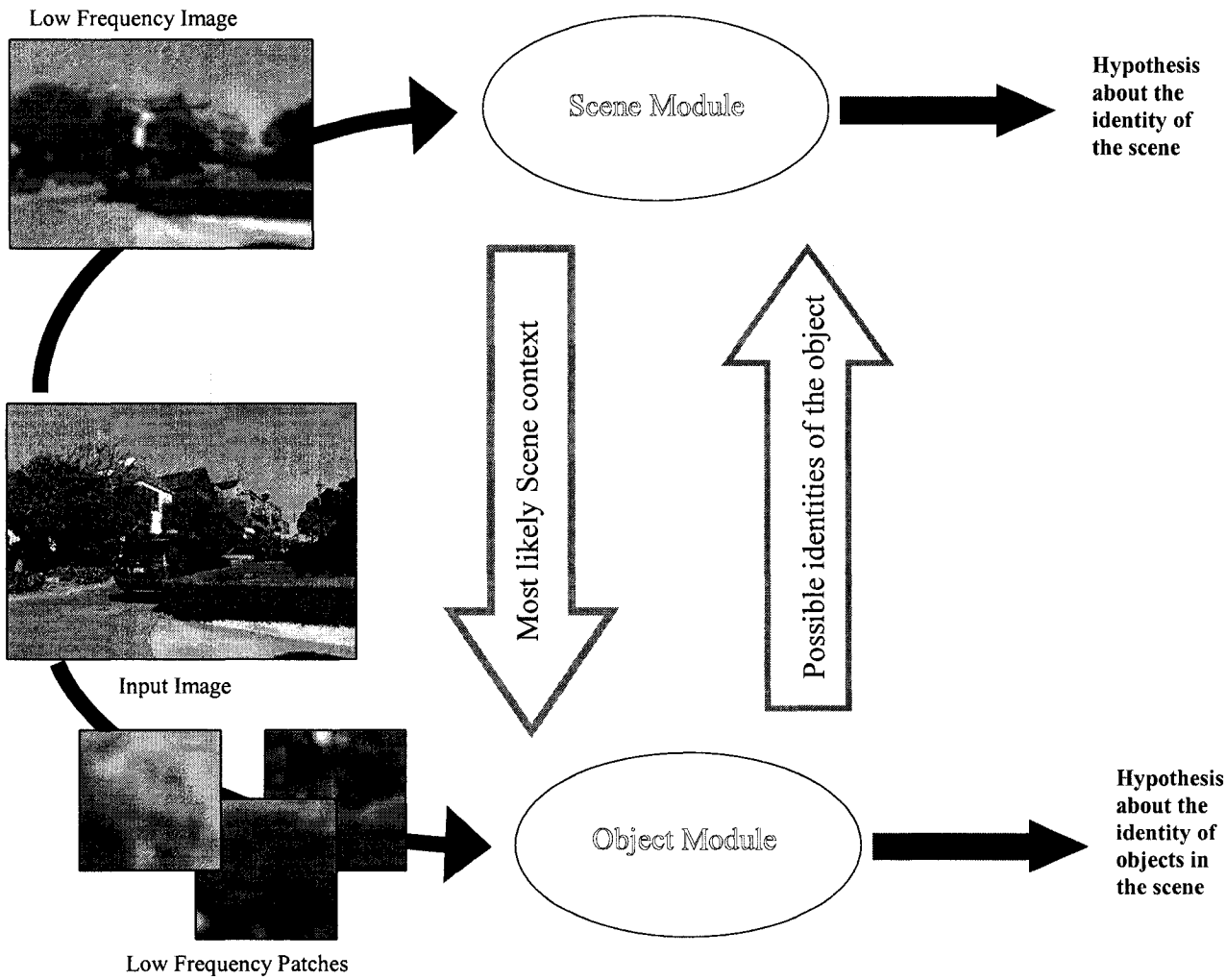

Figure 3.5. The scene module creates hypotheses about the identity of the scene based on the global image features and the object module creates hypotheses about the identity of the objects present in the scene based on local image features.

Chapter 4

Coupling of the Scene Classification Module and the Object Classification Module

In this chapter we present the mathematical methodology we have developed through which the information produced by the two sensory information processing modules, the scene classification module and the object classification module, can become available to each other and be considered as part of the information processing problem solved in each module. The methodology we present here is motivated by the field of data fusion, which is concerned with the methods of combining various information sources. In section 4.1 we motivate our proposed methodology in the framework of Bayesian data fusion. In section 4.2 we distinguish between two classes of data fusion implementations, the weak coupling and the strong coupling architectures. In section 4.3 we propose two approaches for implementing the interactions between the scene classification and the object classification modules based on a Bayesian strongly coupled data fusion architecture.

4.1 Data Fusion

Data fusion deals with the question of fusing separate sensory information processing components in order to achieve a globally "better" solution to the sensory information processing problem at hand, as compared to the solutions given by each of the individual components. The global system improves the performance of the task at hand by producing a solution which is more accurate than the components' solutions or by

producing a unique solution when the individual components are not able to produce any unique solutions individually. The latter aspect of data fusion algorithms have been described by Clark and Yuille [14] in terms of regularization of ill-posed problems.

Clark and Yuille view the problem of image understanding or "perception" as a process of inverting the world-to-sensed-data mapping. Since the sensing process produces a non-invertible projection of the world (i.e. the mapping from the world structures to the image space is many to one), in order to invert this mapping one must constrain the set of possible world interpretations of the sensed-data to a degree where the mapping from the reduced space to the image space becomes invertible. In other words sensing involves a non-invertible projection of the world which makes perception (sensory information processing task) an ill-posed problem; therefore in order to regularize such an ill-posed problem, and for a sensory processing module to operate adequately (being able to produce unique solutions to the task at hand), constraints of one form or another must be imposed on the solution process. These constraints can be "physical constraints", "natural constrains", or "artificial constraints". Physical constraints are based on rules of physics and mathematics and rule out solutions which are physically impossible. Natural constraints are derived from observations from the environment and represent conditions which are normally and naturally true in that domain (examples of natural constraints used in computer vision problems are surface smoothness, object rigidity, Lambertian surface reflectance). Artificial constraints embed expectations about the state of the world based on high level knowledge of the domain, formed from previous estimates of the state of the world. Physical constraints are universally valid, but natural and artificial constraints are not. Furthermore, it is

sometimes not possible to find natural and artificial constraints which are always valid, even within the specific domain of the problem. In cases where the constraints imposed on the information processing module are not valid, or are insufficient, the module may produce a wrong solution or be unable to find a unique solution to the problem.

One way to address this problem is to use the information produced by another information processing unit to correct the answer of the module. In this way combining or fusing results obtained from several modules enhances the performance of the system as a whole. So fusion of information produced by different components of a sensory system can reduce the dependency of the solution of the system on invalid or insufficient constraints imposed on the solution process within each module. In this sense, data fusion can be seen as a method of regularizing the ill-posed problem of perception (or any other ill-posed problem for that matter) not only by means of a priori constraints (constraints not based on current sensory data), but also by constraining it by information which comes from a "partial" solution to the problem and is obtained from independent sensory information processing modules (based on the current sensory data).

In the Bayesian approach to solving sensory information processing problems, different possible solutions are assigned a probability based on the models of the sensing process (likelihood model) and models representing general assumptions made about the world (a priori models). One of the advantages of the Bayesian formulation is that it provides a suitable form for embedding constraints into the solution process. Some of the constraints required for the solution process are incorporated and embedded into the likelihood models when these models are being estimated using sensory measurements. One can also choose the a priori models to enforce the necessary constraints on the

solution process. Usually the a priori models incorporate constraints which are based on general assumptions made about the domain (before any measurements are made), but the priors can also be influenced by the previous measurements (as in the case of active vision). The likelihood models typically involve physical, and to a lesser extent natural constraints, while the prior models typically involve natural and artificial constraints [14].

In the Bayesian approach that we have chosen for determining the semantic context of a scene and for determining the presence or absence of certain object classes in the scene, scene and object classification are formulated as estimating the following *a posteriori* conditional probabilities:

$$P(S_j|V_G) = \frac{P(V_G|S_j)P(S_j)}{P(V_G)} \tag{4.1}$$

$$P_{T_l}(O_i|V_L) = \frac{P_{T_l}(V_L|O_i)\,P_{T_l}(O_i)}{P_{T_l}(V_L)} \tag{4.2}$$

The conditional probabilities $P(V_G|S_j)$ and $P_{T_l}(V_L|O_i)$ represent probabilities of occurrence for the input measurement data on the event that it is known that the measurements belong to scene class S_j or object class O_i respectively. The likelihood $P(V_G|S_j)$ represents the mapping from the class of scenes S_j to the space of image features V_G and similarly $P_{T_l}(V_L|O_i)$ represents the mapping from the class of objects O_i to the image features V_L. Universally valid physical constraints and certain domain specific natural constraints (e.g. certain structural rules normally valid for most

contextually meaningful scenes such as sky above earth, horizontal layers along dominant horizon) are embedded into these conditional probabilities during the learning stage through the training patterns.

On the other hand the *a priori* models $P(S_j)$ and $P_{T_l}(O_i)$ constrain the solution with general assumptions made about the scene classes S_j and object classes O_i. In the previous chapter we mentioned that the *a priori* models $P(S_j)$ and $P_{T_l}(O_i)$ are computed using the statistics of the database to represent how likely a given scene or object is, before any measurements are made. But it is not always possible to estimate an informative *a priori* model for the problem this way (for example a training database where all the scene and object classes have equal probability of presence will produce a uniform *a priori* model for the problem). In cases where the a priori models are uninformative, the solutions to equations (4.1) and (4.2) are reduced to a maximum likelihood estimation of the two equations.

In cases where the constraints embedded in the likelihood models or a priori models are not valid or are insufficient, the scene classification module or the object classification module may produce a wrong solution or be unable to find a unique solution to the problem. In such a case one can supplement the a priori constraints (constraints not based directly on the measurements from the sensory data) with extra constraining information obtained from the other information processing module. For example in the problem of scene classification of a given image, if the object module has independently determined with a high reliability that certain objects exist in the image, but the scene module is not able to classify the image reliably, then the knowledge about

the objects present in the scene can be used for further constraining the scene module solution process. For example knowledge of the relationships between scene categories S_j and object categories O_i, in the form of conditionals $O_i|S_j$ and $S_j|O_i$ can be used to develop a more informative a priori model for the scene module. It is this Bayesian view of data fusion which forms the theoretical basis for our proposed method of implementing informative interactions between the scene and the object modules.

Based on the Bayesian interpretation of data fusion, information from independent information processing modules can be used to impose constraints on either the likelihood models or the prior models of a Bayesian estimation process. The alteration of either the likelihood models or the prior models, in order to accommodate information coming from an independent source, is the basis for distinguishing between two methods of coupling the object and the scene modules, as proposed later in this chapter. Before describing our proposed method for "constraint embedding" or "data fusion" between the scene classification and the object classification modules, it is necessary to distinguish between weakly versus strongly coupled data fusion architectures.

4.2 Weakly and Strongly Coupled Architectures for Data Fusion

The research performed on data fusion systems has been carried out largely within the engineering community [15][102][105] and overlaps substantially with the work on multiple classifier systems in the area of pattern recognition. In this body of work different architectures (for example serial, parallel, hierarchical) have been considered for implementing data fusion, but often the adopted architectures are developed in an *ad*

hoc manner dictated by the practical application at hand. Two major classes of fusional architectures have been distinguished by Clark and Yuille [14]; that of weakly coupled and strongly coupled data fusion. These two classes differ in the way the constraints (information from other sensory modules) are embedded into the solution processes.

In the weakly coupled data fusion model the outputs of several sensory information processing modules are combined in a fusion module to produce a global system solution for the desired task. The general architecture for a weakly coupled data fusion system is presented in figure (4.1). As illustrated in figure (4.1) the modules M_1, M_2,..., M_L process the feature space, and the information processing function performed by the modules are independent from each other. In the weakly coupled architectures the supplementary constraints required for the solution process are imposed through the fusion module. From a Bayesian point of view the likelihood models and the *a priori* models of different modules do not depend on the output of any other module, and the solution process of the component modules are not altered to accommodate extra constraints from other sources.

The information fusion models studied in the area of pattern recognition under the title of "classifier fusion models" are weakly coupled architectures. Examples of these models are the classifier combiners based on Bayesian decision rules proposed by Kittler *et al* [49], classifier combiners based on class predictions proposed by Lam and Suen [51] and Huang and Suen [43], combiners based on stack generalization, mixture of expert models proposed by Jacobs *et al* [47] and Jordan and Jacobs [48], bagging [10], boosting methods proposed by Freund and Schapire [28] [29], and dynamic classifier selection method proposed by Woods *et al* [109]. These models deal with the

problem of combining predictions from multiple classifiers to yield a single class prediction, and represent special cases of the weakly coupled architecture presented here.

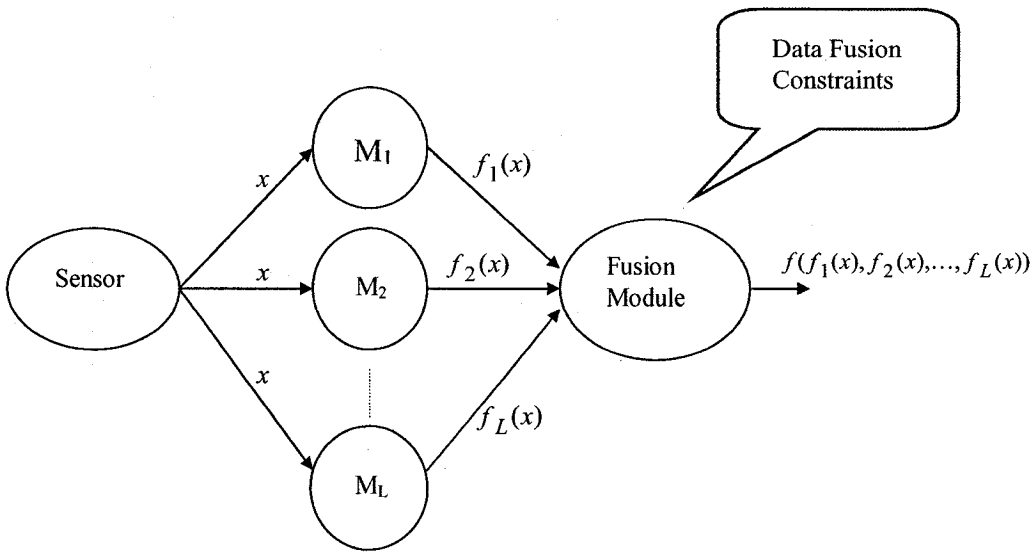

Figure 4.1 The general architecture of a weakly coupled data fusion model is represented with L sensory information processing modules. The modules are defined on the feature space x, each performing independent sensory information processing tasks represented by functions $f_1(x)$, $f_2(x)$, ... The fusion module combines the results produced by the individual modules to produce a global function represented by $f(f_1(x), f_2(x), \ldots, f_L(x))$.

The strongly coupled data fusion architecture differs from the weakly coupled architecture in the sense that the functions of the modules are affected by the outputs of other modules, so that the functions and the outputs of individual modules are not independent from each other [14]. In figure (4.2) the general form of a strongly coupled architecture is presented. Two variations of the strongly coupled architecture are shown in figure (4.2). The feed-forward architecture (4.2.a) is the case where the output of an otherwise independently functioning module affects the function of another component module. In a recurrent architecture (4.2.b) the functionality of both modules are altered based on the mutual outputs, so none of the modules function independently. As illustrated in figure (4.2.b) the function of module M_1 is affected by the function of

module M_2, which has in turn been affected by M_1 (and vice versa). The term recurrent points to this feedback loop created between the two modules. In the Bayesian view point of strongly coupled architectures, either the likelihood or the *a priori* models of the component modules (or both) are altered based on the output from the other module in order to incorporate sufficient constraints for the solution process.

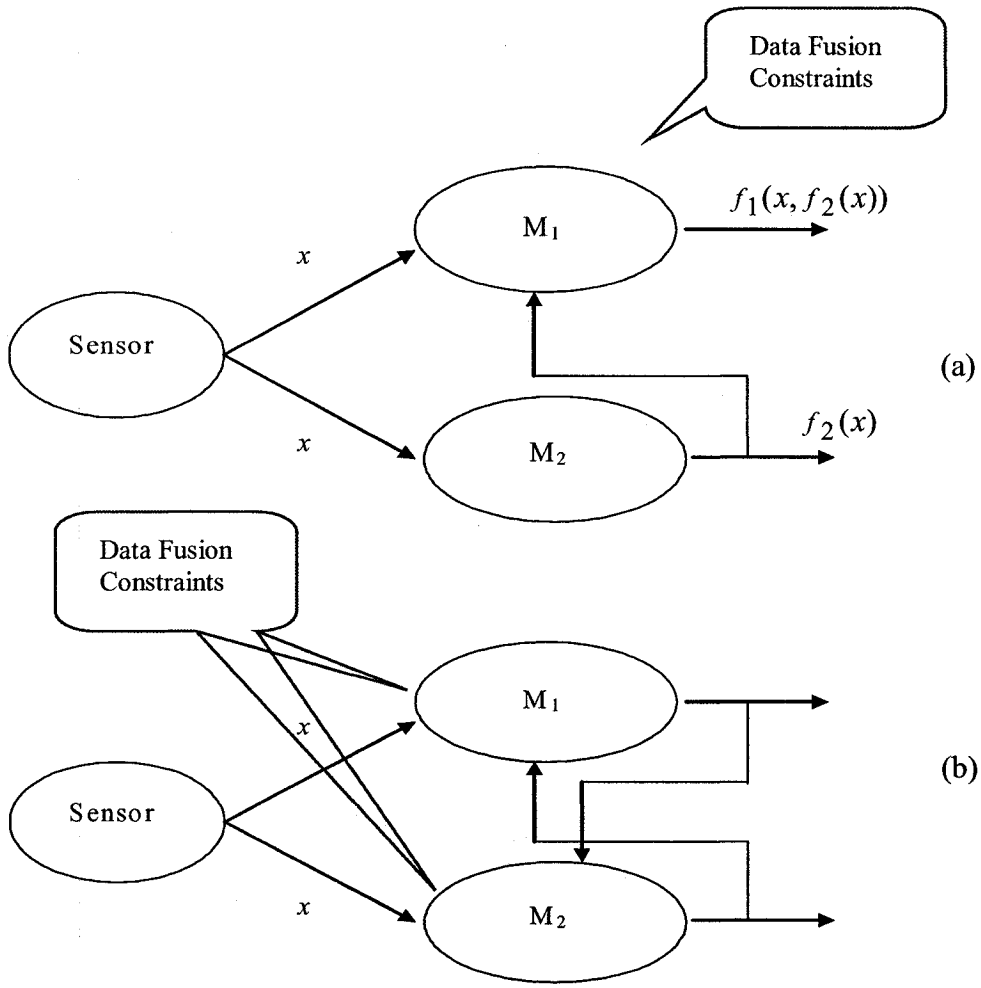

Figure 4.2 The general architecture of strongly coupled data fusion models are represented, (a) represents a feed forward architecture where the likelihood or the prior model of one sensory information processing module is constrained based on the output of another independent functioning module, (b) represents a recurrent architecture where the likelihood or the prior models of both sensory information processing modules are constrained based on output from the other module.

An example of strongly coupled data fusion architecture in literature is the Kalman filtering method [32]. The Kalman filter estimates a variable which represents a sequence of changing states of the world, and involves recursively updating the *a priori* model of the state variable based on previous and current estimates of the state variables and updating the estimate of the state variable based on the current *a priori* model, the system model, and the measured data. The Kalman filter is a strongly coupled model in the sense that the *a priori* model is adapted in a data dependant way.

A general characterization of the function of a module in the Bayesian implementation of a strongly coupled data fusion model is given by Clark and Yuille [14] as follows:

$$p(v \mid x) = \frac{p(x \mid v\ ; z_1, z_{2,\ldots,} z_n) p(v\ ; z_1, z_{2,\ldots,} z_n)}{p(x\ ; z_1, z_{2,\ldots,} z_n)} \tag{4.3}$$

where the function of the module is to determine a parameter v by optimizing the conditional density $p(v \mid x)$, where x is the measured data input to the Bayesian parameter estimation module, and $z_1, z_{2,\ldots,} z_n$ are the data from the other sensory information producing modules. The likelihood model, the *a priori* model, and the data model all can be seen as functions of $z_1, z_{2,\ldots,} z_n$. The output z_k of a given module which influences the estimation process of parameter v, can itself in turn be influenced by the function of this module. This formulation includes the adaptation of both the *a priori* model and the likelihood models.

4.3 Strongly Coupled Data Fusion between Scene and Object Modules

In the previous section we mentioned that in cases where the *a priori* constraints built into the scene classification module and the object classification module fail to provide a unique solution for one of the modules, the knowledge inferred from the other module can be combined as part of the module estimation process in order to further constrain the solution. We are motivated by the strongly coupled data fusion architecture illustrated in figure (4.2) and the general formulation in equation (4.3) to modify our Bayesian solutions for the scene and the object classification modules in order to incorporate possibility of information sharing between the two modules. As discussed in the previous section the strongly coupled data fusion architecture allows two approaches to implementing the interactions between the two modules. In the first approach, the two modules interact through the prior terms of the Bayesian formulation. In this approach the *a priori* models of the scene and object modules are modified in order to allow constraints built into the solution process based on information coming from the other module. This variation of the model is strongly coupled in terms of priors. In the second approach, the likelihood models of each module are reformulated in order to allow data fusion with the other module. This variation of the model is strongly coupled in terms of likelihoods. For both variations of the model we present are examples of recurrent strongly coupled architecture.

4.3.1 Adaptive Priors Model

The key idea in this approach is that the any previously acquired knowledge about the scene identity affects the *a priori* models used for the object identification process, and likewise any previously acquired knowledge about the objects present in the scene

affects the *a priori* models used for the scene identification process. In our proposed model we revise the Bayesian estimation equations (4.1) and (4.2) in order to embed a feedback interaction between the two modules. In order to make feedback connections possible between the two modules, the *a priori* terms in equations (4.1) and (4.2) are expanded as following:

$$P(S_j) = \sum_i P(S_j, O_i) = \sum_i P(S_j | O_i) P(O_i) \tag{4.4}$$

$$P_{T_l}(O_i) = \sum_j P_{T_l}(O_i, S_j) = \sum_j P_{T_l}(O_i | S_j) P(S_j) \tag{4.5}$$

Expanding the *a priori* terms as in equations (4.4) and (4.5) exploits the dependency of the scene level priors and the object level priors to provide a way to feed back the output of the one module to the other module. Equation (4.4) shows how the *a priori* term $P(S_j)$ can be modified based on knowledge of the probability of the presence of different object classes in the scene. If there is no previous knowledge of the different object classes present in the scene, the *a priori* term $P(S_j)$ of equation (4.1) can be determined based on the statistics of the database or be assumed equal for all scene classes (as done for the first iteration of the model), but once the object module has made inferences about the probability of the presence of different object classes in the scene, this knowledge can be used to provide a new estimation of the *a priori* term $P(S_j)$ based on equation (4.4), where the term $P(O_i)$ in equation (4.4) is updated based on the new *a posteriori* distribution $P(O_i | \{V_L\})$ produced by the object module. Similarly equation (4.5) shows how the knowledge acquired by the scene module about the probability of the image belonging to different scene classes can affect the *a priori* probability of the presence of different objects in the scene. The new estimation of the

prior term $P_{T_l}(O_i)$ is estimated by updating the terms $P(S_j)$ in equation (4.5) based on the new *a posteriori* $P(S_j|V_G)$ produced by the scene module.

The data dependent alteration of the *a priori* terms distinguishes this model as a strongly coupled architecture. The mutual feedback between the two modules characterizes the model as a recurrent feedback system. At the first iteration of the model the scene and object modules perform their Bayesian estimation process independently and without any feedback from the other module; therefore, the result of first iteration shows how well the modules can function on their own and if there is any need for information sharing between the modules. If there is no reliable estimate made by either of the two modules then the feedback connections are activated, and new estimates of scene and object classes are made through the recurrent feedback between the two modules.

The feedback is designed to use the new information inferred by the system at each iteration, to determine a more accurate *a priori* model for the specific scene class. The *a priori* models representing different scene classes in the Bayesian equation (4.1) are not the same if there is any previously acquired knowledge of the type of objects found in the scene. Also the *a priori* models representing different object classes in the Bayesian equation (4.2) are not the same if there is any previously acquired knowledge of the image scene type. Expanding the *a priori* models $P(S_j)$ and $P_{T_l}(O_i)$ as in equations (4.4) and (4.5) allows the readjustment of the weights of the conditional probabilities $P(S_j|O_i)$ and $P_{T_l}(O_i|S_j)$ in order to incorporate the effect of the knowledge acquired by the other module.

It is important to show that the modification of the priors given in equations (4.4) and (4.5) produces valid *a priori* probability distributions. In order to have valid *a priori* and *a posteriori* probability distributions in equations (4.1) and (4.2), we have to show that $\sum_j P(S_j)=1$ and $\sum_i P_{T_l}(O_i)=1$, when $P(S_j)$ and $P_{T_l}(O_i)$ are estimated using equations (4.4) and (4.5). Since

$$\sum_j P(S_j)=\sum_j\sum_i P(S_j\,|\,O_i)P(O_i)=\sum_i P(O_i)\sum_j P(S_j\,|\,O_i) \tag{4.6}$$

and also given that $P(O_i)$ are replaced by the *a posteriori* distributions $P(O_i\,|\,\{V_L\})$, which are computed so that $\sum_i P(O_i\,|\,\{V_L\})=1$, in order to show that $\sum_j P(S_j)=1$, we must show that for $\forall O_i$, $\sum_j P(S_j\,|\,O_i)=1$. And similarly, since

$$\sum_i P_{T_l}(O_i)=\sum_i\sum_j P_{T_l}(O_i|\,S_j)P(S_j)=\sum_j P(S_j)\sum_i P_{T_l}(O_i|\,S_j) \tag{4.7}$$

and given that $P(S_j)$ are replaced by the *a posteriori* distribution $P(S_j|V_G)$ which are computed so that $\sum_j P(S_j|V_G)=1$, in order to show that $\sum_i P_{T_l}(O_i)=1$, we must show that for $\forall S_j$, $\sum_i P(O_i\,|\,S_j)=1$. Computing the conditional probabilities $P(S_j|O_i)$ and $P_{T_l}(O_i|S_j)$ simply based on enumeration of database items ensures the conditions $\sum_j P(S_j\,|\,O_i)=1$ and $\sum_j P(S_j|V_G)=1$. $P(S_j|O_i)$ is computed as the total number of images containing object category O_i, which belong to the scene category S_j divided by the total number of images in the database which contain object class O_i (being any scene type). And similarly $P_{T_l}(O_i|S_j)$ is computed as the total number of image patches

of given scale T_l belonging to images from scene category S_j which contain an object from class O_i divided by the total number of image patches of scale T_l (containing any of the object categories) which belong to an image from scene category S_j. One can view the approach explained in this section as having a set of different *a priori* models for solving a given Bayesian estimation problem, where each of these *a priori* models are appropriate to be used in a given domain. The information from the other sensory module is used to determine which domain is being operated and which one of the *a priori* models are to be selected and used. The updating of the *a priori* model based on the knowledge acquired from the other sensory information processing module may have the effect of changing a uniform or uninformative prior model to an informative prior model.

4.3.2 Adaptive Likelihoods Model

In the second approach to strong coupling of the scene and object classification modules, the likelihood models of the Bayesian equations (4.1) and (4.2) are modified in order to incorporate constraints based on the inferences made by the other module. For this purpose the likelihood term of the scene classification module is modified as $P(V_G, \hat{P}(O_1), \hat{P}(O_2), \ldots, \hat{P}(O_N) \mid S_j)$, which represents a joint distribution of the global image features V_G and $\hat{P}(O_i)$, which is an estimate of the probabilities of object classes O_i being present in the scene ($i = 1 \ldots N$ where N is the number of object classes). $\hat{P}(O_i) = P(O = O_i \mid V_L)$ and $P(O = O_i \mid V_L)$ are estimated using the posterior probabilities of the object classes as estimated by the object module. The likelihood term of the object classification module is also modified as

$P_{T_l}(V_L, \hat{P}(S_1), \hat{P}(S_2), \ldots, \hat{P}(S_M) \mid O_i)$ which represents a joint distribution of the local image patch features V_L and $\hat{P}(S_j)$, which is an estimate of the probability of different scene classes S_j ($j = 1 \ldots M$ where M is the number of scene classes). $\hat{P}(S_j) = P(S = S_j \mid V_G)$ and $P(S = S_j \mid V_G)$ are estimated using the posterior probabilities of the scene classes as estimated by the scene module. The adaptive likelihood solution for scene and object classification is given as the following:

$$P(S_j \mid V_G, \hat{P}(O_1), \ldots, \hat{P}(O_N)) = \frac{P(V_G, \hat{P}(O_1), \ldots, \hat{P}(O_N) \mid S_j) P(S_j)}{P(V_G, \hat{P}(O_1), \ldots, \hat{P}(O_N))} \tag{4.8}$$

$$P_{T_l}(O_i \mid V_L, \hat{P}(S_1), \ldots, \hat{P}(S_M)) = \frac{P_{T_l}(V_L, \hat{P}(S_1), \ldots, \hat{P}(S_M) \mid O_i) P_{T_l}(O_i)}{P_{T_l}(V_L, \hat{P}(S_1), \ldots, \hat{P}(S_M))} \tag{4.9}$$

The model thus defined is strongly coupled in terms of likelihoods. Similar to the adaptive priors model, the modules initially implement the independent solutions given by equations (4.1) and (4.2). In case information fusion is necessary for a reliable scene or object classification, the initial values of the parameters $\hat{P}(O_i)$ and $\hat{P}(S_j)$ are determined using the most current *a posteriori* estimates of $P(O \mid \{V_L\})$ and $P(S \mid V_G)$ (*a posteriori* distributions estimated by the original equations (4.1) and (4.2)) and are then used for implementing the coupled solutions given by equations (4.8) and (4.9). Thus at each iteration the likelihood terms of each module are re-evaluated based on the inferences made by the other module, while the prior terms remain unchanged. A learning stage is required in order to estimate distributions $P(V_G, \hat{P}(O_1), \hat{P}(O_2), \ldots, \hat{P}(O_N) \mid S_j)$ and $P_{T_l}(V_L, \hat{P}(S_1), \hat{P}(S_2), \ldots, \hat{P}(S_M) \mid O_i)$, using a

training set of images for which $\hat{P}(O_i)$ and $\hat{P}(S_j)$ have been determined using equations (4.1) and (4.2). The estimation of the probability distribution $P(V_G|S_j)$ involves learning the characteristics of the feature clusters which represent scene classes S_j. For the probability distribution $P(V_G, \hat{P}(O_1), \hat{P}(O_2), \ldots, \hat{P}(O_N)|S_j)$, the clusters formed in the joint space of V_G and $\hat{P}(O_i)$, not only depict the variability of the features V_G for different scene classes S_j, but also depict the relationship between different object classes O_i and the scene classes S_j. The clusters representing features from images belonging to different scene class S_j have peaks close to those values of parameters $\hat{P}(O_i)$ which represent object classes O_i that are often found in relationship with scene class S_j. Similarly for the probability distributions $P_{T_l}(V_L, \hat{P}(S_1), \hat{P}(S_2), \ldots, \hat{P}(S_M)|O_i)$, the clusters formed in the joint space of V_L and $\hat{P}(S_j)$ not only depict the variability of the features V_L of the image patches of scale T_l which contain an object from class O_i, but also depict the relationship between the different scene classes S_j and the object classes O_i. The feature clusters representing patches containing O_i have peaks (are most dense) close to those values of parameters $\hat{P}(S_j)$ which represent scene classes S_j that most often contain objects O_i.

Chapter 5

Experimental Results for the Strongly Coupled Scene and Object Classification Models

In this chapter we present the experimental results from implementing the strongly coupled scene and object classification models presented in sections 4.3 and 4.4. We demonstrate selected examples where the scene module or the object module cannot perform the scene or the object classification task reliably when they function independently, but where the strong coupling of the two modules improves the initial classification results. We demonstrate how the initial inferences made about the scene and the object classes change as the scene module interacts with the object module, and as the prior model estimations or the likelihood model estimations vary in time. We also measure the performance of the strongly coupled models as classification tools using receiver operating characteristic (ROC) curves.

In section 5.1 we give a description of the database we created for the purpose of the experiments. In section 5.2 we discuss the choice of some important model parameters such as the orientations and scales of the Gabor filters and the number of Gaussian mixtures used for modeling the likelihood densities based on their effect on the classification performance. In section 5.3 we demonstrate the effect of the strong coupling of the two modules on the scene and object classification performance. In this section we also present the statistical evaluation of the model performance and address the issues of statistical meaningfulness of the presented results. The statistical evaluation

of the adaptive priors and the adaptive likelihood models provide a basis for comparing these two models.

5.1 Experimental Image Database

A database of 1000 natural images from different scene categories was created for the purpose of these experiments. Each image is 256x256 pixels in size. These images include pictures taken by a digital camera and images downloaded from the web. The images have been gathered according to the following scene categories: street scenes, park scenes, indoor scenes, downtown scenes, and residential (suburban) scenes. The object classes identified in the images are vehicles, trees, people, buildings, and furniture. Sample images of different scene categories are presented in figure (5.1) and samples of the different object categories are given in figure (5.2).

The images in this database have been gathered under varied times of the year and different times of the day, and therefore lighting conditions vary among different images in each scene category. Also there has not been any artificial control of the scales in which the objects appear in the scenes. Our goal has been to gather a set of images that captures the natural frequency of the appearance of different object types in their different scales, as experienced by the human eye in scenes encountered everyday.

Natural images depicting scenes of the same basic-level categories (such as forest, mountain, beach, street, buildings, indoors) share common features. According to the discussion in chapter 2 the study of the power spectrum of the natural images shows that images belonging to the same basic-level scene categories share common spectral features, and these features can be used for classifying scenes. What gives rise to a particular spectral shape for a certain scene category is the similarity in the distribution

of structural patterns (textures) in scenes of the same category. But the distribution of the structural patterns and the spectral features of the scene vary based on both the viewpoint of the observer and also the scale of the images. By scene scale we mean the mean depth range, i.e. the mean distance between the observers and the elements in the scene. This issue is important for us, since it sets the constraints for the scene scales and point of views we gather for the database. It is important to consider, for the purpose of gathering images for the database, how the statistics of the spectral features of the scene images vary as a function of point of view and mean depth range.

One can intuitively see that the ecological parameters (i.e. parameters that depend on the interactions between the world and the observer of the world) affecting the shape of the image power spectra are also strongly constrained by the way scene images are defined. Although we treat scenes and objects almost in a parallel fashion in our model, there is an inherent difference between scenes and objects. An object is a concept that exists independently of the observers' ecological factors, while a scene is a concept, based on deductions made by the observer, and strongly correlated with the observers' ecological factors. An object remains the same object, no matter from which point of view or depth of range it is viewed, while the semantic meaning of an image viewed by an observer changes when point of view or depth of range changes (the view of a street by a pedestrian walking in a street and by an airplane passenger flying over the street do not belong to the same scene category).

With our chosen observer being a human standing up (straight), the viewpoints for our chosen scene categories (indoors, streets, parks, etc.) are strongly constrained, with the main components composing the scene also being strongly constrained in orientation (buildings, cars, trees, furniture, most people) with pronounced horizontal

and vertical alignments for most objects. Torralba and Oliva [94] made a study of the variations of the spectral features of scenes based on changes in the scene scale. Their results show that significant differences exist between spectral features of images when the mean depth range changes more than a factor of 10. For the images we have gathered by digital camera, we controlled the scene scale by maintaining a fixed range of mean depth for images of the same scene category. Specifically the mean distance of the observer with the main components of the scene do not vary by more than 10 meters from one image to another (no control is used for indoor scenes). The mean depth of the images collected from the web was controlled by comparing the average scales of the main components of the scenes, and making them similar to values computed on the digital camera images.

Ecological constraints, which define a scene category, also constrained the objects found in the scene. Our database of object patches does not contain an infinite number of point of views of objects. Also, the scales of the main objects found in the scenes are correlated with the scene category. So our database of object patches is constrained both in point of view and scale. Therefore we do not require an object classification system (or set of object features) which is spatially invariant or scale invariant.

Figure 5.1 Sample images of the five scene categories are presented. The scene categories presented in each column, from left to right, are street, park, indoors, downtown, and residential scenes.

Figure 5.2 Sample images of the five object categories are presented. The object categories presented from top to bottom are people, buildings, cars, furniture, trees.

5.2 Choice of Model Parameters

The global and local image feature vectors V_G and V_L are computed by convolving the images with Gabor filters tuned to radial frequencies $f_r = (\frac{1}{4}, \frac{1}{8}, \frac{1}{16}, \frac{1}{32})$ and orientations $\theta = (\frac{\pi}{6}, \frac{\pi}{3}, \frac{\pi}{2}, \frac{2\pi}{3}, \frac{5\pi}{6}, \pi)$. This image representation encodes spatially localized structural information. In order to reduce the dimensionality of the representation, and also to capture the variability of the features, the responses of the images to different Gabor filters are decomposed to their principal components. The global/local features of each image/image-patch are produced by projecting the filtered images onto the corresponding principal components. In these experiments four eigenvectors have been chosen for feature extraction. This choice is based on a study of the classification performance of the uncoupled scene model (figure (5.3)). In these experiments the size of the training set extracted from 800 training images using 24 Gabor filters and four eigenvectors is 2.38 Gigabytes.

One other important parameter of the model is the number of Gaussians used in the mixture model used for the likelihood probability distributions in the Bayesian formulation of the scene and object modules. We have chosen a mixture of 2 Gaussians for modeling the likelihood distributions based on experimental results from the model. ROC curves for scene classification results, for model implementations with one Gaussian and mixtures of 2 and 3 Gaussians, are shown in figure (5.4). All curves in this figure show the classification performance for the uncoupled scene model for 200 test images. Performance of the model with mixture of 3 Gaussians shows no significant improvement over the performance of model with mixture of 2 Gaussians.

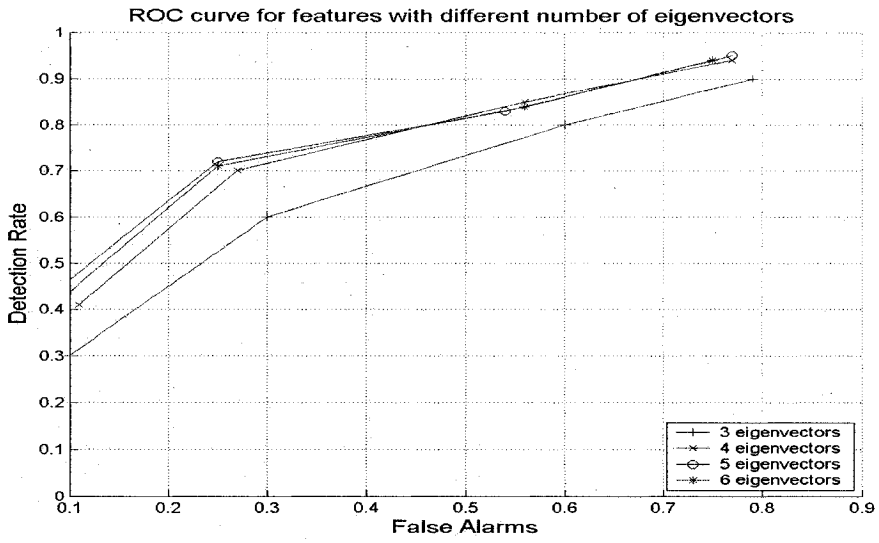

Figure 5.3. The classification performance for the uncoupled scene model for 200 test images is presented. Each curve shows performance for a different choice of the number of eigenvectors used for the feature extraction process. Performance of the model using 5 or 6 eigenvectors shows no significant improvement over the performance of model using 4 eigenvectors.

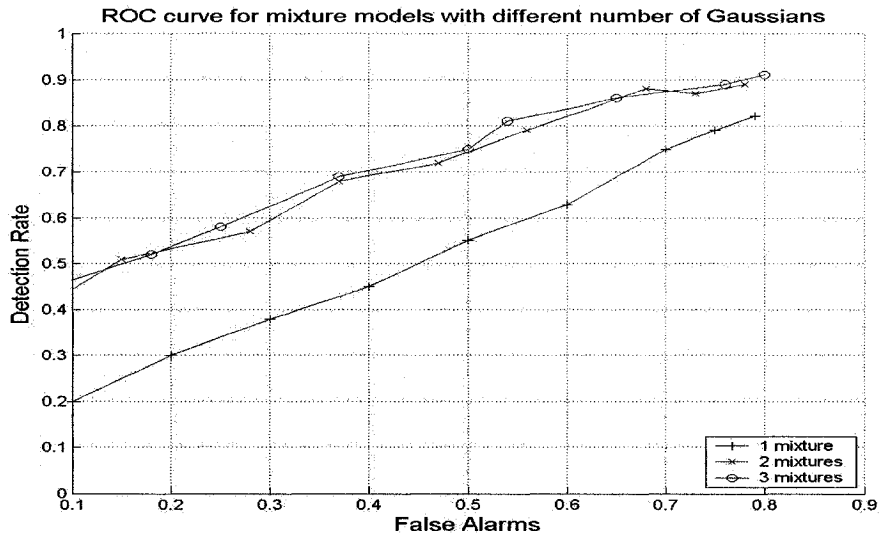

Figure 5.4. The classification performance for the uncoupled scene model for 200 test images is presented. Each curve shows performance for mixture models with different number of Gaussians. Performance of the model with mixture of 3 Gaussians shows no significant improvement over the performance of model with mixture of 2 Gaussians.

5.3 Experimental Results for the Strongly Coupled Scene and Object Modules

Having discussed the issues of the creation of the database and the choice of important parameters affecting the model performance, we now present the experimental results from the implementation of the adaptive priors and the adaptive likelihoods models as presented in chapter 4. In section 5.3.1 we present selected examples of the models' behaviors for chosen images of the test set. For each model we have chosen 7 examples which represent different types of the behavior of the model under a variety of input images. By studying the behavior of the model in these sample cases we intend to gain a deeper understanding of the model function and also to examine how the information flow between the two modules will affect the inferences made by each module. These cases represent selective behaviors of the model, so a statistical study which measures the general performance of model as a classification tool is presented in section 5.3.2. ROC curves which present the performance of the two models for varying decision thresholds are presented in section 5.3.2.

All images in the database have been labeled by 3 human observers. The observers have been asked to label the images by one of the five scene category labels: street scene, downtown area, residential area, indoors, and park. The observers have also been asked to label the patches containing objects as representing one of the 5 object categories: vehicles, plants, buildings, furniture, and people. The scene images left uncategorized or categorized as ambiguous by at least one of the observers have been discarded from the database and replaced by non-ambiguous images, so all the images in the database are uniquely assigned to one of the 5 scene categories by all 3 observers (examples of images which have ambiguous class assignments by human observers are

kept for some experiments, but are not included in the training or the test sets unless mentioned in the experiments.) The same strategy has also been taken with object images. Image patches left uncategorized or categorized as ambiguous by at least one of the observers have been discarded and replaced, so that all image patches used for the training of the object module are uniquely assigned to one of the 5 object categories by all 3 observers.

For the purpose of these experiments we divided the database of images into 800 images for training and 200 images for testing. Equal numbers of images are used for training the modules for different scene or object categories. In order to be able to estimate confidence levels for statistical analysis of the classification results, we have chosen the strategy of rotating the test set, i.e. at each trial, alternative subsets of the image database are chosen as test images, and the scene and object modules are trained using the remaining 800 images in the database. Five different subsets of the database have been used to compute the confidence levels in the classification results. The mean standard deviation error is computed for the classification results obtained from each rotating training image set.

Once a test image is given to the model, the model classification result falls into one of the following three categories: correctly classified, misclassified, and unclassified images. The results of classification are a function of both the iteration number and also the threshold levels we choose for accepting the probability levels as a correct decision. The image category label given by the human observers is used as the criteria for validating the model classification results. We specify our exact definition of an image being correctly classified, unclassified, and misclassified by the model at each section.

5.3.1 Case Studies for the Adaptive Priors and Adaptive Likelihood Models

In this section we present 7 examples of the behavior of the adaptive priors and the adaptive likelihood model. In this section an image is defined as unclassified when the difference of the two highest module *a posteriori* probabilities is less than a fixed range (chosen as ± 0.1 for the purpose of these experiments). An image is defined as correctly classified when the image is not unclassified and the module MAP solution for the image category agrees with the human classification. An image is defined as misclassified when the image is not unclassified and the module MAP solution for the image category does not agree with the human classification.

Figure (5.5) shows the percentages of correct scene classifications for different scene classes of a test set of 200 images. Results are averaged for the two coupled models. The averaged percentages of correct classifications are shown for iterations 1, 50, 100, 150, 200, and 250 of the two coupled models, given a fixed decision threshold.

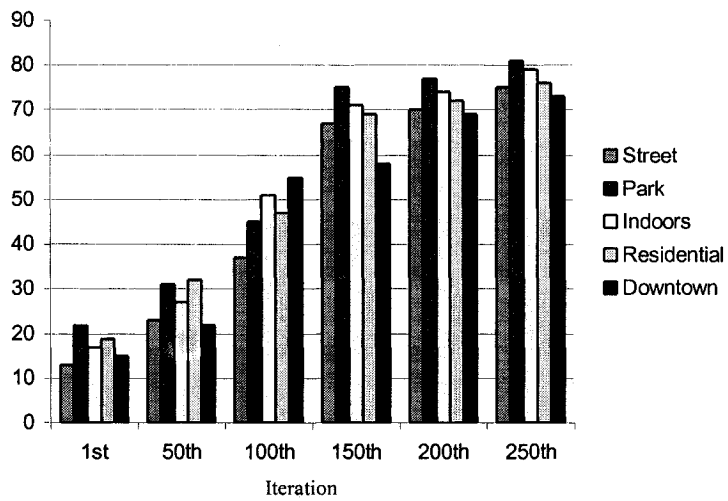

Figure 5.5. Percentages of correct scene classification results for different scene categories averaged for the two coupled models are shown. Results are shown for different iterations, given a fixed decision threshold.

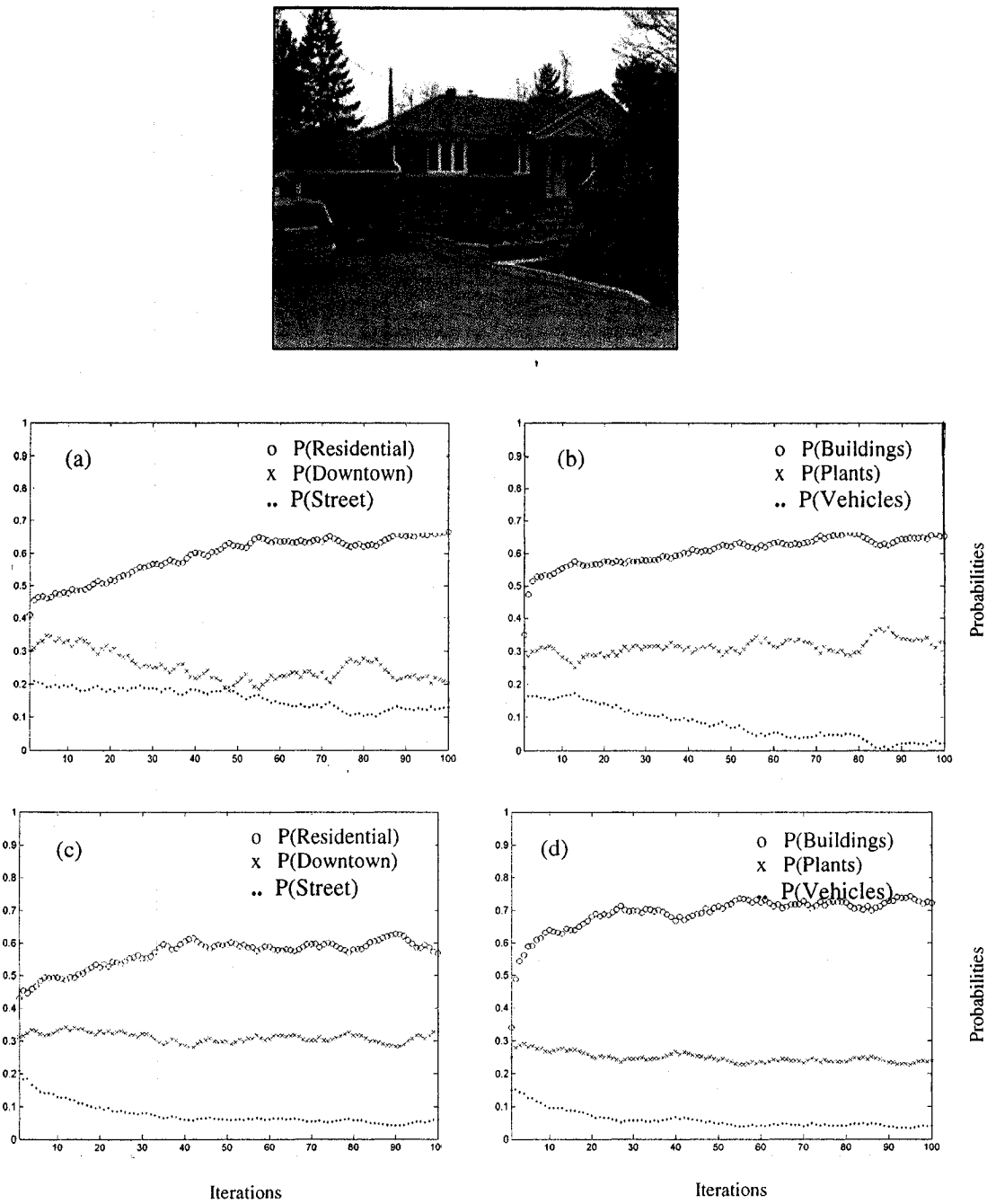

Figure 5.6. The scene and object hypotheses created by the first 100 iterations of the two models for a sample image belonging to the residential category are presented, (a) shows the posterior scene probabilities computed by the adaptive priors model, (b) shows the posterior object probabilities computed by the adaptive priors model (c) shows the posterior scene probabilities computed by the adaptive likelihood model, (d) shows the posterior object probabilities computed by the adaptive likelihood model.

As the first example for the behavior of the adaptive priors and the adaptive likelihood model we have chosen a sample image belonging to the residential scene category as the input to the two models (figure (5.6)). Graphs (5.6.a) and (5.6.b) show the posterior probabilities computed by the scene and the object module of the adaptive priors model. Graph (5.6.a) shows the posterior scene class probabilities computed for this image during the first 100 iterations of the adaptive priors model. The image is correctly classified as a residential scene at the first iteration of the model. The object module is able to provide evidence for the presence of buildings, plants, and vehicles in the image as shown in graph (5.6.b). The local image information about the objects present in the scene reinforces the correct scene module hypothesis about the category of the scene. Graphs (5.6.c) and (5.6.d) present the posterior probabilities computed by the scene and object modules of the adaptive likelihood model. The scene module of the adaptive likelihood model computed higher probability for the scene belonging to the residential category as shown in graph (5.6.c), and the object module of the adaptive likelihood model computes higher probabilities for the presence of buildings as compared to plants and vehicles. The feedback between the two modules reinforces the original hypotheses made, and by the end of the 100 iterations of the two modules the scene module keeps the correct hypothesis about the identity of the image.

As the second example we have chosen an image that is categorized by the human observer as a residential image. In Figure (5.7) we show the behavior of the two models for reaching a hypothesis about the identity of this image. Graphs (5.7.a) and (5.7.b) illustrate the posterior probabilities computed by the adaptive priors model and graphs (5.7.c) and (5.7.d) present the posterior probabilities computed by the adaptive likelihood model.

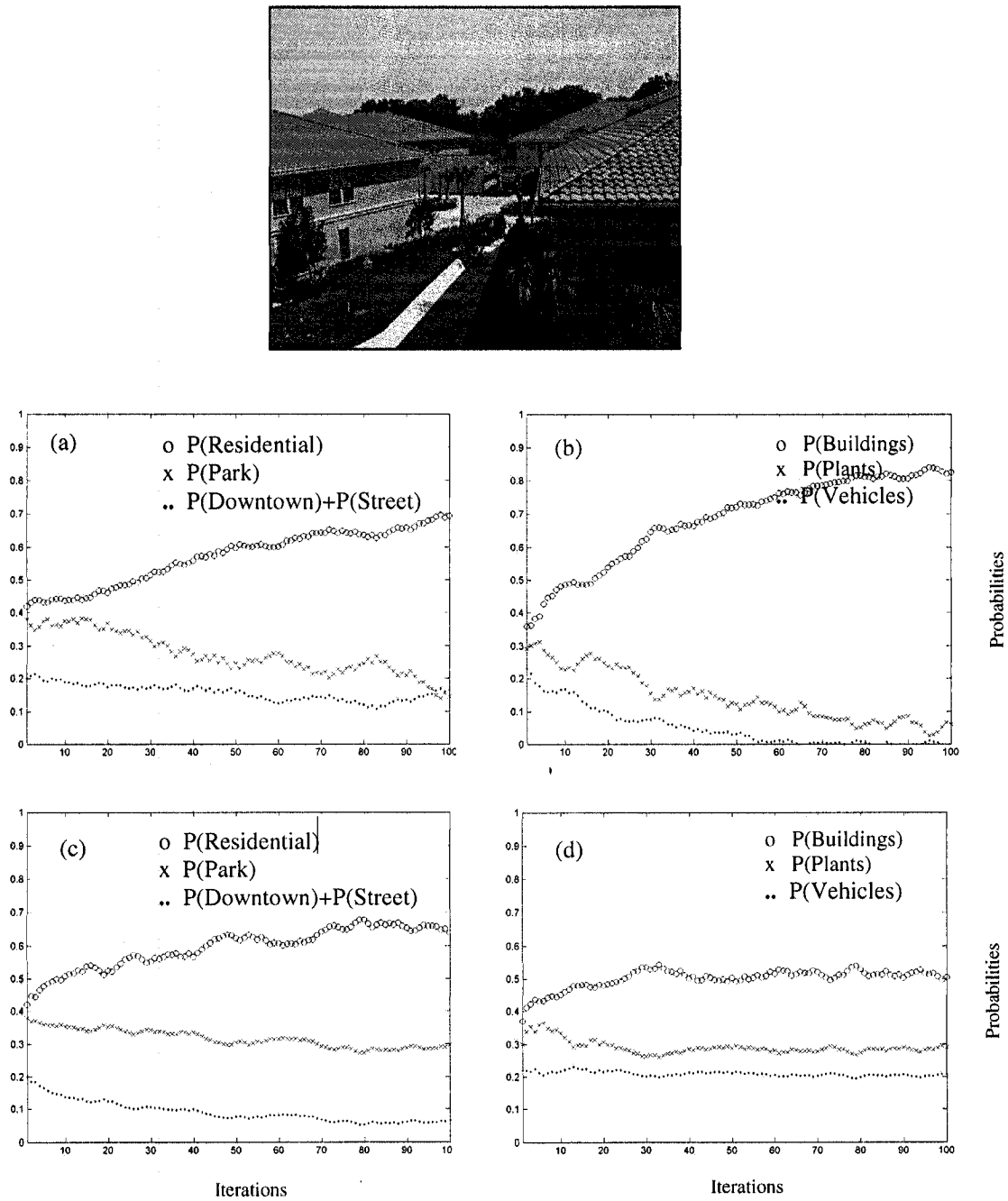

Figure 5.7. The scene and object hypotheses created by the first 100 iterations of the two models for a sample image belonging to the residential category are presented, (a) shows the posterior scene probabilities computed by the adaptive priors model, (b) shows the posterior object probabilities computed by the adaptive priors model (c) shows the posterior scene probabilities computed by the adaptive likelihood model, (d) shows the posterior object probabilities computed by the adaptive likelihood model.

Graph (5.7.a) illustrates the *a posteriori* probabilities of the test image belonging to the residential category or the park category, as produced by the scene module, for the first 100 iterations of the adaptive priors model. The image is unclassified by the scene module at the first iteration of the model since the difference of the probabilities of the scene belonging to the residential or the park category is less than 0.1. The three curves in graph (5.7.b) illustrate the *a posteriori* probabilities of image containing buildings, plants, and vehicles, as produced by the object module, at the first 100 iterations of the adaptive priors model. The scene probabilities estimated by the first iteration of the scene module are in fact the results of scene categorization without any feedback from the object module. One can interpret the model behavior as the following: At the first iteration, the scene module is not able to discriminate between the image global features V_G belonging to the residential category or the park category. The object module finds evidence for buildings, plants, and vehicles in the scene. This combination of objects, with their relative probability levels, provide an object profile which modifies the prior model of the scene module in a way which favors the probability of image being a residential scene versus a park scene. At the same time the scene *a posteriori* distribution propagates to the object module, and modifies the prior model of the object module. The modification of the object priors has the effect of changing the original hypothesis made about some of the object patches, and the aggregation of these changes produces new estimates for the probability of presence of buildings, plants, or vehicles in the image. After 100 iterations, the mutual feedback between the scene and the object module has the overall effect of increasing the probability of the scene belonging to the residential category as compared to the park scene. At the end of the 100^{th} iteration more patches

have been labeled as buildings, and with higher probabilities, as the probability level of the presence of buildings has increased as compared to plants, or vehicles.

Graphs (5.7.c) and (5.7.d) in this example show the posterior probabilities computed by the scene and the object module of the adaptive likelihood model. Graph (5.7.c) shows the probability of the scene belonging to the residential or the park category as computed by the adaptive likelihood model. The scene module with no feedback computes similar probabilities for the scene being a residential or a park scene. The likelihood term of the scene module with no feedback computes the likelihood of the scene belonging to different scene categories based only on the global context features of the image V_G. The strong coupling of the likelihood terms of the two modules has the effect of increasing the probability of the scene belonging to the residential category. The likelihood term of the scene module with feedback computes the likelihood of the scene belonging to different scene categories based on the joint probability density of the global context features V_G and the probability of the presence of different object categories such as buildings, plants, and vehicles. Similarly, the likelihood term of the object module with no feedback computes the likelihood of the presence of different object categories based only on the local features V_L. The likelihood term of the object module with feedback computes the likelihood of the presence of different object categories based on the joint probability density of the local features V_L and the probability of the image belonging to different scene categories. The joint scene likelihood function estimates higher probabilities for the image belonging to the residential scene category. The joint object likelihood function estimates higher probability for patches containing buildings.

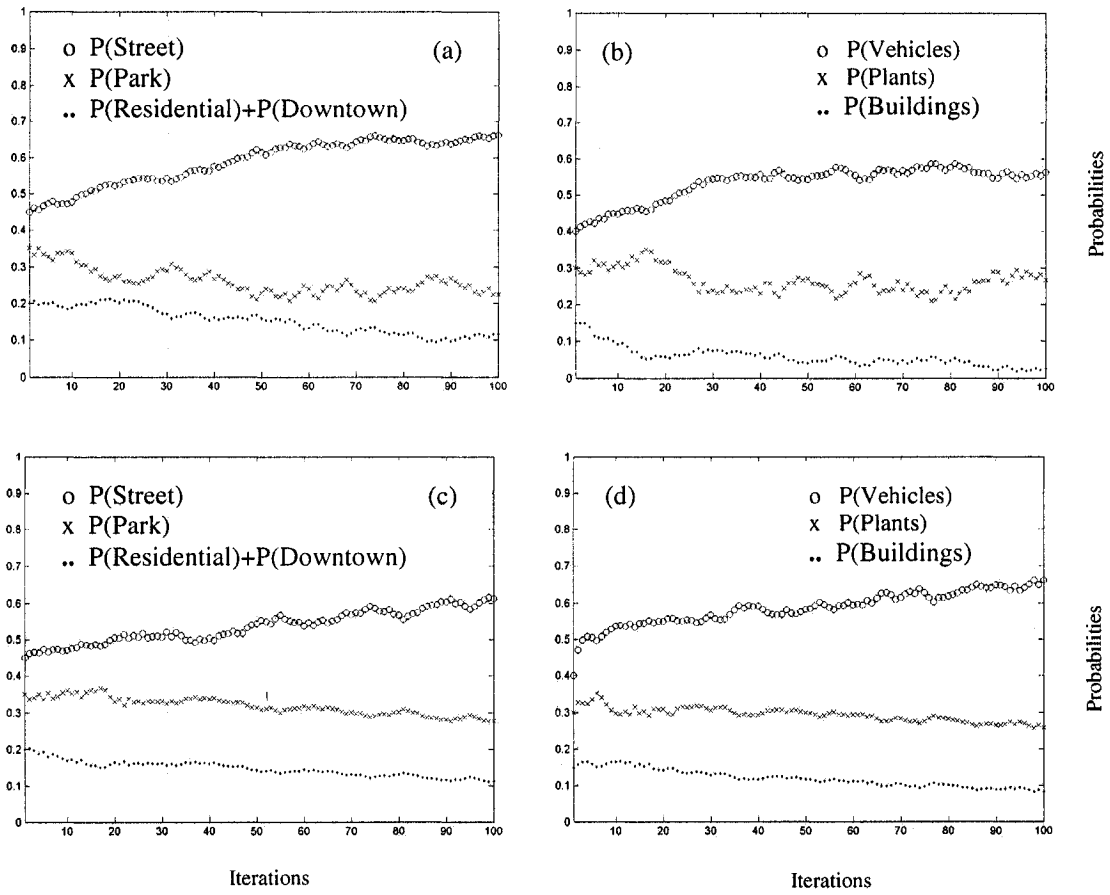

Figure 5.8. The scene and object hypotheses created by the first 100 iterations of the two models for a sample image belonging to the street category are presented, (a) shows the posterior scene probabilities computed by the adaptive priors model, (b) shows the posterior object probabilities computed by the adaptive priors model (c) shows the posterior scene probabilities computed by the adaptive likelihood model, (d) shows the posterior object probabilities computed by the adaptive likelihood model.

Figure (5.8) presents an example for the behavior of the two adaptive models for an image that is categorized by the human observer as belonging to the street category. Graph (5.8.a) illustrates the *a posteriori* probabilities of the test image belonging to the street category or the park category, as produced by the scene module of the adaptive priors model. The three curves in graph (5.8.b) illustrate the *a posteriori* probabilities of image containing vehicles, plants, and buildings, as produced by the object module of the adaptive priors model. The global image features V_G do not provide adequate evidence for the scene module to independently produce a reliable hypothesis about the identity of the image, and in the first iteration, the scene module estimates very close probability values for the image being a street scene or a park scene. The object module is able to independently find evidence for vehicles, plants, and buildings in the scene, as presented in the first object *a posteriori* estimates. The feedback between the two modules has the effect of the enforcement of the hypothesis of the image being a street scene and the weakening of the hypothesis of the image being a park scene.

Each scene class is associated with a prototypical arrangement of objects. The strong coupling of the scene priors and the object priors in fact makes an association between each scene class and its prototypical arrangement of objects. When the object posterior probabilities are projected to the scene module the set of associations that correspond to the relevant scene context are activated and result in an enforcement of the posterior probability of the scene class which is most strongly associated with the present set of objects. In this example the profile of the objects in the scene, a high probability of vehicles and lower probabilities for plants and buildings enforces the hypothesis of the image being a street scene. When the higher probability of image being

a street scene is projected back to the object module, it can strengthen the evidence for the presence of vehicles in some regions of the image through the object priors. After 100 iterations, the mutual feedback between the scene and the object module has the overall effect of increasing the probability of the scene belonging to the street category as compared to the park category. At the end of the 100^{th} iteration more patches have been labeled as vehicles, and with higher probabilities, as the probability level of the presence of vehicles has increased as compared to plants, or buildings.

Graphs (5.8.c) and (5.8.d) in this example show the posterior probabilities computed by the scene and the object module of the adaptive likelihood model. Graph (5.8.c) shows the probability of the scene belonging to the street, park, or residential and downtown category as computed by the adaptive likelihood model. Graph (5.8.d) shows the probability of the object categories vehicles, plants, and buildings being present in the scene. The scene module with no feedback computes close probabilities for the scene being a park or a street scene. The probability of the scene belonging to the street scene category increases when estimated using the coupled scene likelihood model. The probability of vehicles in the image increases when estimated by coupled object likelihood model. The strong coupling of the likelihood terms of the two modules has the effect of increasing the probability of the scene belonging to the street category.

The curves produced by the object module in both models implemented, raise the question of why the probability of vehicles is estimated higher than the probability of plants in this image, eventhough a larger area of the image is covered by plant type texture. We use a weighting scheme in order to balance the effect of the scale of the patches. But in this example the aggregation of the local evidence for vehicles from smaller patches has exceeded the evidence provided by fewer patches of a larger scale.

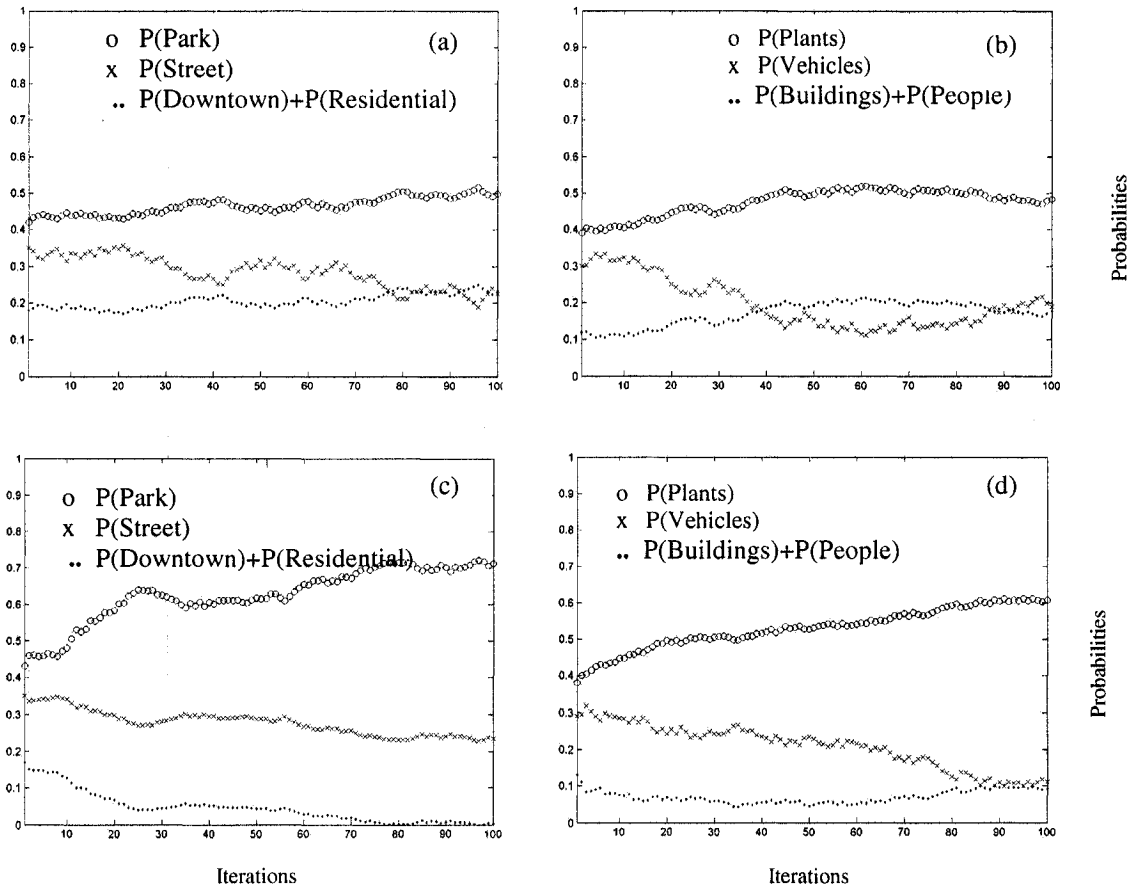

Figure 5.9. The scene and object hypotheses created by the first 100 iterations of the two models for a sample image belonging to the park category are presented, (a) shows the posterior scene probabilities computed by the adaptive priors model, (b) shows the posterior object probabilities computed by the adaptive priors model (c) shows the posterior scene probabilities computed by the adaptive likelihood model, (d) shows the posterior object probabilities computed by the adaptive likelihood model.

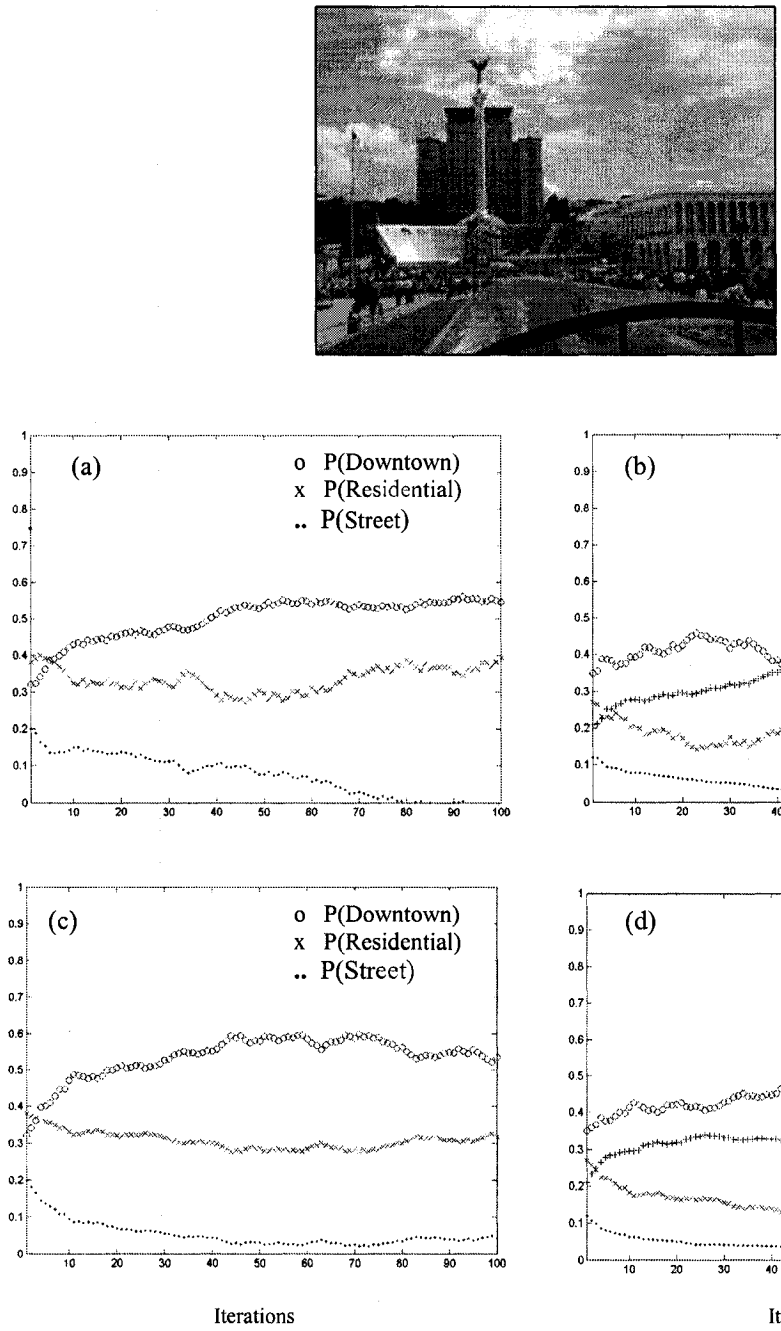

Figure 5.10. The scene and object hypotheses created by the first 100 iterations of the two models for a sample image belonging to the downtown category are presented, (a) shows the posterior scene probabilities computed by the adaptive priors model, (b) shows the posterior object probabilities computed by the adaptive priors model (c) shows the posterior scene probabilities computed by the adaptive likelihood model, (d) shows the posterior object probabilities computed by the adaptive likelihood model.

The fourth example we have chosen for the behavior of the two adaptive models is shown in figure (5.9). Graphs (5.9.a) and (5.9.b) present the scene posterior probabilities and the object posterior probabilities as computed by the scene and the object modules of the adaptive priors model. Graphs (5.9.c) and (5.9.d) compute the scene posterior probabilities and the object posterior probabilities as computed by the scene and object module of the adaptive likelihood model. The image belonging to the park scene category is unclassified by the scene module at the first iteration, with the probability of the scene being a street or a park scene being close. The object module is able to provide evidence for the presence of plants, vehicles, buildings and people in the image. The probability of plants being present in the scene is higher than vehicles. This is not a characteristic of street scenes and the hypothesis for the scene being a street becomes weaker by the 100^{th} iteration.

The fifth example which is a downtown scene is shown in figure (5.10). Graphs (5.10.a) and (5.10.b) illustrate the results from the adaptive priors model. Graphs (5.10.c) and (5.10.d) illustrate the results from the adaptive likelihood model. The scene module at the first iteration misclassifies the image of the downtown street. The probability of the image being a residential scene is higher than the image being a downtown scene. The object module provides evidence for the presence of buildings, plants, people and vehicles in the image. As the model iterates the evidence for vehicles decreases, which can be the result of the feedback from the scene module providing higher probability for the image being a downtown or a residential scene as compared to a street scene. Also, local evidence for people being present in the scene increases, which can be related to the scene module estimating a higher probability for the scene being a downtown scene by the end of the 100^{th} iteration.

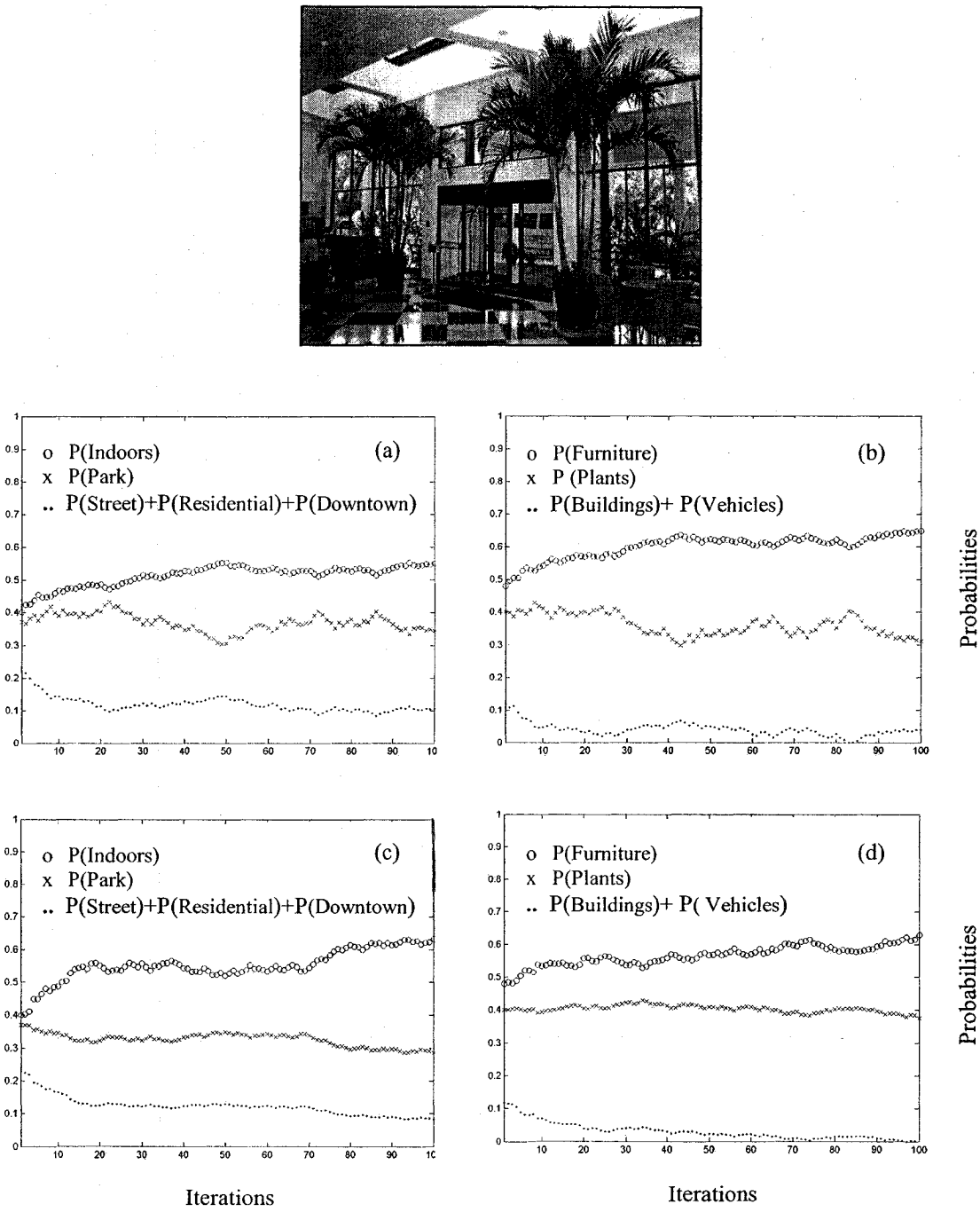

Figure 5.11. The scene and object hypotheses created by the first 100 iterations of the two models for a sample image belonging to the indoors category are presented, (a) shows the posterior scene probabilities computed by the adaptive priors model, (b) shows the posterior object probabilities computed by the adaptive priors model (c) shows the posterior scene probabilities computed by the adaptive likelihood model, (d) shows the posterior object probabilities computed by the adaptive likelihood model.

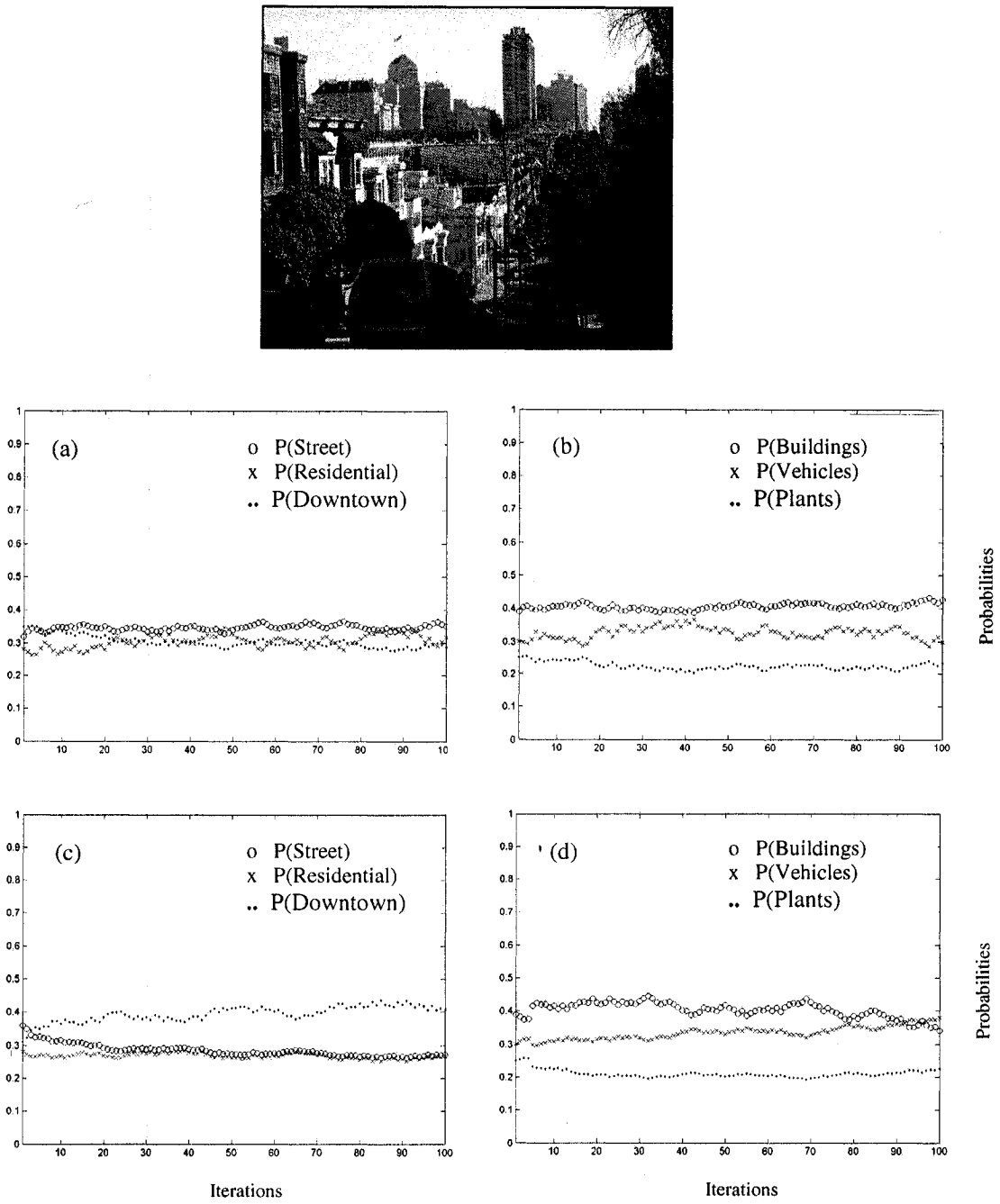

Figure 5.12. The scene and object hypotheses created by the first 100 iterations of the two models for a sample image belonging to the ambiguous category are presented, (a) shows the posterior scene probabilities computed by the adaptive priors model, (b) shows the posterior object probabilities computed by the adaptive priors model (c) shows the posterior scene probabilities computed by the adaptive likelihood model, (d) shows the posterior object probabilities computed by the adaptive likelihood model.

The sixth example is an image which belongs to the indoor scene category. The results related to this example are shown in figure (5.11). This image is initially unclassified by the scene module. The global context features are not adequate for uniquely classifying this image. This may be due to the large windows in the indoor image which show plants from outdoors. The object module finds evidence for the presence of both furniture and plants in the image. The model is able to resolve the ambiguity in the scene identity by the 100^{th} iteration, although the rate of increase in the indoor *a posteriori* probability levels is not uniform, and the model seems to oscillate between the indoor and the park identities.

The last example is an ambiguous image in the sense that the human observers have not been able to uniquely label this image as a street scene, a downtown scene, or a residential scene (figure (5.12)). It is interesting to show that the model is also unable to resolve the ambiguity in the scene identity. Evidence is found as for the presence of buildings, vehicles and plants, but the relative probability levels of the presence of the object categories do not reinforce a specific scene prior and the model oscillate between the three hypotheses.

5.3.2 Statistical Study of the Classification Results

The suggested architectures can be compared from different points of view. In this section we would limit the criteria of the comparison of the two models to their performance in classification tasks. Figure (5.13) presents the comparison of the two models based on their performance in terms of correct classifications of scene identities. Receiver Operator Curves (ROC) demonstrate the performance of the models in terms of their true positive and false positive results and can be used as a tool for quantitatively

measuring and comparing the performance of the models. Plots (5.13.a) and (5.13.b) illustrate ROC curves computed for the coupled priors and the coupled likelihood model respectively. Each of the curves represents results from a fixed iteration and varying decision thresholds of the two models. Each plot shows ROC curves computed from the scene classification results obtained from the first, 50^{th}, 100^{th}, and 150^{th} iteration of the model. Results from the test images in all scene categories have been combined into each curve. A correct detection happens when the estimated probability of the image belonging to the correct scene type is higher than the decision threshold, and the probabilities of the image belonging to the other scene categories are all below the decision threshold. A False alarm happens when the probability of the image belonging to an incorrect scene category is higher than the decision threshold, and the probabilities of the image belonging to all other scene categories are all lower than the decision threshold. The error bars have been computed using the classification results from rotating sets of test images from the data base, so that in each experiment 200 images are chosen as test images, and the remaining 800 images are used as the training set.

Comparing the curves representing performance at the first and the 150^{th} iteration of the two models we can see that scene classification performance is significantly higher at the 150^{th} iteration of both models. The curve representing the results from the first iteration is the same in both models, and represents the scene classification result by the uncoupled scene module. Therefore, one can conclude that in general the feedback between the object and scene module has improved the scene classification performance.

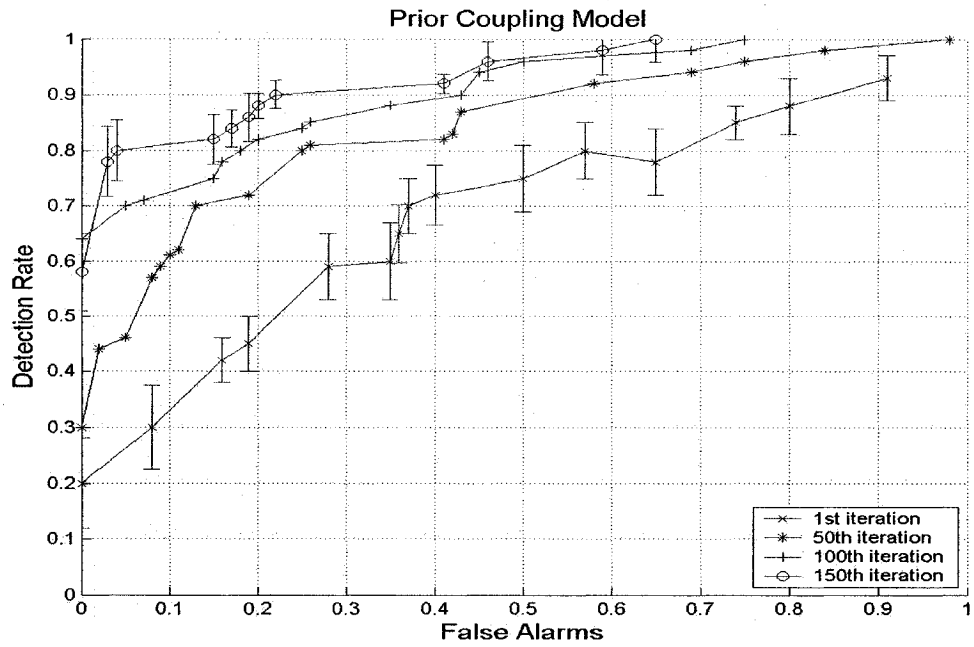

(a)

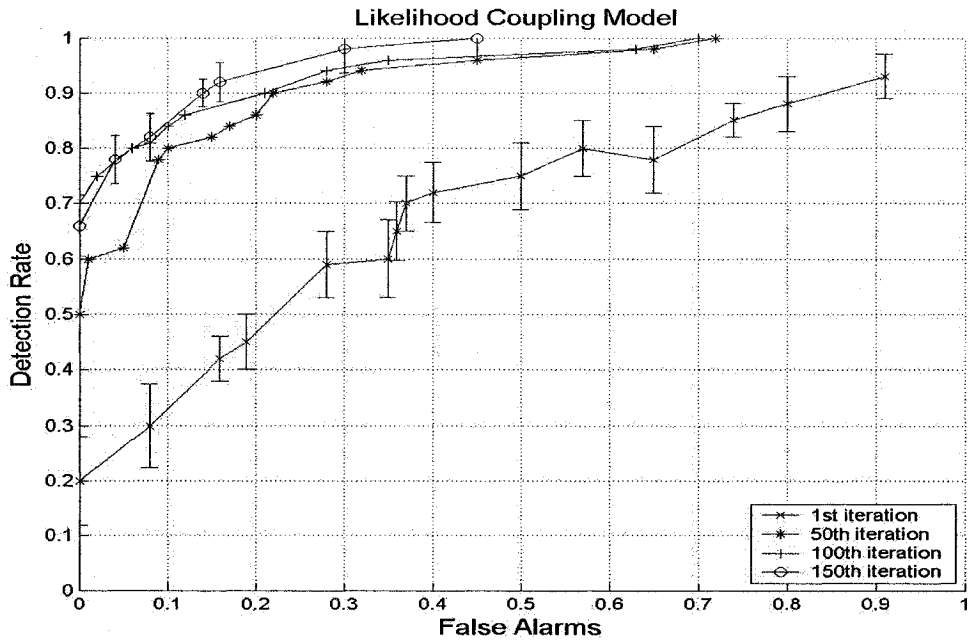

(b)

Figure 5.13. ROC curves for scene classification results of the test images. (a) ROC curves computed for the coupled priors model. (b) ROC curves computed for the coupled likelihood model. Each curve represents results from a fixed iteration.

Chapter 6

Comparison of the Strongly Coupled Scene and Object Classification Models

In the previous chapter we presented the experimental results obtained from implementing the strongly coupled scene and object classification models. The receiver operating characteristic (ROC) curves depicting the performance of each of the strongly coupled models (figure 5.13) shows that in general the feedback mechanism between the object classification module and the scene classification improves the scene classification performance in both models. In this chapter we further analyze the outputs obtained from the two models in order to establish some of the main characteristics of the models such as predictability, speed of response, and robustness of the models. Investigating these questions also provides a basis for comparing the behavior of the two models. In section 6.1 we compare the classification performance of the two models using the corresponding ROC curves. In section 6.2 we investigate the predictability of the two models using cross-correlation plots and in section 6.3 we compare the speed of the two models by estimating the rise times of the models' outputs. In section 6.4 we investigate the robustness of the models to variations of the input image such as changes in image orientations, and additional noise.

6.1 Classification Performance of the Two Models

Plotting the ROC curves representing the scene classification performance of the two models demonstrates a significant difference in their detection rates. In order to

demonstrate this result more clearly, we plot the ROC curves obtained from the two models, for fixed iterations and varying decision thresholds, in the same graph (figure (6.1.a) and (6.1.b)). In figure (6.1.a) the two curves corresponding to the classification results obtained from the 50^{th} iteration of the two models are shown. In figure (6.1.b) the two curves corresponding to the classification results obtained from the 150^{th} iteration of the two models are shown.

The results depicted in figure (6.1.a) and (6.1.b) show that the adaptive likelihood model has a higher detection rate as compared to the adaptive priors model. Based on these experimental results one can empirically conclude that constraining the likelihoods provides better solutions for the scene classification problem compared to constraining the priors, given our choice of image features and image data base. This result also implies that the MAP solutions of the Bayesian estimation problems presented by the functions of the scene and object modules are more sensitive to changes in the shape of the likelihood distributions, as compared to changes in the shape of the prior distributions.

6.2 Predictability of the Two Models

We use autocorrelation plots as tools for checking the predictability of the model. Randomness in a data set is ascertained when the autocorrelation plots have near zero values for all time lag separations. If the data set is non-random one or more of the auto-correlation values is significantly non-zero. We form the auto-correlation plots by computing the auto-correlation coefficient R_h as the following

$$R_h = \frac{C_h}{C_0} \tag{6.1}$$

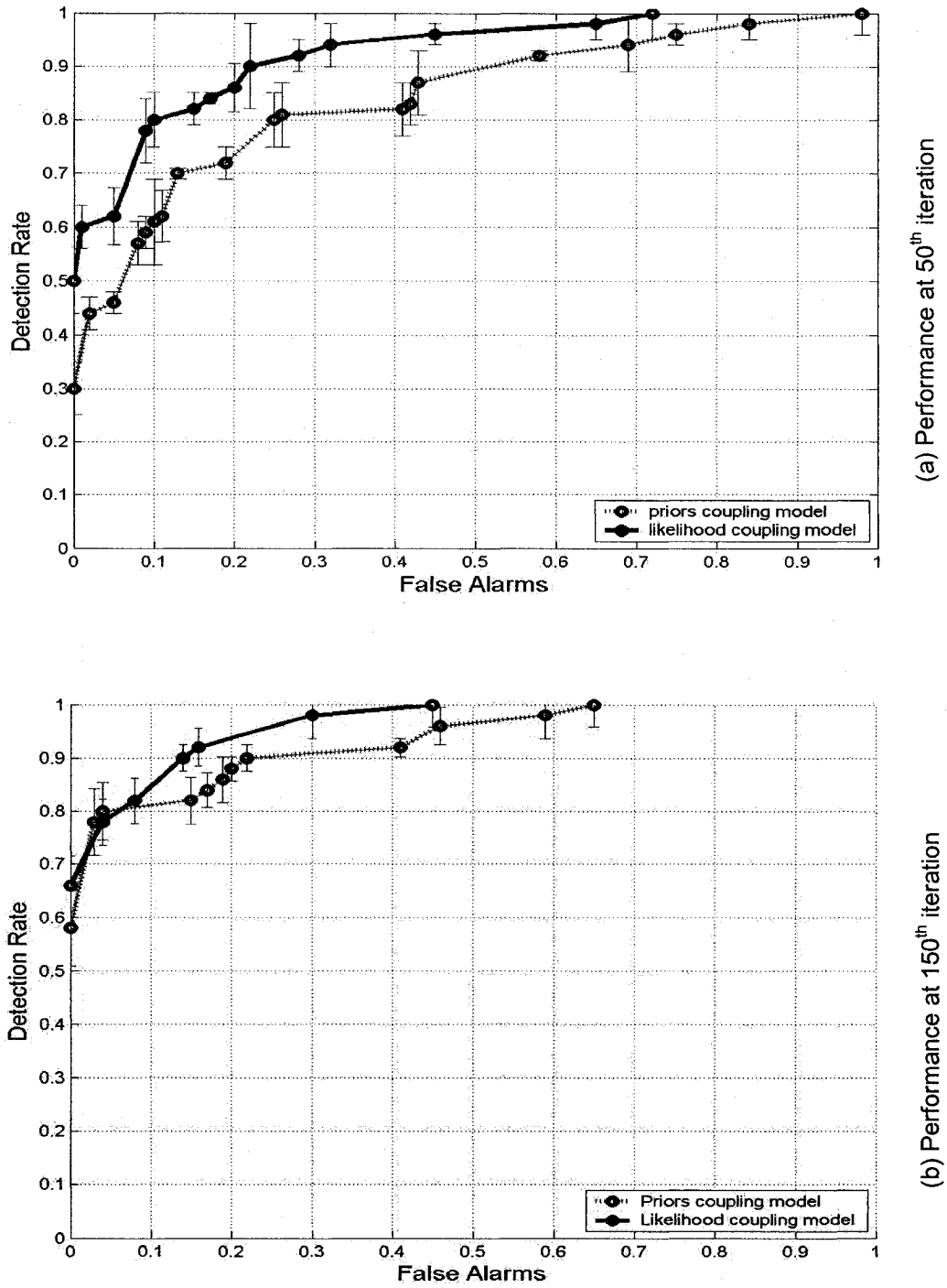

Figure 6.1. ROC curves for scene classification results of the coupled likelihood and coupled priors models, (a) ROC curves representing scene classification results from 50th iteration of the two models, (b) ROC curves representing scene classification results from the 150th iteration of the two models.

where C_h is the auto-covariance function

$$C_h = \frac{1}{N} \sum_{t=1}^{N-h} (x_t - \mu)(x_{t+h} - \mu) \tag{6.2}$$

and C_0 is the variance function

$$C_0 = \frac{\sum_{t=1}^{N} (x_t - \mu)^2}{N} \tag{6.3}$$

We have plotted the autocorrelations of the outputs of the coupled likelihood and the coupled priors model obtained in the previous experiments. Figures (6.2) and (6.3) show the autocorrelation plots for the outputs of the coupled likelihood and coupled priors model respectively. Figures (6.2.a) and (6.3.a) show the averaged autocorrelations that correspond to a correct classification decision given a fixed threshold level at iteration 100. Figures (6.2.b) and (6.3.b) show the averaged autocorrelations that correspond to cases where the scene images remain unclassified or ambiguous given the same fixed threshold level at iteration 100. Figures (6.2) and (6.3) demonstrate significant autocorrelation in both processes; the data does not follow a random or a sinusoidal pattern and represents a predictable process. In all cases the autocorrelation starts with moderately higher values at smaller lags and gradually decreases. One can observe that the autocorrelation plots from the coupled priors model show a faster decay compared to the autocorrelation plots from the coupled likelihood model. Based on this observation one can empirically conclude that the coupled likelihood process provides a higher degree of predictability compared to the coupled priors model. Also comparing the plots from the correct classification cases to the plots from unclassified and ambiguous cases, one can observe that the autocorrelation plots corresponding to the correct classification cases decay slower.

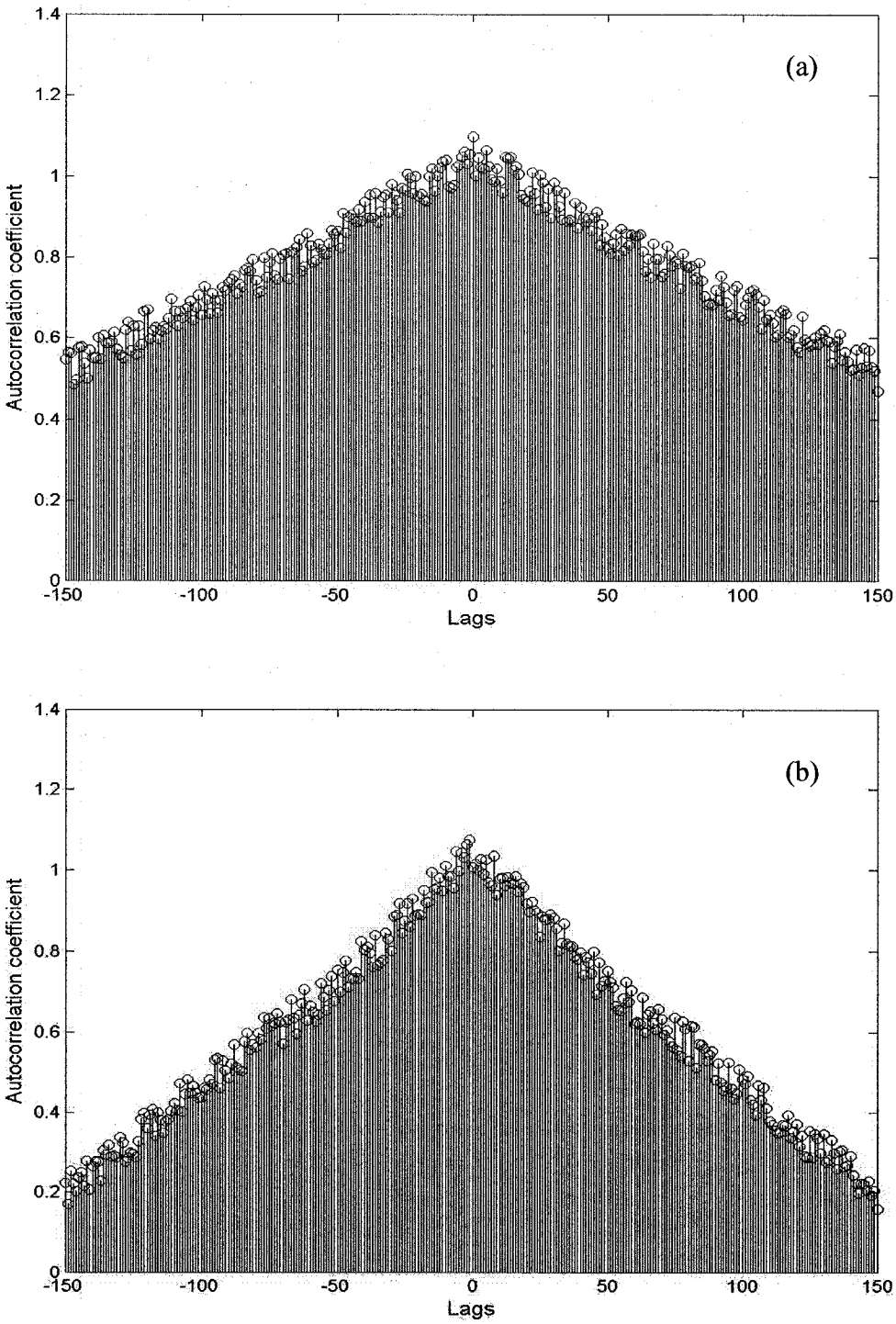

Figure 6.2. Autocorrelation plots for the outputs of the coupled likelihood model, (a) shows the averaged autocorrelations plot of the model outputs which correspond to a correct classification decision, (b) shows the averaged autocorrelations plot of the model outputs which correspond to cases where the scene images remain unclassified or ambiguous.

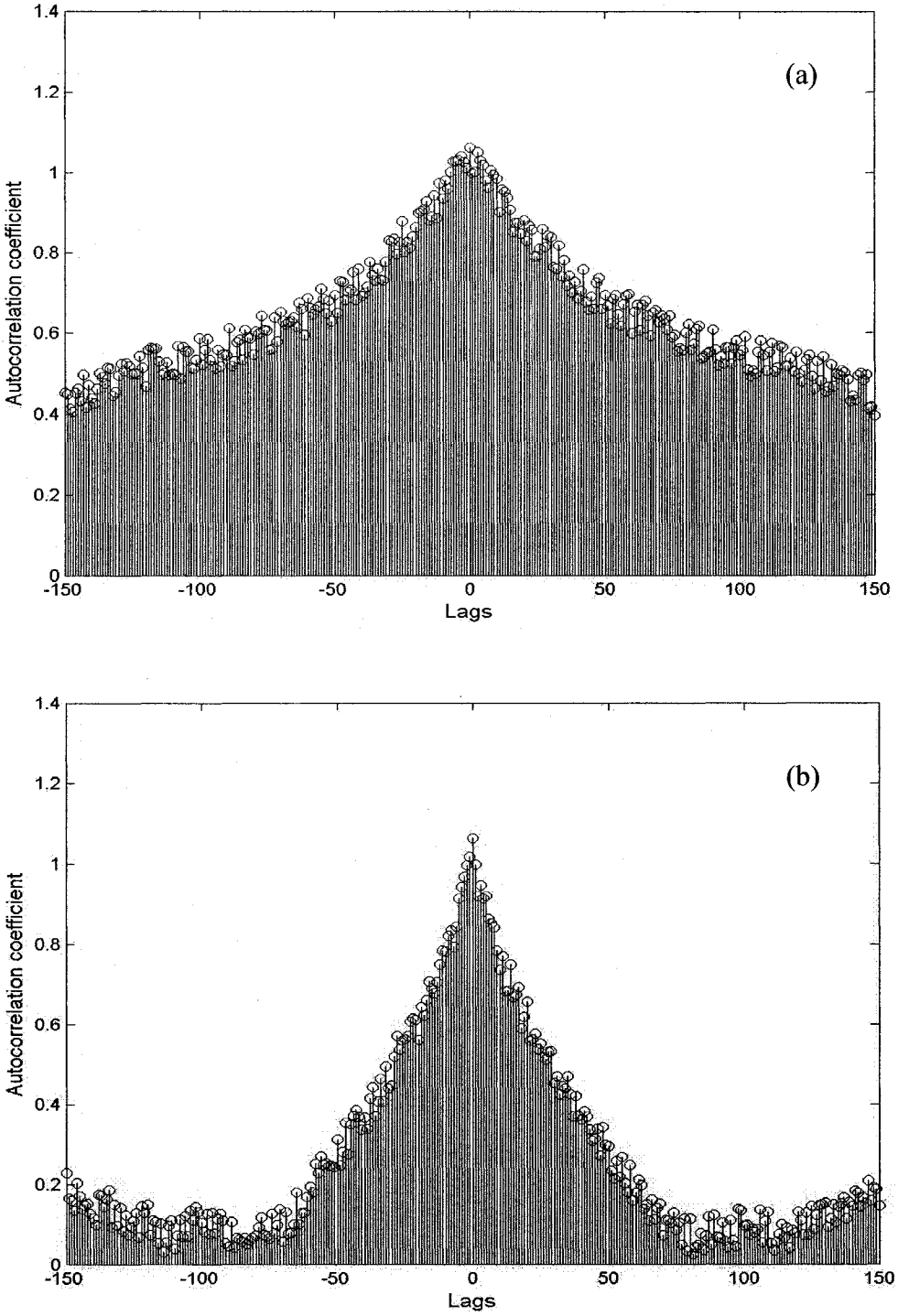

Figure 6.3. Autocorrelation plots for the outputs of the coupled priors model, (a) shows the averaged autocorrelations plot of the model outputs which correspond to a correct classification decision, (b) shows the averaged autocorrelations plot of the model outputs which correspond to cases where the scene images remain unclassified or ambiguous.

6.3 Speed of the Two Models

In this section we compare the speed of the two approaches. In order to evaluate the speed of the two models we use the model outputs that represent a correct classification by the 100^{th} iteration given a fixed threshold. We use two methods for evaluating the rise times of the model outputs.

1) We fit the model outputs y with a first order step response given by the exponential function $1 - A\exp(\frac{-t}{\tau})$. In order to do so we use a regression method to fit a straight line to $\ln(1-y)$. The slope of the fitted line is equal to $\frac{-1}{\tau}$. The time constant τ provides a way for comparing the rise times of the model outputs.
2) We determine the iteration number where the model response has risen %63 of the way from its original value at the first iteration to the value of the threshold.

Tables (6.1) and (6.2) show the results computed from the two models' outputs corresponding to different scene types. Results from table (6.1) show that a higher time constant is estimated for the coupled priors model's outputs, consistently over all scene classes. This translates into slower rise times for the outputs obtained from the coupled priors model.

	Time Constant	
Scene Type	Coupled Likelihood Model	Coupled Priors Model
Street	666.7 ± 70	1250.2 ± 300
Park	555.5 ± 100	909.1 ± 300
Indoors	476.2 ± 50	1111.1 ± 400
Downtown	625.3 ± 100	1740 ± 500
Residential	769.2 ± 70	2500.0 ± 300

Table 6.1. Comparison of the speed of the two models using time constants obtained from fitting the model outputs with a first order step response.

	Iteration Number	
Scene Type	Coupled Likelihood Model	Coupled Priors Model
Street	43 ± 10	78 ± 12
Park	24 ± 14	53 ± 9
Indoors	27 ± 10	45 ± 15
Downtown	51 ± 7	74 ± 11
Residential	37 ± 12	62 ± 17

Table 6.2. Comparison of the speed of the two models using the iteration number in which the model responses rise %63 of the way from their original value at the first iteration, to the value of the threshold.

We choose a second method for comparing the speed of the two processes since the first order step response function does not always provide a good model for fitting the models' output data. The results obtained from the second method explained above are shown in table (6.2). These results support the findings from figure (6.1) that outputs from the coupled likelihood model have shorter rise times. One can observe that in most cases the coupled likelihood model outputs reach %63 of the difference between their original values and the threshold values in significantly fewer iterations compared to the coupled priors outputs.

6.4 Robustness of the Two Models to Input Variations

In this section we study how the models' classification results change with variations to the input images. At first we experiment with images with added Gaussian noise of zero mean and σ=0.1, 0.01, and 0.001. Figure (6.4) shows examples of the noisy images generated from an example image of the test set. Table (6.3) shows the classification results obtained from a test set of 50 images chosen from different scene categories. These results are obtained using a fixed decision threshold at the iteration 150.

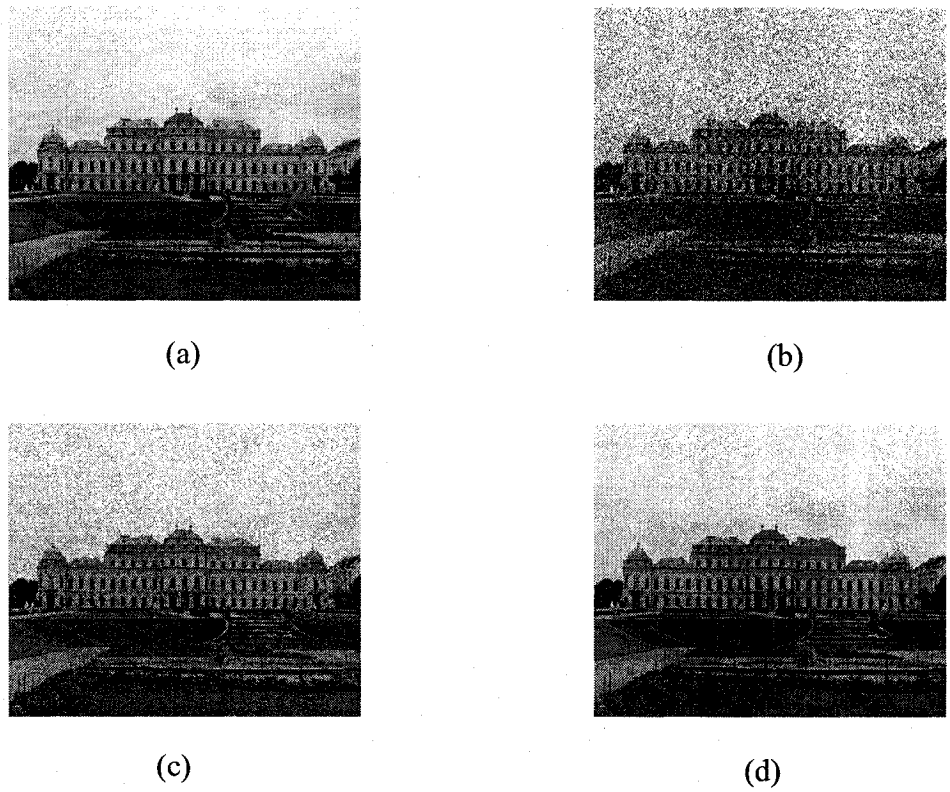

Figure 6.4. Examples of noisy images, (a) original image, (b) image with added Gaussian noise of zero mean and σ=0.1, (c) image with added Gaussian noise of zero mean and σ=0.01, (d) image with added Gaussian noise of zero mean and σ=0.001.

Noise Type	**Coupled Likelihood Model**		**Coupled Priors Model**	
	Detection Rate	False Alarm	Detection Rate	False Alarm
No added noise	%80 ± 0.5	%8	%77 ± 0.3	%14
Added Gaussian μ=0, σ=0.001	%80 ± 0.5	%8	%77 ± 0.3	%14
Added Gaussian μ=0, σ=0.01	%76 ± 0.8	%13	%68 ± 0.5	%15
Added Gaussian μ=0, σ=0.1	%56 ± 0.7	%27	%43 ± 0.2	%19

Table 6.3. Classification performance for noisy test images.

Based on the results shown in table (6.3) one can observe that an additional Gaussian noise of σ=0.001 has no effect on the scene classification results of the chosen test data set. Detection rates computed for the images with an additional Gaussian noise of σ=0.001 are lower than detection rates of the original images, but this difference is not statistically significant. Detection rates corresponding to images with added Gaussian noise of σ=0.1 shows significant decrease compared to the other cases. In fact these detection rates are as low as the detection rates computed for uncoupled scene modules. This result may be explained by the fact that the Gaussian noise of σ=0.1 strongly distorts the fine details in the image. Although the models use low spatial frequency features for both the scene and object representations, the performance of object classification, especially for objects with smaller scales, declines and therefore the object related information passed from the object module to the scene module is no longer useful.

In the last part of these experiments we investigate the effect of changing the input image orientations. In order to create images of different orientations we change the upright camera orientation we had used for capturing the images in the database and capture images with the camera rotated at 45, 90, and 180 degrees. It is interesting the images rotated 180 degrees show the least decrease in the detection rates, compared to detection rates obtained from images rotated by 45 or 90 degrees. This may seem counter-intuitive since we experience a significant effect on our ability of recognizing scenes and objects when presented with upside images. But based on the scene and object representations used in the models, the dominant horizontal or vertical structures

present in the image and also the dominant horizon line in the images, remain in the same orientation within a 180 degree rotation.

Degree of Rotation	**Coupled Likelihood Model**		**Coupled Priors Model**	
	Detection Rate	False Alarm	Detection Rate	False Alarm
No Rotation	%97 ± 0.5	%14	%92 ± 0.5	%15
+45° Rotation	%82 ± 0.7	%15	%86 ± 0.3	%13
+90° Rotation	%63 ± 0.5	%21	%61 ± 0.2	%22
180° Rotation	%94 ± 0.2	%11	%91 ± 0.5	%14

Table 6.4. Classification performance for test images with variations in orientation.

Chapter 7

Attentional Feature Tuning

In the previous section we demonstrated the effect of the strong-coupling of the scene and object modules on scene categorization results. The object classification and the scene classification module make inferences about high-level concrete (object) or semantic (scene) concepts based on local or global low level sensory features extracted from the power spectrum of the images. The strongly-coupled feedback incorporated in the model uses the inference made related to one of the high-level concepts to influence and adjust the inference made about the other high-level concept. It is also possible to create a top-down feedback between the high-level inference processes and the lower level feature extraction processes with the objective of creating an attentional modulation effect which would make the scene or object classification process more efficient. For example when the scene categorization module creates a hypothesis about the identity of a scene based on the global features V_G of the image, in the cases that the identity of the image is ambiguous, meaning that the probability of the scene belonging to two or more classes are smaller than a certain threshold, the feedback between the object and the scene module may resolve this ambiguity based on evidence for presence of object classes which can more clearly identify the scene. One other way of resolving such ambiguity is to tune the features V_G extracted from the scene image in order to create higher discriminability between the ambiguous scene classes. In this chapter we present the implementation and the experimental results of such a feature tuning scheme

where the hypothesis generated about the identity of the scenes is used to modify the feature extraction process.

In the previous chapters we talked about the experiments by Oliva and Torralba which show that the distribution of energy across the different scales and orientations of the Gabor filter bank are stable enough among images belonging to the same scene category, and therefore these distributions can be used as signatures representing the scene classes [94]. In this chapter we propose using the energy distribution characterizing each scene category to tune the Gabor filter bank used for producing the low level features V_G based on the scene hypothesis produced by the scene module. The Bayesian inference function of the scene module represents the bottom-up flow of information in the model, where scene identities are inferred from the low level features image features. The feature tuning represents the top-down flow of information, where the high-level information inferred from the scene identification module is used to tune the low-level features. This approach has conceptual similarity to the winner-take-all model introduced by Tsotsos *et al* [97], but instead of the top-down winner-take-all selection process biasing the features in some region of the image, representing the focus of attention to that region, we use the hypothesis formed by the scene module to bias global image responses to selected spatial frequencies and orientations, therefore attending to certain frequencies and orientations and not to a certain location in the image.

For this purpose we first study the energy levels of image responses to the Gabor filter bank for images of different scene classes. We compute the average energy level of the image responses from each scene class to each Gabor filter (with specific orientation

and scale), and thus we create a "Gabor index" for each scene class. At the first iteration of the model, the feature vector V_G is extracted from the image without any *a priori* hypothesis about the scene category, therefore the image responses to filters of different scales and orientations are all used with equal weight for forming V_G. But once the probability of the image belonging to a scene class is estimated, this value can be used to weight the image responses to different Gabor filters based on the corresponding "Gabor Index". In this way we intend to enhance the image responses to filters with higher energy levels and inhibit the image responses to filters with lower energy levels. The newly formed V_G is used in estimating the likelihoods $P(V_G | S_j)$ for the next iteration. We study the effect of combining the feature modulation and the feedback between the object and the scene module on the scene classification performance.

7.1 Feature Tuning Scheme

In order to compute dominant power spectrum information for images belonging to each scene class we use the total energy of the image responses to the bank of Gabor filters. For a given image $I(\xi,\eta)$ the image response to a Gabor filter tuned to radial frequency f_r and orientation θ is given by

$$V(x, y, f_r, \theta) = \left| \sum_{\xi,\eta=1}^{N} I(\xi,\eta) G_{f_r,\theta}(x-\xi, y-\eta) \right| \tag{7.1}$$

The total energy of the image response $V(x, y, f_r, \theta)$ is given by

$$E_{f_r,\theta} = \sum_x \sum_y \left| V(x, y, f_r, \theta) \right|^2 \tag{7.2}$$

The average energy of the image responses to each Gabor filter tuned to radial frequency f_r and orientation θ , for all images in the database belonging to scene class S_j is given as follows:

$$E_{f_r,\theta,S_j} = \frac{\sum_{i=1}^{N} E_{f_r,\theta}(V_{ij})}{\sum_{j=1}^{M}\sum_{i=1}^{N} E_{f_r,\theta}(V_{ij})} \tag{7.3}$$

where the subscript $j = 1...M$ denotes the scene classes S_j, and the subscript $i = 1...N$ denotes the N images in each scene class S_j of the database. We call the average energy E_{f_r,θ,S_j} of images belonging to scene class S_j, the index of Gabor filter $G_{f_r,\theta}$ for scene class S_j. The Gabor indices provide an energy profile for each scene category which can serve as a basis for tuning the image features which provide higher energy responses for each scene category. Figure (7.1) shows the Gabor index thus computed for the four scene classes, downtown, residential, park, indoors, and street scenes.

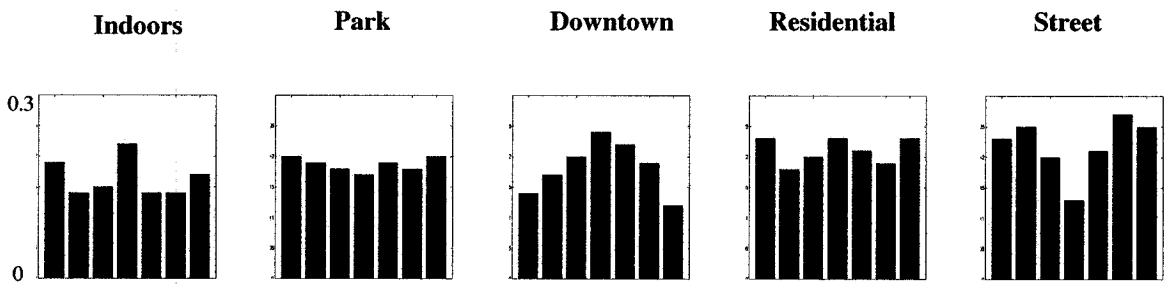

Figure 7.1. The Gabor indices computed for five scene categories, indoors, park, downtown, residential, and street scenes are presented for $\lambda = 8$ and $\theta = 0,30,60,90,120,150,180$ degrees. Each Gabor index is obtained by averaging the total energy of the database images in each scene category.

Given an input image to the model, we can use the hypothesis formed by the scene module to bias the image responses to selected Gabor filters which provide higher discrimination for scene classes with higher probabilities. We weigh the image response to a Gabor filter with radial frequency f_r and orientation θ according to the probability value of each scene class S_j and index of the Gabor filter $G_{f_r,\theta}$ for each scene class S_j as the following:

$$\hat{V}(x, y, f_r, \theta) = \sum_{j=1}^{M} P(S_j | V_G) \frac{E_{f_r,\theta,S_j}}{\sum_{f_r}\sum_{\theta} E_{f_r,\theta,S_j}} V(x, y, f_r, \theta) \tag{7.4}$$

In each iteration of the model, in order to incorporate the top-down feature tuning scheme based on the hypotheses created by the scene module, the modulated image responses $\hat{V}(x, y, f_r, \theta)$ are weighed based on the probability values estimated for each of the scene classes at the previous iteration. The modulated image responses $\hat{V}(x, y, f_r, \theta)$ replace $V(x, y, f_r, \theta)$ for computing the global image features V_G used at the current iteration of the model. Updating of the global image features V_G, based on the modulated image responses, means that the likelihood model estimations vary at each iteration of the model.

For the adaptive prior model the estimate of the likelihood $P(V_G | S_j)$ varies based on the updated values of V_G, and for the adaptive likelihood model the estimate of the likelihood $P(V_G, P(O = O_1), \ldots, P(O = O_N) | S_j)$ varies not only based on the new estimates for the object class probabilities, but also based on the new global image features V_G. As the model iterates, if one of the scene category probabilities computed

by the model dominates the other scene category probabilities, the corresponding Gabor index gains more weight for the modulation of the image responses. In the next section we show examples of how such a process affects the function of the scene classification module, and in general the scene classification performance of the model.

7.2 Experimental Results

Figures (7.2) and (7.3) present results of the model function when combined with feature tuning effect as explained in the previous section. Figure (7.2) illustrates an example of the behavior of the coupled likelihoods model when combined with the feature tuning effect and figure (7.3) illustrates an example of the behavior of the coupled priors model when combined with the feature tuning effect.

The sample image in figure (7.2.a) is a street scene. The probabilities of buildings, plants, and vehicles being present in the scene, as computed by the coupled likelihood model, without any feature tuning is shown in figure (7.2.b). The probabilities of the image belonging to the scene categories street, park, downtown, and residential, as computed by the coupled likelihood model, without feature tuning, is shown in figure (7.2.c). Initially the model computes close probability values for the image belonging to the street category and the park category, but the object module finds more evidence for vehicles being present in the image as compared to plants. The object probabilities provide enough information for the scene module in order to gradually estimate higher probabilities for the scene being a street scene. Figure (7.2.d) shows the probabilities of this image belonging to the mentioned scene classes when the coupled likelihoods model is combined with the feature tuning effect. Comparing figure (7.2.c) and (7.2.d) one can

say that for the shown iterations of the sample image, the effect of the feature tuning is to increase the speed of the model achieving a correct scene classification result.

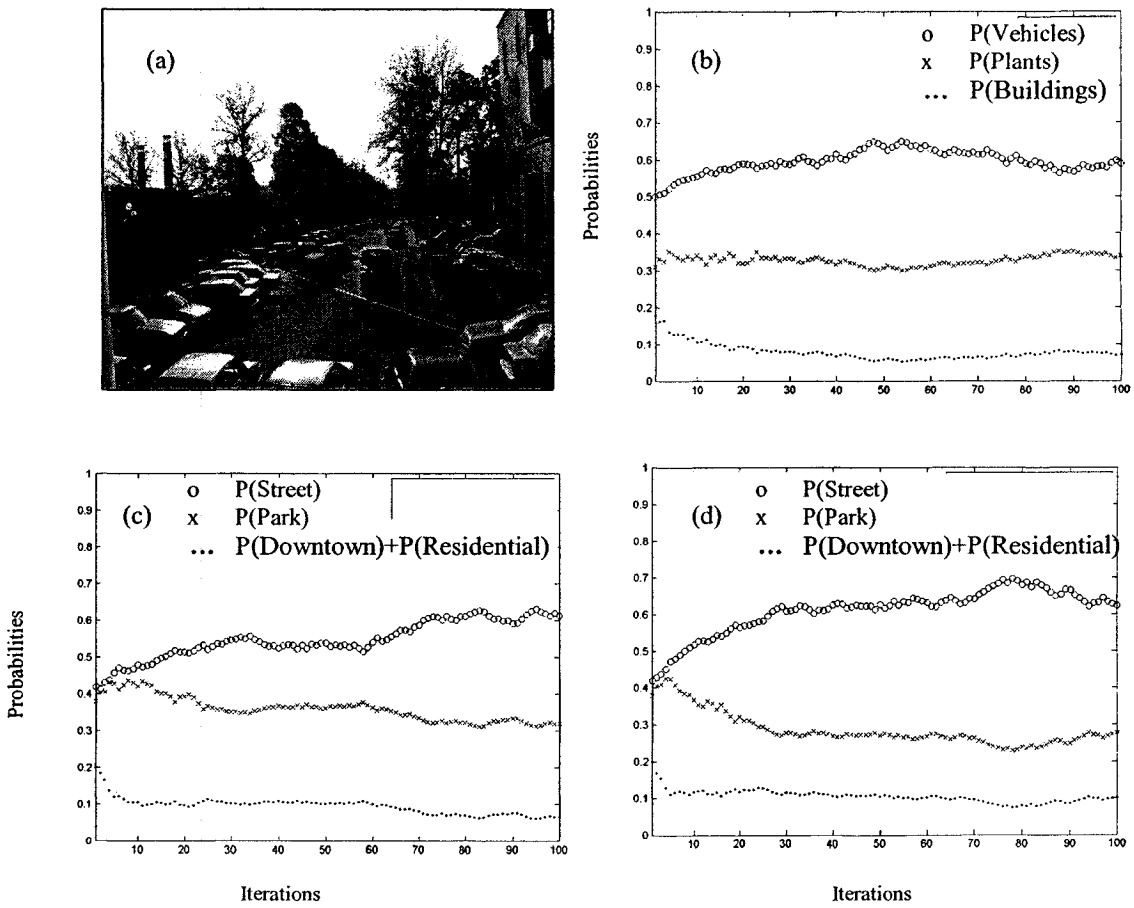

Figure 7.2. An example of the function of the coupled likelihoods model as combined with feature tuning effect is presented (a) sample input image (b) the probabilities of different objects being present in the scene, as computed by the coupled likelihoods model, without any feature tuning (c) the probabilities of the image belonging to different scene classes, as computed by the coupled likelihoods model, without any feature tuning and (d) the probabilities of the image belonging to different scene classes, as computed by the coupled likelihoods model, combined with feature tuning.

Figure (7.3) illustrates a similar example for the coupled priors model. The sample image in (7.3.a) belongs to the downtown scene category. Figure (7.3.b) and (7.3.c) show the object class and scene class probability values as estimated by the coupled priors model without any feature tuning effect. Initially the model computes

close probability values for the image belonging to the downtown category and the street category, but the object module finds little evidence for vehicles being present in the image as compared to buildings.

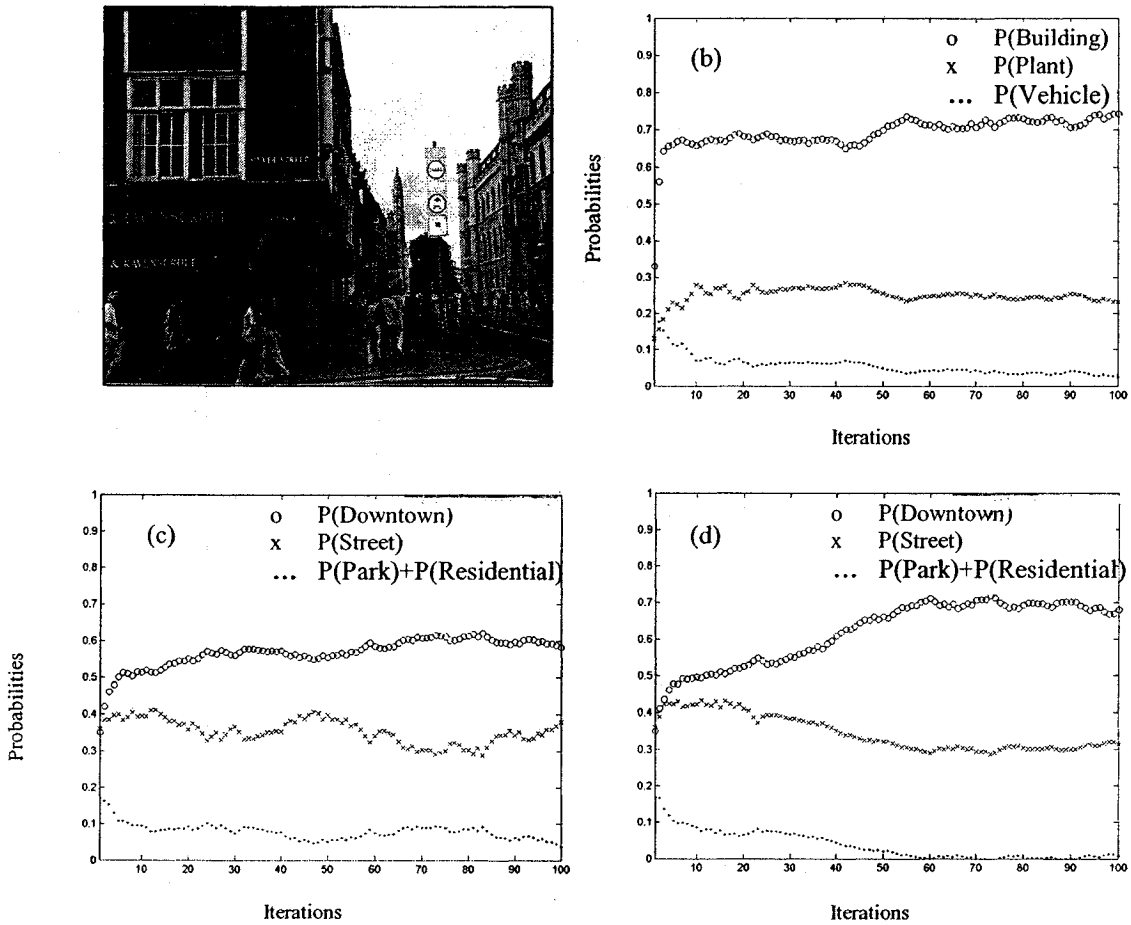

Figure 7.3. An example of the function of the coupled priors model as combined with feature tuning effect is presented (a) sample input image (b) the probabilities of different objects being present in the scene, as computed by the coupled priors model, without any feature tuning (c) the probabilities of the image belonging to different scene classes, as computed by the coupled priors model, without any feature tuning and (d) the probabilities of the image belonging to different scene classes, as computed by the coupled priors model, with feature tuning.

In this example the feedback from the object module to the scene module has the effect of decreasing the probability of the scene belonging to street scene category. Figure

(7.3.d) shows the behavior of the model when the coupling of the priors is combined with the feature tuning effect. Similar to the example above the effect of feature tuning for this sample image is that the model achieves higher probabilities for the correct scene class identity in earlier iterations.

Examples in the previous two figures have been selected among experimental results in order to illustrate the capability of the feature tuning to increase the scene classification performance. In order to make a statistically valid conclusion about the effect of feature tuning on the scene classification performance we plot ROC curves. Figure (7.4) and (7.5) contain the receiver operating characteristic (ROC) curves for scene classification task performed by the coupled priors and coupled likelihoods models when their functionality is combined with the feature tuning effect. In figures (7.4) and (7.5) each curve represents results from varying decision thresholds of a fixed iteration of the model. Comparing the curves representing performance at the first and the 100^{th} iteration of the two models we can see that classification performance is higher at the 100^{th} iteration in both models. It is also important to compare the performances of the two models with feature tuning with the performances of the two models without any feature tuning. Therefore, we have included relevant plots in figures (7.4) and (7.5) to make the comparisons easier. One can observe that the models with feature tuning achieve higher classification performance at the 100^{th} iteration as compared to the models without feature tuning. In general one can conclude that the effect of combining feature tuning with the strongly coupled models is that on average a higher detection rate is achieved with fewer iterations, at least within the first 100 iterations of the model.

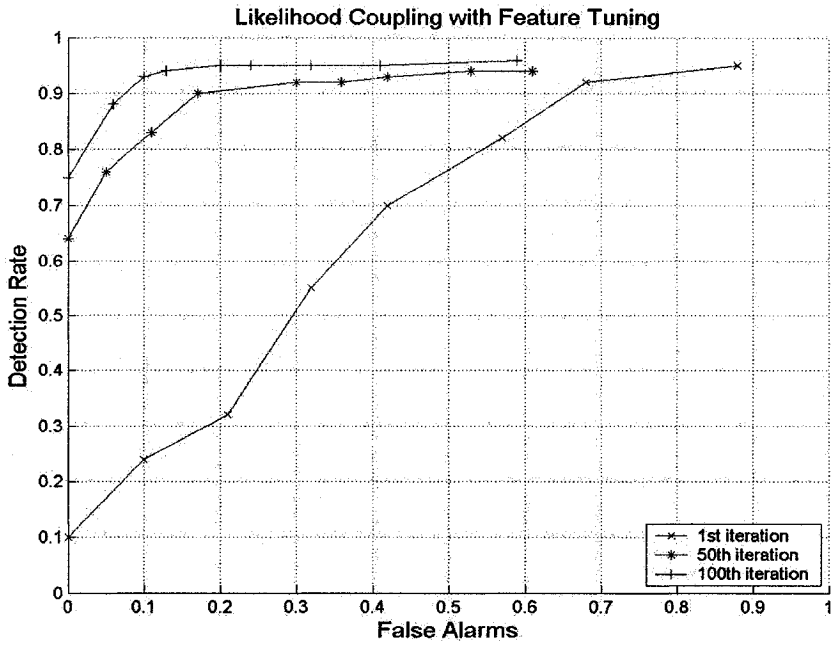

(a)

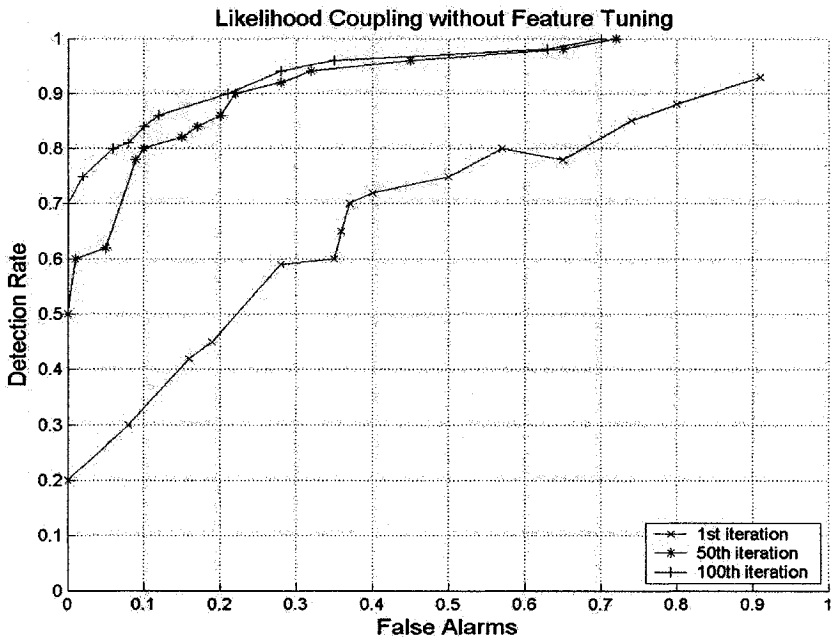

(b)

Figure 7.4. (a) ROC curves computed for the coupled likelihood model when combined with top-down feature tuning effect. (b) ROC curves computed for the coupled likelihood model without any feature tuning effect. Each curve represents results for varying decision thresholds for a fixed iteration of the model.

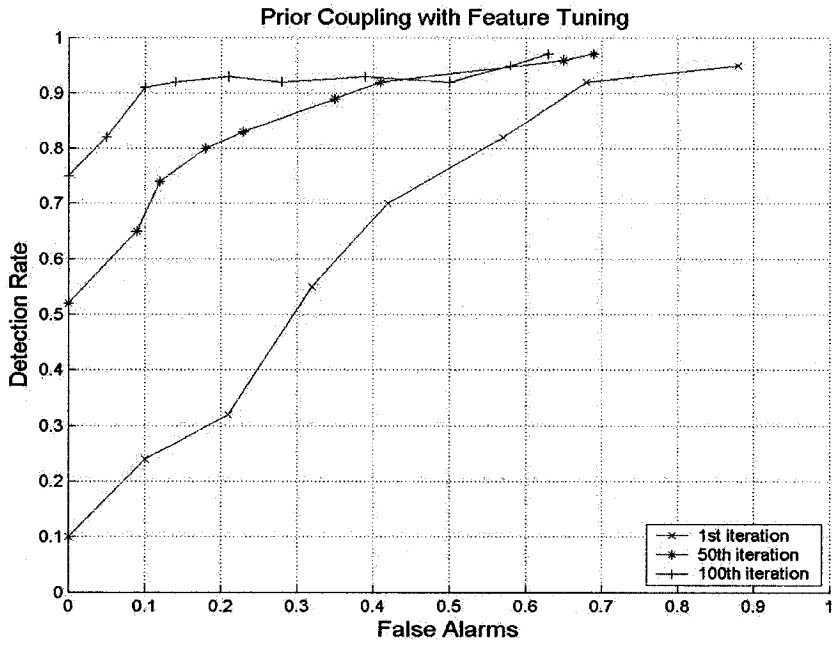

(a)

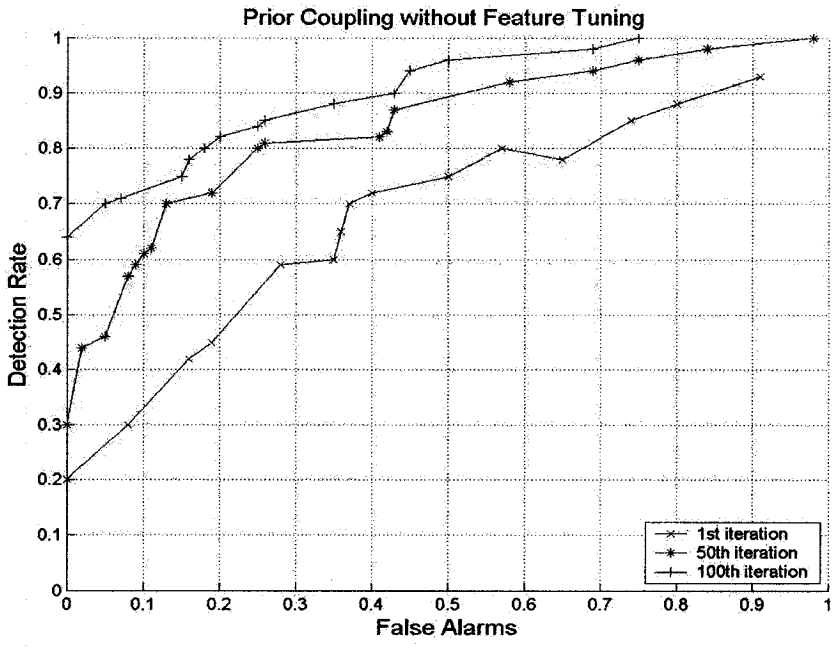

(b)

Figure 7.5 (a) ROC curves computed for the coupled priors model when combined with top-down feature tuning effect. (b) ROC curves computed for the coupled priors model without any feature tuning effect. Each curve represents results for varying decision thresholds for a fixed iteration of the model.

Chapter 8

Conclusions and Future Work

8.1 Conclusions

In this thesis, we have presented a strongly coupled data fusion architecture within a Bayesian framework that models the associations between the scene and object classification mechanisms. Based on findings from the domains of neurophysiology and psychophysics there is adequate experimental evidence to suggest that the scene perception mechanism and the object perception mechanism in human vision do not function in isolation. There is experimental evidence which shows that scene-contextual constraints are available early enough and are robust enough to influence the object recognition mechanism, also rapid recognition of familiar objects influences the scene recognition mechanism. These experimental results imply the presence of a bidirectional flow of information between the scene and the object recognition mechanisms, while contradicting a strictly hierarchical relationship between the two processes in any order. These findings have motivated us to develop an architecture that can give a computational account of how such a relationship is possible between the object classification and the scene classification processes. The most important characteristic of the architecture proposed in this thesis is that it avoids a hierarchical relationship between the two processes, so that each of the processes can function independently in case of lack of feedback from the other process. A feedback channel is provided between the two processes so that as soon as any of the two processes extracts any information

about the identity of the scene or the identity of the objects present in the scene, this information becomes available to the other process.

Our proposed architecture is derived from Clark and Yuille's [14] work. In their work they present a general architecture for strongly-coupled data fusion of separate sensory information processing modules, with the purpose of regularizing the ill-posed problem involved with each sensory information processing task. We have used this general structure and have adapted it to the specific problem of the strong coupling of two modules which are specialized in the scene classification and the object classification tasks. The strong coupling of the two modules provide additional constraints for each module's solution process based on the information obtained from the independent process of the other module. The Bayesian approach taken for solving the tasks assigned to each module has the advantage of providing a suitable form for embedding constraints either in the likelihood models or the prior models of the modules' solution processes. In this thesis we have presented novel schemes for modifying the Bayesian solutions for the scene and object classification tasks which allow data fusion between the two modules based on the constraining of the priors or the likelihoods.

We have implemented the two proposed models and tested the model functions using a data base of natural images created for this purpose. We have presented examples of the model outputs for images of different scene categories which illustrate how the feedback between the two modules can improve the initial scene classification results obtained from the uncoupled scene module. The ROC curves plotted for the likelihood coupling and the prior coupling models show that the scene classification

performance improves significantly in both models as a result of the strong coupling of the scene and object modules. The shapes of the autocorrelation plots obtained from both models' outputs demonstrate the predictability of the two models' processes. We have also tested the robustness of the two models to variations to the input test images such as added noise. ROC curves depicting the scene classification performance of the two models also show that the likelihood coupling model achieves a higher detection rate compared to the prior coupling model. We have also computed the average rise times of the models' outputs as a measure of comparing the speed of the two models. The results show that the likelihood coupling model outputs have a shorter rise time. Based on these experimental findings one can conclude that imposing constrains on the likelihood models provide better solutions to the scene classification problems compared to imposing constraints on the prior models. This result is compatible with the general concept that the prior models represent smoother functions compared to the likelihood models. Imposing constraints on the likelihood models, which are more sensitive functions compared to the prior models, improves the Bayesian solution more than imposing constraints on prior models, which are smoother, slower varying functions.

We have also proposed an attentional feature modulation scheme, which consists of tuning the input image responses to the bank of Gabor filters based on the scene class probabilities estimated by the model and the energy profiles of the Gabor filters for different scene categories. Experimental results based on combining the attentional feature tuning scheme with the likelihood coupling and the prior coupling methods show a significant improvement in the scene classification performances of both models.

The question of coupling the object classification process and the scene classification process has been addressed by other researchers in the field of machine learning such as Murphy *et al* [65]. The approach taken by these researchers is to combine the tasks of scene classification and object presence detection using a tree-structural graphical model, where the message passing runs first bottom-up (objects to scenes) and then top-down (scenes to objects). The graphical model encodes a conditional joint probability density model of the scene class and the object classes present in the scene as constrained by the global contextual features. Our approach to combining the scene classification and the object classification tasks differ from this approach in a fundamental way. Our main goal in developing the proposed architecture was its biological relevance, and not necessarily building a model for efficient scene or object classification. Therefore, we imposed certain constraints to our model, such as avoiding a hierarchical relationship between the object and scene classification modules, in order to develop a computational scheme which would explain the relationship between the scene and object recognition process in human visual system based on psychophysical findings.

8.2 Future Work

Our main challenge in developing a model where the scene processing and the object processing modules would interact, was to find a way to combine results from local and global sources of information. There are three types of local information produced by the object processing module, the identity of the objects, the location of the objects, and the scale of the objects. In the present implementation of the model the local information

extracted about the identities of the objects are combined with each other and interact with the global source of information, but we make no use of the objects' locations and scales, while both the scales of the objects and their locations provide strong constraints for the scene classification problem. Therefore, the proposed model can be enhanced by modifying the present formulation in order to include scales and locations of the objects as part of the information passed between the modules.

Our present method of identifying objects in a scene is based on sliding a detector over the whole scene and classifying the patches at each location and scale. We can improve the speed and the accuracy of our object classification module by reducing the search space for objects. This can be implemented either by using prior constraints from the scene classes inferred from the scene classification module. Scene classes provide strong constraints on the locations where certain object classes may be found. We can also reduce the search space for the objects by using an attentional scheme which would highlight the most conspicuous locations of the scene. This may provide a way to reduce the amount of irrelevant information processed and to focus on the most informative or the most interesting locations of the scene. Such a scheme would also be closer to how humans fixate on different locations in a scene, rather than covering the whole scene with a pre-assigned order.

What we consider a very challenging and interesting issue to be addressed in future work is the issue of moving from a highly supervised model, such as the model presented in this thesis, to an unsupervised model, where new scene and object categories can be learned from the data. Also the choice of levels of abstractions for scene and object classes in a supervised model is a challenging decision. While

designing the experiments for the implementation of our model we had to deal with the problem of choosing appropriate levels of abstraction for the scene and object categories, in order to allow useful information being produced for the use of the other model. Changing the levels of abstraction from basic level categories such as the ones we have used in our experiments to more general or finer discrimination categories may involve modifications to the proposed model which has to be investigated further.

References

[1] G. K. Aguirre., "The parahippocampus subserves topographical learning in man," *Cortex,* vol. 6, pp. 823-829, 1996.

[2] R. Baddeley, "The correlational structure of natural images and the calibration of spatial representations," *Cogn. Sci.* vol. 21, pp. 351-372, 1997.

[3] M. Bar and S. Ullman, "Spatial context in recognition," *Perception*, vol. 25, pp.343-352, 1996.

[4] M. Bar and E. Aminoff, "Cortical analysis of visual context," *Neuron* vol. 38, pp. 347-358, 2003.

[5] I. Biederman, "Perceiving real-world scenes," *Science*, vol. 177, pp. 77-80, 1972.

[6] I. Biederman, "On the semantics of a glance at a scene," *Perceptual Organization*, pp. 213-254, 1981.

[7] I. Biederman, R. C. Teitelbaum, and R. J. Mezzanotte, "Scene perception: a failure to find a benefit from prior expectancy or familiarty," *J. of Exp. Psychol.*, vol. 9(3), pp. 411-429, 1983.

[8] I. Biederman, "Recognition-by-Components: A theory of human image understanding," *Psychological Review*, vol. 94, pp. 115-147,

[9] S. J. Boyce, A. Pollatsek, and K. Rayner, "Effect of background information on object identification," *J. Exp. Psychol. Hum. Perc. and Perf.*, vol. 15(3), pp. 556-566, 1989.

[10] L. Breiman, "Bagging predictors," *Machine Learning*, vol. 26(2), pp. 123-140, 1996.

[11] J. Bullier and L. G. Nowak, "Parallel versus serial processing: new vistas on the distributed organization of the visual system," *Curr. Opin. Neurobiol.*vol. 5, pp. 497-503 1995.

[12] M. Burl and P. Perona, "Recognition of planar object classes," *Proc .of Computer Vision and Pattern Recognition*, pp. 223-230, 1996.

[13] S. Belongie, C. Carson, H. Greenspan, and J. Malik, "Color and texture based image segmentation using EM and its application to image querying and classification," *Proc. of the Int. Conf. Computer Vision*, pp. 675-672, 1998.

[14] J. J. Clark and A. L. Yuille, *Data Fusion for Sensory Information Processing Systems*, USA: Kluwer Academic Publishers, 1990.

[15] B. V. Dasarthy, *Decision Fusion*, Los Alamitos, CA: IEEE Computer Society Press.

[16] P. De Graef, D. Christiaens, and G. d'Ydewalle, "Perceptual effects of scene context on object identification," *Psychol. Res.*, vol. 52, pp. 317-329, 1990.

[17] P. E. Downing., "A cortical area selective for visual processing of the human body," *Science* vol. 293, pp. 2470-2473, 2001.

[18] T. Ehtiati and J. J. Clark, "A Bayesian Model for the Bi-directional Influences between the Scene and the Object Identification Processes", *Proc. of the International Workshop on the Representation and Use of Prior Knowledge in Vision (WRUPKV),* in association with the 9th European Conference on Computer Vision (ECCV), pp. 126-139, 2006.

[19] T. Ehtiati and J. J. Clark, "A Strongly Coupled Architecture for Contextual Object and Scene Identification", *Proc. of the 17th IEEE International Conference on Pattern Recognition (ICPR)*, vol. 3, pp. 69-72, 2004.

[20] R. A. Epstein, "The cortical basis of visual scene processing," *Visual Cogn,* vol. 12, pp. 954-978, 2005.

[21] R. Epstein and N. Kanwisher, "A cortical representation of the local visual environment," *Nature,* vol. 392, pp. 598-601, 1998.

[22] L. Fei-Fei, R. Fergus, and P. Perona, "Learning generative visual models from few training examples: an incremental Bayesian approach tested on 101 object categories," Workshop on Generative-Model Based Vision, 2004 (in press).

[23] L. Fei-Fei, R. VanRullen, C. Koch, and P. Perona, "Rapid natural scene categorization in the near absence of attention," *Proc. Nat. Acad. Sci.*, vol. 99(14), pp. 9596-9601, 2002.

[24] L. Fei-Fei, R. Fergus, and P. Perona, "A Bayesian approach to unsupervised one-Shot learning of object categories," *Proc. of Int. Conf. on Computer Vision*, pp. 1134-1141, 2003.

[25] L. Fei-Fei, R. Fergus, and P. Perona, "One-Shot learning of object categories," *IEEE Trans. on Pattern Analysis and Machine Intelligence*, vol. 28(4), pp. 594-611, 2006.

[26] R. Fergus, P. Perona, and A. Zisserman, "Object class recognition by unsupervised scale-invariant learning," *Proc. of Computer Vision and Pattern Recognition*, pp. 264-271, 2003.

[27] M. Flickner and H. Sawhney, "Query by image and video content: The QIBC system," *IEEE Computer*, vol. 28(9), pp. 23-32, 1995.

[28] Y. Freund and R. E. Schapire, "Experiments with a new boosting algorithm," *Proc. of the Thirteenth Int. Conf. on Machine Learning*, pp. 148-156, 1996.

[29] Y. Freund and R. Schapire, "A short introduction to boosting," *Journal of Japanese Society for Artificial Intelligence*, vol. 14(5), pp. 771-780, 1999.

[30] A. Friedman, "Frame pictures: the role of knowledge in automatized encoding and memory for gist," *J. of Exp. Psychol. General*, vol. 108(3), pp.316–355, 1979.

[31] J. D. Gabrieli, R. A. Poldrack, and J. E. Desmond, "The role of left prefrontal cortex in language and memory," *Proc. Natl Acad. Sci. USA,* vol. 95, pp.906–913, 1998.

[32] A. Gelb, *Applied Optimal Estimation.* Cambridge, MA: MIT Press 1974.

[33] F. Germeys and G. d'Ydewalle, "Revisiting scene primes for object locations," *Quart. J. Exp. Psychol.*, vol. 54A(3), pp. 683–693, 2001.

[34] M. Gorkani and R. W. Picard, "Texture orientation for sorting photos at a glance," *Proc.of the Int. Conf. on Pattern Recognition*, vol. 1, pp. 459-464, 1994.

[35] C. V. Gottesman and H. Intraub, "Wide-angle memories of close-up scenes: a demonstration of boundary extension,", *Behav. Res. Methods Instrum. Comp.*, vol. 31(1), pp. 86-93, 1999.

[36] K. Grill-Spector, Z. Kourtzi, and N. Kanwisher, "The lateral occipital complex and its role in object recognition," *Vision Res.,* vol. 41, pp. 1409–1422, 2001.

[37] K. Grill-Spector and N. Kanwisher, "Visual recognition: as soon as you know it is there, you know what it is," *Psychol. Sci.*, vol. 16 (2) , pp. 152-160, 2005.

[38] A. Gupta and R. Jian, "Visual information retrieval," *Communications of the ACM*, vol. 40(5), pp. 71-79, 1997.

[39] J. V. Haxby, "Distributed and overlapping representations of faces and objects in ventral temporal cortex," *Science,* vol. 293, pp. 2425–2430, 2001.

[40] J. M. Henderson and A. Hollingworth, "High-level scene perception," *Annu. Rev. Psychol.*, vol. 50, pp. 243-271, 1999.

[41] A. Hollingworth and J. M. Henderson, "Object identification is isolated from scene semantic constraint: evidence from object type and token discrimination," *Acta Psychol (Amst),* vol. 102(2-3), pp. 319-343, 1999.

[42] J. Huang, S. R. Kumar, and R. Zabih, "An automatic hierarchical image classification scheme," *Proc. of Sixth ACM Intl. Multimedia Conf.*, pp. 219-228, 1998.

[43] Y. S. Huang and C. Y. Suen, "A method of combining multiple experts for recognition of unconstrained handwritten numerals," *IEEE Trans. on Pattern Analysis and Machine Intelligence,* vol. 17 (1), pp.90-94, 1995.

[44] D. H. Hubel and T. N. Wiesel, "Receptive fields and functional architecture of the monkey striate cortex," *Journal of Physiology*, vol. 195, pp.215-243, 1968.

[45] D. Hubel and T. Wiesel, " Binocular interaction and functional architecture in the cat's visual cortex," *Journal of Physiology*, vol. 160, pp. 106-154, 1962.

[46] H. Intraub, "Boundary extension for briefly glimpsed photographs: do common perceptual processes result in unexpected memory distortions?" *J. Mem. Lang.,* vol. 35, pp. 118-134, 1996.

[47] R. A. Jacobs, M. I. Jordan, S. J. Nowlan, and G. E. Hinton, "Adaptive mixtures of local experts," *Neural Computation*, vol. 3, pp. 79-87, 1991.

[48] M. I. Jordan and R. A. Jacobs, "Hierarchical mixtures of experts and the EM algorithm," *Neural Computation*, vol. 6, pp. 181-214, 1994.

[49] J. Kittler, M. Hatef, R. P. W. Duin, and J. Matas, "On combining classifiers," *IEEE Trans. on Pattern Analysis and Machine Intelligence*, vol. 20(3), pp. 226-239, 1998.

[50] S. M. Kosslyn, R. A. Flynn, J. B. Amsterdam, and G. Wang, "Components of high-level vision: A cognitive neuroscience analysis and accounts of neurological syndromes," *Cognition*, vol. 34, pp. 203-277, 1990.

[51] L. Lam and C. Y. Suen, "Optimal combinations of pattern classifiers," *Pattern Recognition letters,* vol. 16, pp. 945-954, 1995.

[52] Y. LeCun, L. Bottou, Y. Bengio, and P. Haffner, "Gradient-based learning applied to document recognition," *Proc. of the IEEE*, vol. 86(11), pp. 2278–2324, 1998.

[53] T. Leung, M. Burl, and P. Perona, "Finding faces in cluttered scenes using labeled random graph matching," *Proc. Int. Conf. on Computer Vision*, pp. 637–644, 1995.

[54] I. Levy, "Center-periphery organization of human object areas," *Nature Neurosci.,* vol. 4, pp. 533–539, 2001.

[55] P. Lipson, "Context and Configuration Based Scene Classification," *EECS dept,* PhD thesis MIT, 1996.

[56] G. R. Loftus, W. W. Nelson, and H. J. Kallman, "Differential acquisition rates for different types of information from pictures," *Q. J. Exp. Psychol.* vol. 35A, pp. 187-198, 1983.

[57] E. A. Maguire., "Knowing where things are: parahippocampal involvement in encoding object locations in virtual large-scale space," *J. Cogn. Neurosci.*, vol. 10, pp. 61-76, 1998.

[58] J. M. Mandler and R. E. Parker, "Memory for descriptive and spatial information in complex pictures," *J. of Exp. Psychol.*, vol. 2(1), pp. 38-48, 1976.

[59] D. Marr, *Vision*, USA: W.H. Freeman, 1981.

[60] G. J. McLachlan and T. Krisshnan, *The EM Algorithm and Extenstions*, USA: John Wiley & Sons Inc. 1997.

[61] W. H. Merigan and J. H. Maunsell, "How parallel are the primate visual pathways?" *Annu. Rev. Neuroscie.*, vol. 16, pp. 369–402, 1993.

[62] R. L. Metzger and J. R. Antes, "The nature of processing early in picture perception," *Psychol. Res.*, vol. 45, pp. 267-274, 1983.

[63] T. P. Minka and R. W. Picard, "Interactive learning using a society of models," *Proc. of CVPR IEEE Computer Society*, pp. 447-452, 1996.

[64] M. Mishkin, L. G. Ungerleider, and K. A. Macko, "Object vision and spatial vision: Two cortical pathways," *Trends Neurosci.*, vol. 6, pp. 414–417, 1983.

[65] K. Murphy, A. Torralba, and W. Freeman, "Using the forest to see the trees: a graphical model relating features, objects and scenes," *Neural info. Processing Systems*, Vancouver, B.C., 2004.

[66] A. Oliva and P. G. Schyns, "Coarse blobs or fine edges? Evidence that information diagnosticity changes the perception of complex visual stimuli," *Cognitive Psychology*, vol. 34, pp. 72-107, 1997.

[67] A. Oliva and P. G. Schyns, "Colored diagnostic blobs mediate scene recognition," *Cognitive Psychology*, vol. 41, pp.176-210, 2000.

[68] A. Oliva and A. Torralba, "Modeling the shape of the scene: a holistic representation of the spatial Envelope," *Int. Journal of Computer Vision*, vol. 42(3), pp. 145-175, 2001.

[69] A. Oliva and A. Torralba, "Scene-Centered Description from Spatial Envelope Properties," *Proc. 2nd Workshop on Biologically Motivated Computer Vision*, Tubingen, Germany, 2002.

[70] A. Oliva, A. Torralba, A. Guerin-Dugue, and J. Herault, "Global semantic classification of scenes using power spectrum templates," *Proc. of The Challenge of Image Retrieval.* Electronic Workshop Computer Series, Springer-Verlag, 1999.

[71] A. Oliva, "Gist of a Scene," *Neurobiology of Attention,* Academic Press, Elsevier pp. 251-256.

[72] J. K. O'Regan and A. Noë, "What it is like to see: A sensorimotor theory of visual experience," *Synthese*, vol. 129(1), pp. 79-103, 2001.

[73] J. K. O'Regan, R. A. Rensink, and J. J. Clark, "Blindness to scene changes caused by "mudsplashes"," *Nature*, vol. 398, pp. 34, 1999.

[74] S. E. Palmer, "Visual perception and world knowledge: notes on a model of sensory-cognitive interaction," *Explorations in Cognition*, pp. 279-307. LNR Res. Group, San Francisco, 1975.

[75] T. Poggio and S. Edelman, "A network that learns to recognize 3D objects,",*Nature* vol. 343, pp. 263-266, 1990.

[76] M. C. Potter, "Short-term conceptual memory for pictures," *J. of Exp. Psychol. Hum. Learning and Mem*, vol. 2, pp. 509-522, 1976.

[77] M. C. Potter, A. Staub, J. Rado, and D.H. O'Connor, "Recognition memory for briefly presented pictures: the time course of rapid forgetting," *J. Exp. Psychol: Hum. Perc. and Perf*, vol. 28(5), pp. 1163-1175, 2002.

[78] A. Puce, T. Allison, M. Asgari, J. C. Gore, and G. McCarthy, "Differential sensitivity of human visual cortex to faces, letterstrings, and textures: a functional magnetic resonance imaging study," *J. Neurosci.,* vol. 16, pp. 5205-5215, 1996.

[79] A. L. Ratan and W. E. L. Grimson, "Training templates for scene classification using a few examples," *Proc. of IEEE Workshop on Content-Based Access of Image and Video Libraries*, pp. 90-97, 1997.

[80] R. A. Rensink, J. K. O'Regan, and J. J. Clark, "To see or not to see: the need for attention to perceive changes in scenes," *Psychol. Sci.*, vol. 8(5), pp. 368-373, 1997.

[81] G. Rousselet, M. Fabre-Thorpe, and S. Thorpe, "Parallel processing in high-level categorization of natural images," *Nature Neuroscience*, vol. 5, pp. 629–630, 2002.

[82] H. Rowley, S. Baluja, and T. Kanade, "Neural network-based face detection," *IEEE Trans. On Pattern Analysis and Machine Intelligence.*, vol. 20(1), pp. 23-38, 1998.

[83] A. M. Schmid and M. Bar, "Activation of multiple candidate object representations during top–down facilitation of visual recognition," *Soc. Neurosci. Abstr.* vol. 128(5), 2003.

[84] H. Schneiderman and T. Kanade, "A statistical approach to 3D object detection applied to faces and cars," *Proc. of Computer Vision and Pattern Recognition*, pp. 746-751, 2000.

[85] J. R. Smith and S. F. Chang. "Visualseek: A fully automated content-based image query system," *ACM Multimedia*, pp. 87-98, 1996.

[86] L. Standing, "Learning 10,000 pictures," *Quarterly Journal of Experimental Psychology,* vol. 25, pp. 207-222, 1973.

[87] L. Standing, J. Conezio, and R. N. Haber, "Perception and memory for pictures: Single-trial learning of 2,500 visual stimuli," *Psychonomic Science*, vol. 19, pp. 73-74, 1970.

[88] C. E. Stern, "The hippocampal formation participates in novel picture encoding: evidence from functional magnetic resonance imaging," *Proc. Natl Acad. Sci.,* vol. 93, pp. 8660–8665, 1996.

[89] K. Sung and T. Poggio, "Example-based learning for view-based human face detection," *IEEE Trans. on Pattern Analysis and Machine Intelligence*, vol. 20(1), pp. 39-51, 1998.

[90] M. Szummer and R. Picard, "Indoor-outdoor image classification," *Int. Workshop on Content-based Access of Image and Video Databases*, 1998.

[91] K. Tanaka, "Neuronal mechanisms of object recognition," *Science,* vol. 262, pp. 685-688, 1993.

[92] M. Tarr and H. Bulthoff, "Is human object recognition better described by geon structural descriptions or by multiple views? Comment on Biederman and Gerhardstein (1993)," *J. Exp. Psychol. Hum. Percept. Perform*, vol. 21, pp. 1494-1505, 1995.

[93] S. Thorpe, D. Fize, and C. Marlot, "Speed of processing in the human visual system," *Nature*, vol. 381, pp. 520-522, 1996.

[94] A. Torralba and A. Oliva., "Statistics of natural image categories," *Network: computation in neural systems*. vol. 14, pp.391-412, 2003.

[95] A. Torralba and A. Oliva, "Depth estimation from image structure," *IEEE Trans. on Pattern Analysis and Machine Intelligence,* vol. 24(9), pp. 1226-1238, 2002.

[96] A. Treisman and G. Gelade, "A feature-integration theory of attention," *Cogn. Psychol.*, vol. 12, pp. 97-136, 1980.

[97] J. K. Tsotsos, S. Culhane, W. Wai, Y. Lai, N. Davis, and F. Nuflo, "Modeling visual attention via selective tuning," *Artificial Intelligence*, vol. 78(1-2), pp. 507-547, 1995.

[98] L. G. Ungerleider and M. Mishkin, "Two cortical visual systems," *Analysis of Visual Behavior*, pp. 549-586, MIT press, Cambridge, Mass., 1982.

[99] A. Vailaya, M. Figueiredo, A. Jain, and H. Zhang, "Image classification for content-based indexing," *IEEE Trans. on Image Processing*, vol. 10, 2001.

[100] A. Vailaya, M. Figueiredo, A. Jain, and H. Zhang, "A Bayesian Framework for Semantic Classification of Outdoor Vacation Images," Proc. *of SPIE Conference on Electronic Imaging*, San Jose, California, 1999.

[101] D. C. Van Essen, "Functional organization of primate visual cortex," *Cerebral Cortex*, vol. 3, pp. 259-329. Plenum Press, 1985.

[102] P. K. Varshney, *Distributed Detection and Data Fusion*, New York: Springer Verlag, 1997.

[103] P. Viola and M. Jones, "Rapid object detection using a boosted cascade of simple features," *Proc. of Computer Vision and Pattern Recognition*, vol. 1, pp. 511-518, 2001.

[104] P. Viola, M. Jones, and D. Snow, "Detecting pedestrians using patterns of motion and appearance," *Proc. of the Int. Conf. on Computer Vision*, pp. 734-741, 2003.

[105] E. Waltz and J. Llinas, *Multisensor Data Fusion*, Boston: Artech House, 1990.

[106] M. Weber, M. Welling, and P. Perona, "Unsupervised learning of models for recognition," *Proc. of the European Conf. on Computer Vision,* vol. 2, pp. 101-108, 2000.

[107] J. M. Wolfe, "Visual search," *Attention*, pp. 13-74, Psychology Press Ltd., 1998.

[108] J. M. Wolfe, "Visual memory: what do you know about what you saw?" *Curr. Bio*, vol. 8, pp. R303-R304, 1998.

[109] K. Woods, W. P. Kegelmeyer, and K. Bowyer, "Combination of multiple classifiers using local accuracy estimates," *IEEE Trans. on Pattern Analysis and Machine Intelligence,* vol. 19, pp. 405-410, 1997.

[110] E. C. Yiu, "Image classification using color cues and texture orientation," *dept. EECS* , Masters's thesis MIT, 1996.

[111] H. Yu and W. Wolf, "Scenic classification methods for image and video databases," *Proc. SPIE, Digital Image Storage and Archiving Systems*, pp. 363-371, 1995.

[112] H. J. Zhang and D. Zhong, "A scheme for visual feature based image indexing," *Proc. SPIE Conference on Storage and Retreival for Image and Video databases*, San Jose, CA, pp. 36-46, 1995.

[113] D. Zhong, H. J. Zhang, and S. F. Chang, "Clustering methods for video browsing and annotation," *Proc. SPIE Conference on Storage and Retreival for Image and Video databases*, San Jose, CA, 1995.